

MANAFOUR AEROSPACE
PRESENTS

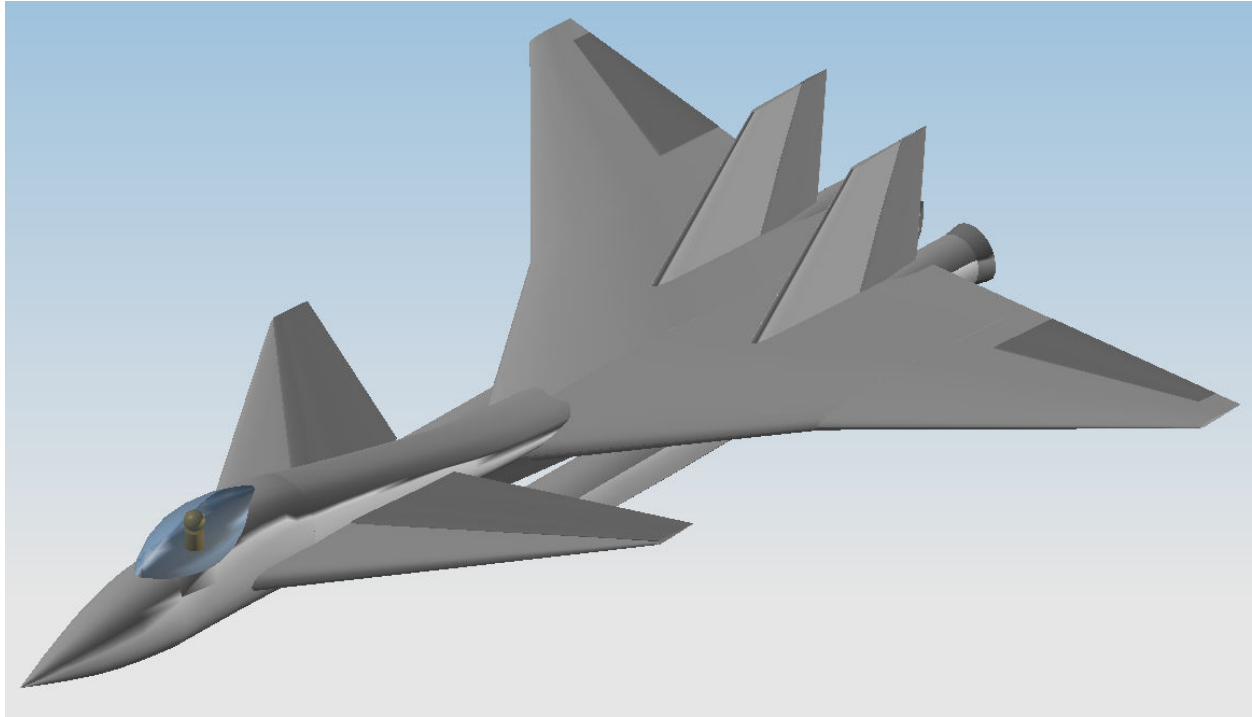
THE HEDGEHOG



A HOMELAND DEFENSE INTERCEPTOR
2005-2006 AIAA UNDERGRADUATE TEAM
AIRCRAFT DESIGN COMPETITION

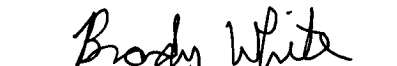
VIRGINIA TECH
AEROSPACE ENGINEERING
MAY 10, 2006

MANAFOUR AEROSPACE




Christopher Bright
Materials, Structures
AIAA#: 239398


Dane Morgan
CAD, Configuration
AIAA#: 268378


Brady White
Aerodynamics, Stability & Control
AIAA#: 225963


Stanton Krycinski
Aircraft Systems
AIAA#: 267361


Jena Rosebrock
Team Leader, Weights and Balance
AIAA#: 261657


Sam Wozniak
Cockpit Layout, CAD
AIAA#: 270082


Paul McChesney
Mission Analysis
AIAA#: 248187


Bradford Smith
Propulsion
AIAA#: 268377


William H. Mason
Advisor

Executive Summary

In response to the 2005-06 AIAA Foundation Undergrad Team Aircraft Design Competition Request for Proposal (RFP)¹, Manafour Aerospace has designed a homeland defense interceptor (HDI), The *Hedgehog*. In an attempt to design the best aircraft, different concepts were developed and analyzed. Through an iterative process, analyses were done in the following areas: missions, aerodynamics, weights, structures, stability, and systems. This helped the team to determine the best design to meet or supersede all of the proposed requirements.

The *Hedgehog* is a canard configured aircraft with a cranked wing. It is powered by two F414 engines, enabling it to loiter for four hours and dash at Mach 2.2. *Hedgehog* is capable of carrying 4 AIM – 120 AMRAAMs, 4 AIM – 9M Sidewinder Missiles, and a M61A1 20 mm Cannon. It can also endure significant loads during the 18 deg/sec instantaneous turn. All of these capabilities were met while keeping the flyaway cost under 15 million dollars assuming a 1000 unit lot.

Table of Contents

List of Figures	v
List of Tables	vi
Nomenclature	vii
1. Introduction	1
1.1 Background	1
1.2 AIAA RFP Requirements	2
2. Design Concepts	3
3. Mission and Performance Analysis	13
3.1 Mission	13
3.1.1 The Defensive Counter-Air Patrol Mission	13
3.1.2 The Point Defense Intercept Mission	13
3.1.3 The Intercept/Escort Mission	14
3.2 Other Design Considerations	15
3.3 Initial Sizing	16
3.4 Performance	18
3.4.1 Maximum Thrust Maneuvering Performance	18
3.4.2 Point Performance Requirements	20
3.4.3 Takeoff and Landing	22
4. Aerodynamics	22
4.1 Wing Geometry	22
4.2 High-Lift Devices	25
4.3 Lift and Drag	25
5. Propulsion	31
5.1 Research	31
5.2 Inlet Design	33
5.3 Installed Thrust	36
5.4 General Configuration Comments	38
6. Materials	38
6.1 Material Selection	38
6.2 Composites	38
6.3 Metals	40
7. Structures	40
7.1 Loads	40
7.2 Wings	42
7.3 Canard and Tail	43
7.4 Fuselage	43
8. Weights and Balance	45
8.1 Structural Weight	45
8.2 Fuel Weight and Corresponding Cg Shift	46
8.3 Mass Moments of Inertia	50
9. Stability and Control	51
9.1 Canard and vertical tail sizing	51
9.2 Control surfaces and trim	52
9.3 Stability and control derivatives and flying qualities	55
10. Systems and Avionics	57
10.1 Integrated Avionics	57
10.2 Common Integrated Processor	57
10.3 Fire Control Systems	58
10.4 Cockpit Layout and Instrumentation	59
10.5 Additional Equipment	61
10.6 Cockpit Layout	61
10.7 Landing Gear Location and Sizing	62
10.8 Systems Layout	64
11. Cost Analysis	68

11.1	Research Development Test and Evaluation	68
11.2	Flyaway Cost	69
11.3	Operations and Maintenance Costs.....	70
11.4	Total Cost	71
11.5	Life-Cycle Cost.....	72
12.	Conclusion.....	74
Appendix A: Mission Requirements ¹		75
Appendix B: Minimum Performance Requirements ¹		77
Appendix C: Government Furnished Equipment ¹		78
Appendix D: Configuration Drawings		79
References.....		83

List of Figures

Figure 2.1	Delta Wing Design	3
Figure 2.2	Variable Wing Design	4
Figure 2.3	Arrow Wing with Canard Design	5
Figure 2.4	Initial Changes of the Arrow Wing with Canard	6
Figure 2.5	Final Design Progression	7
Figure 2.6	Three View Drawing with Dimensions	8
Figure 2.7	Three View Structural Drawing	9
Figure 2.8	Inboard Profile Drawing	10
Figure 2.9	Top View	11
Figure 2.10	Side View	11
Figure 2.11	Front View	12
Figure 2.12	Systems Layout Drawing	12
Figure 3.1	Defensive Counter-Air Patrol Mission Profile	13
Figure 3.2	Point Defense Intercept Mission Profile	14
Figure 3.3	Intercept/Escort Mission Profile	15
Figure 3.4	Instantaneous Turn Rate vs. Mach Number	15
Figure 3.5	Design Space	18
Figure 3.6	Maximum Thrust Maneuvering Performance at 10,000 ft	19
Figure 3.7	Maximum Thrust Maneuvering Performance at 30,000 ft	19
Figure 3.8	Maximum Thrust Maneuvering Performance at 50,000 ft	20
Figure 3.9	1-g Maximum Thrust Specific Excess Power Envelope	21
Figure 4.1	Wing Planform	23
Figure 4.2	Wing, Canard, and Vertical Tail Airfoils	23
Figure 4.3	Lift Curves at Various Flap Deflections	26
Figure 4.4	Zero Lift Drag Coefficients	27
Figure 4.5	Aircraft Area Distribution	28
Figure 4.6	Takeoff and Landing Drag Polar	29
Figure 4.7	Loiter Drag Polar	30
Figure 4.8	Dash Drag Polar	30
Figure 5.1	Inlet Pressure Recovery versus Deflection Angle	34
Figure 5.2	Sketch of Side View of Inlet with Shocks	36
Figure 5.3	Maximum Allowable D/q	37
Figure 7.1	Structural V-n Diagram	41
Figure 7.2	Shear Diagram	41
Figure 7.3	Bending Moment Diagram	42
Figure 7.4	Honeycomb Spar Construction	42
Figure 7.5	Structural Drawing of Wing, Canard, and Vertical Tails	44
Figure 7.6	Structural Drawing of Fuselage	44
Figure 7.7	Structural Drawing of Entire Aircraft	45
Figure 8.1	Cg Plot for Defensive-Air Patrol Mission	47
Figure 8.2	Cg as %MAC Plot for Defensive-Air Patrol Mission	48
Figure 8.3	Cg Plot for Point Defense Intercept Mission	48
Figure 8.4	Cg as %MAC Plot for Point Defense Intercept Mission	49
Figure 8.5	Cg Plot for Intercept/Escort Mission	49
Figure 8.6	Cg as %MAC Plot for Intercept/Escort Mission	50
Figure 9.1	Sizing X-Plot for Canard	51
Figure 9.2	Top View of Canard and Elevator	53
Figure 9.3	Top View of Wing and Flaperons	54
Figure 9.4	Side View of Vertical Tails and Rudder	54
Figure 10.1	Integrated Electronic Warfare System	58
Figure 10.2	AESA	59
Figure 10.3	ATFLIR	59
Figure 10.4	F-22 Cockpit Instrument Panel	60

Figure 10.5	ACES II	61
Figure 10.6	Cockpit Layout	62
Figure 10.7	Landing Gear Layout	63
Figure 10.8	Systems – Profile View	64
Figure 10.9	Systems – Bottom View	65
Figure 10.10	Integrated Structural and Systems Drawing	66
Figure 10.11	Fuel Storage Drawing	66
Figure 10.12	Actuator Diagram	67
Figure 11.1	Cost Estimation for Production Run	68
Figure 11.2	Production Learning Curve	69
Figure 11.3	Flyaway Cost Estimation for Production Run	70
Figure 11.4	Total Cost Breakdown	71
Figure 11.5	Average Life-Cycle Cost	72
Figure 11.6	Average Life-Cycle Cost Breakdown	73
Figure D.1	Top View	79
Figure D.2	Side View	80
Figure D.3	Front View	80
Figure D.4	Isometric View	81
Figure D.5	Isometric Systems Layout	82

List of Tables

Table 1-1	RFP Requirement	2
Table 2-1	Mission Decision Matrix	6
Table 2-2	Overall Concept Decision Matrix	6
Table 3-1	Fuel Fractions for Defensive Counter-Air Patrol Mission	16
Table 3-2	Fuel Fractions for Point Defense Intercept Mission	17
Table 3-3	Fuel Fractions for Intercept/Escort Mission	17
Table 3-4	1-g Specific Excess Power – Military Thrust	21
Table 3-5	1-g Specific Excess Power – Maximum Thrust	21
Table 3-6	5-g Specific Excess Power – Military Thrust	21
Table 3-7	Sustained Load Factor – Maximum Thrust	22
Table 3-8	Take-off and Landing Roll Distance	22
Table 4-1	Wing Geometry Parameters	23
Table 4-2	Maximum Lift Coefficients	25
Table 4-3	Zero-Lift Drag Build-up	27
Table 4-4	Thrust and Drag Analysis	28
Table 5-1	Engine Data	33
Table 6-1	Composite Comparison	39
Table 6-2	Thermoplastics Properties	40
Table 6-3	Aluminum Alloy Comparison	40
Table 7-1	Bulkhead Functions	43
Table 8-1	Scaling Factors and Multipliers for Empty Weight Calculations	45
Table 8-2	Weights for Each Component	46
Table 8-3	Fuel Weight Predictions	47
Table 9-1	Canard Geometry Parameters	52
Table 9-2	Vertical Tail Geometry Parameters	52
Table 9-3	Flight Conditions for DATCOM	55
Table 9-4	Stability and Control Derivatives	55
Table 9-5	Static Margin at Crucial Points in Flight Envelope	56
Table 9-6	Level 1 Flying Qualities (Class A and C)	56
Table 9-7	Level 1 Flying Qualities (Class B)	57
Table 11-1	Operations and Maintenance Cost	70
Table 11-2	Total Initial Cost	71

Nomenclature

$\%T_{Loss}$	=	Percentage of thrust lost due to inlet and duct pressure recovery
$(P/P_0)_{actual}$	=	Actual pressure ratio
$(P/P_0)_{ref}$	=	Reference pressure ratio
A^*	=	Cross sectional area of duct where $M=1$
A_{Duct}	=	Cross sectional area of duct at front face of engine
A_{Inlet}	=	Cross sectional area of inlet just downstream of normal shock
A_{max}	=	Maximum area
C_{D0}	=	Drag coefficient
C_{D0wave}	=	Wave drag coefficient
C_{Lmax}	=	Maximum lift coefficient
$C_{Lmaxturn}$	=	Maximum lift coefficient for turn
C_{ram}	=	Ram recovery factor
D	=	Total drag
I_{xx}	=	Mass moment of inertia
L/D_{max}	=	Maximum lift to drag ratio
M	=	Mach number
M_∞	=	Freestream Mach number
MMC	=	Metal Matrix Composite
P_s	=	Specific Excess Power
q	=	Dynamic pressure
R_x	=	Radius of gyration
T/W	=	Thrust to weight ratio
$T_{Installed}$	=	Installed thrust
T_{Lost}	=	Thrust lost due to auxiliary power generation requirements
$TOGW$	=	Take-off Ground Weight
$TSFC$	=	Thrust specific fuel consumption
$T_{uninstalled}$	=	Uninstalled thrust
$T_{Uninstalled}$	=	Uninstalled thrust
W/S	=	Wing loading
γ	=	Ratio of specific heats
δ	=	Flow deflection angle
σ	=	Shock wave angle

1. Introduction

1.1 Background

Since the turn of the century there has been a new threat to the United States and the world. This new threat has come in the form of terrorism and has changed the way the United States and the world looks at national defense. No longer is our nation focused on a massive land attack by another world super power, but on two hijacked airliners crashing into the World Trade Center buildings killing over 2,000 people. This new breed of terrorism also brings to the table the threat of nuclear, biological, and chemical weapons that could be deployed from a single aircraft. US researchers predict that one bomb of anthrax dropped on a major city would kill over 123,000 people even if every victim received treatment.² Biological and chemical weapons pose the greatest threat due to their low cost and high kill ratio. The low cost of these weapons makes them attainable by most of the terrorist cells in the world, and thus a threat to the nations hated by the terrorist cells, mostly the United States. This threat of solo “kamikaze” missions requires a new kind of affordable defense platform to protect the lives of American people. The 2005-2006 AIAA Request for Proposal calls for a new affordable homeland defense interceptor.¹ This homeland defense interceptor will be required to protect this nation from any kind of airborne threat, whether nuclear, biological or chemical, brought by terrorists. The current defense interceptors that the United States has in their inventory include the F-14, F-15, F-18, F-16. Most of these aircraft are at the end of their projected service life or will by the year 2020. As technology changes, these aircraft will become obsolete and incapable of properly defending our nation. The new current fighters that the Air Force is producing such as the F-22 and F-35 are designed for operation against the world’s state of the art aircraft and are very expensive. Due to the high cost of these aircraft they would not be ideal in providing homeland defense for the approximated 12,383 miles of United States coastline not including the borders of Canada or Mexico.³ Therefore there is a demand for an affordable homeland defense interceptor that could be mass produced to defend the borders of our country while at the same time not leaving a gigantic hole in the budget of the Department of Defense. This demand for a fast, maneuverable, and inexpensive fighter aircraft led to the design proposal of the *Hedgehog*, designed by Manafour Aerospace, for the 2005-06 AIAA competition. This aircraft design proved the most efficient and cost effective out of the ideas considered. The *Hedgehog* meets all the RFP design requirements and would be the best choice in defending our great nation against the terrorist threat of the future.

1.2 AIAA RFP Requirements

The 2005-2006 AIAA RFP required that the homeland defense interceptor be small, fast, and affordable. Table 1 shows the RFP requirements for the AIAA homeland defense interceptor.

Table 1-1. RFP Requirements.¹

RFP Requirements	RFP Referenced Section
Design a homeland defense interceptor including an engine data package	2.1
Design should be cost effective and perform the two given design missions	2.2
An intercept escort mission will be evaluated	2.3
All systems must be designed for one pilot with equipment weighing a total of 250 lbs. Or pilot can control the aircraft remotely if the operational concept accomplishes positive threat identification as well as addressing all communication bandwidth issues related to the unmanned approach.	3.1
Design must allow easy access to and removal of primary elements of all major systems, and minimize requirements for unique support equipment.	3.2
Design limit load factors are +7 and -3 vertical g's in the clean configuration with 50% internal fuel.	3.3
Structure should withstand a dynamic pressure of 2,133 psf (M = 1.2 at sea level)	3.3
A factor of safety of 1.5 shall be used on all design ultimate loads	3.3
Primary structures should be designed for durability and damage tolerance	3.3
Design service life is 12,000 hours	3.3
Primary design fuel is standard JP-8 or Jet-A (6.7 lb/gal)	3.4
All fuel tanks will be self sealing	3.4
External fuel tanks if carried for design missions, must be retained for the entire mission	3.4
Unaugmented subsonic longitudinal static margin (S.M.) shall be no greater than 10% and no less than 10%	3.5
A digital flight control system is mandatory for designs that are statically unstable in the longitudinal axis	3.5
The aircraft must operate in all weather from existing NATO runways (8,000 ft), shelters, and maintenance facilities and from austere bases without support equipment	3.6
The aircraft must be capable of all-weather interception and weapon delivery	3.6
Flyaway cost per aircraft for a 1000 aircraft buy will not exceed \$15 million in 2005 U.S. dollars	3.7
All practical measures will be taken to minimize total life cycle costs	3.7

Appendix A shows the three missions the aircraft has to perform along with the requirements in those missions. Appendix B exhibits the minimum performance requirements and constraints, the maximum weapons carriage

capability, and the engine cycle requirements. Appendix C shows the government furnished equipment that will be required on the aircraft along with its weight, volume and cost.

2. Design Concepts

During the brainstorming process of the design project many concept ideas were discussed. The first item to be considered was whether the aircraft should be manned or unmanned. The unmanned concept was not chosen due to the higher flyaway cost and time lag issues. The major factor in an interceptor is a swift and decisive strike against the incoming plane. The plane needs to be able to quickly identify and respond to any maneuvers made by the opposing pilot.

Ideas were discussed to best meet the RFP design requirement and complete each of the missions. Out of these ideas three design concepts were picked for further research. These three concepts were thought to be the best designs to carry out the missions and meet the RFP requirements. These three concepts included a delta wing design, a variable swept wing design, and an arrow wing canard configuration.

The first concept design was the delta wing design which is shown in Figure 2.1.

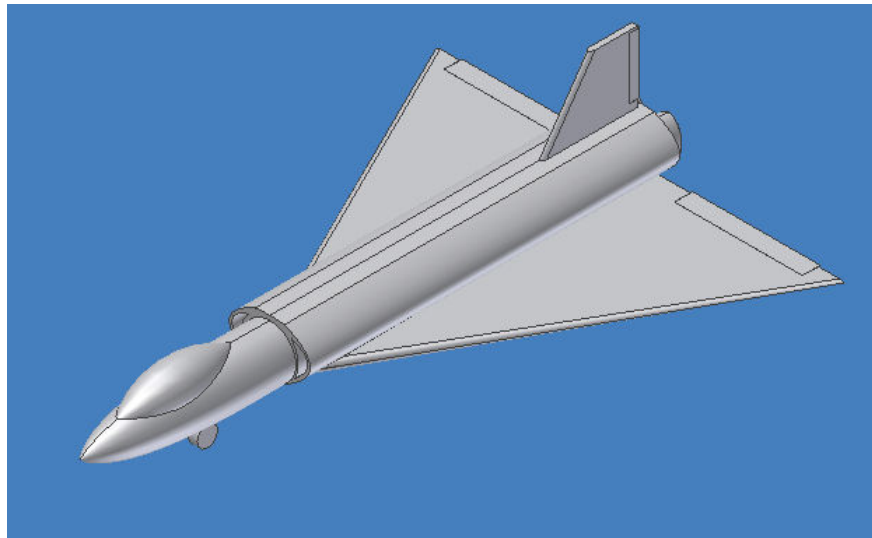


Figure 2.1. Initial concept drawing of the delta wing design.

The delta wing configuration was a credible design because of its good performance at high Mach numbers. One of the major mission drivers in the RFP is the dash at Mach 2.2. Due to this requirement a need for a design that performed well at high speeds was necessary. With the delta wing design this high speed dash requirement would be attainable. Although the delta wing design performed very well at high speeds, its performance in the low speed range fell short. It was found that the pure delta wing design did not have the low speed performance necessary to

attain the four hour loiter mission requirement. Another advantage to the delta wing design is that its simplistic nature makes it structurally sound and fairly inexpensive to manufacture. However, due to the fact that the pure delta wing concept had poor low speed performance, which would not be able to meet the RFP's loiter requirement, it was dismissed as a final design concept.

The next design concept discussed was a variable swept wing design seen in Figure 2.2.

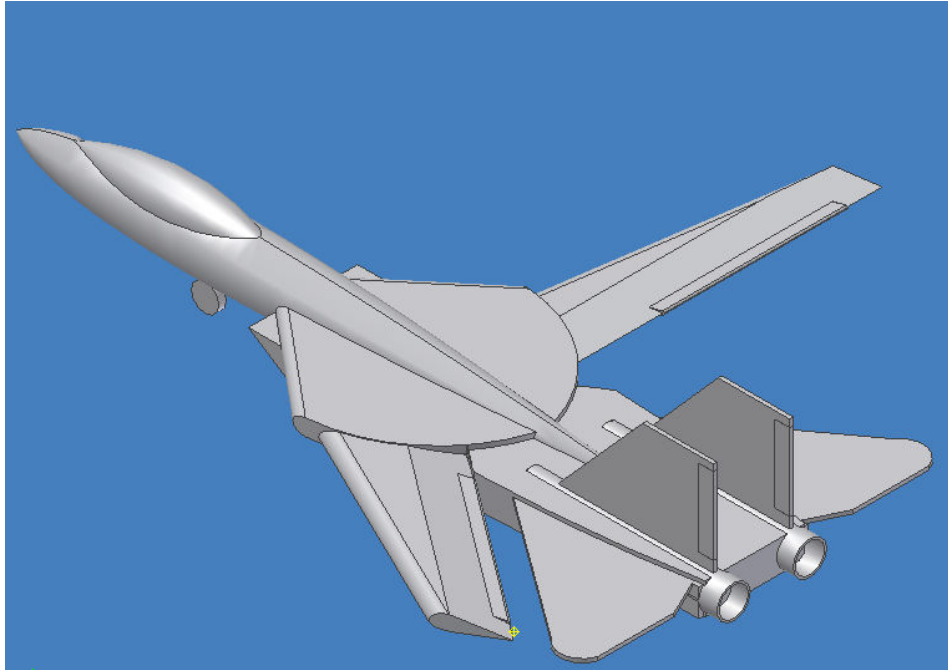


Figure 2.2. Initial concept drawing of the variable wing design.

It was thought that this design would give us the ability to meet the high speed dash requirement as well as the low speed loiter requirement of the RFP. The ability to extend the wings during flight to increase the span would allow the variable sweep design to achieve a much better low speed flight performance. After researching this design further it was found that the extended wing configuration of the aircraft did give a substantial increase in performance during low speed flight. However, the disadvantage to the variable sweep design is that process of sweeping the wings forward and back during flight would make the mechanics of the aircraft very complicated. The mechanical devices to perform such a task would be complicated, as well as the control of the aircraft due to the shift in the center of gravity and aerodynamic chord. A larger concern for the variable sweep design was that of the cost. Through research it was discovered that the process to create the parts for a variable sweep aircraft, such as the

USN F-14 Tomcat, was very expensive. This rise in price was due to the complicated nature of manufacturing process required to make the sweeping devices for the wing. Since the RFP required that the aircraft have a flyaway cost of \$15 million US dollars, it was decided that this design was would become too expensive to manufacture and produce, and was eventually ruled out as a final design concept.

The last design concept considered was the arrow wing canard design seen in Figure 2.3.

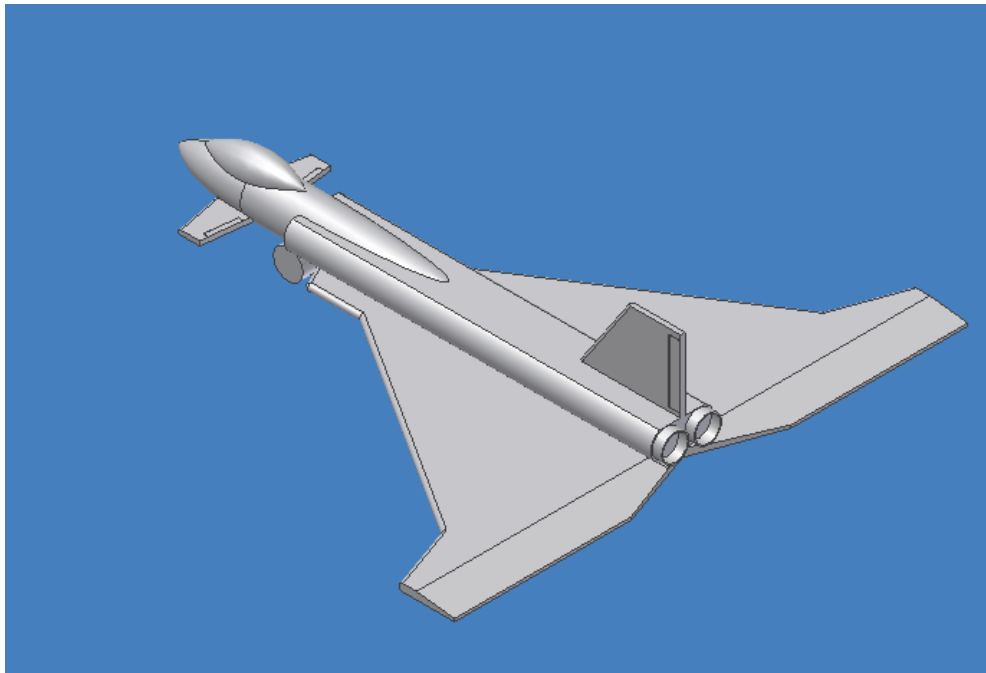


Figure 2.3. Initial concept drawing of the arrow wing with canard design.

This design incorporated a cranked wing design to increase the wing span and give it better performance at low speeds. The semi delta wing shape would give the aircraft the performance need in the high speed flight regime while the cranked wing would allow it to perform well at low speed flight regimes. The canards in this configuration would add to the stability and control of the aircraft as well as possibly double for a second lifting surface. This design concept was also very structurally sound and nowhere near as complex as the swept wing concept. Its fairly simple design would also help keep the cost of the aircraft down. A comparison matrix for the three aircraft was drawn up using criteria thought import for the final design, which can be seen in Tables 2-1 and 2-2. Each criterion was given a weighted value and then the three concept aircraft were rated for each criterion. In the end the arrow wing canard configuration was the design concept with the best results and chosen for our final design concept.

Table 2-1. Mission decision matrix.

	Loiter	Supersonic	Turn Rate	Minimum Cruise Speed	Total
Percentage	30	30	30	10	100
Delta Wing	2	9	5	4	5.2
Arrow Wing	5	9	7	8	7.1
Variable Sweep	8	8	4	7	6.7

Table 2-2. Overall decision matrix.

	Structures	Stability	Aero	Mission	Weights	Systems	Fuel Storage	Costs	Total
Importance	15	5	20	20	15	5	5	15	100
Delta Wing	9	5	6	5.2	4	8	8	9	65.9
Arrow Wing	7	6	8	7.1	9	8	8	8	77.2
Variable Sweep	5	8	9	6.7	7	4	6	4	64.4

As more research was done on the arrow wing canard concept the configuration of the concept underwent drastic changes. As seen in Figures 2.4 and 2.5, the concept went through changes in wing shape, canard shape, fuselage shape, and intake shape as well as many other changes.

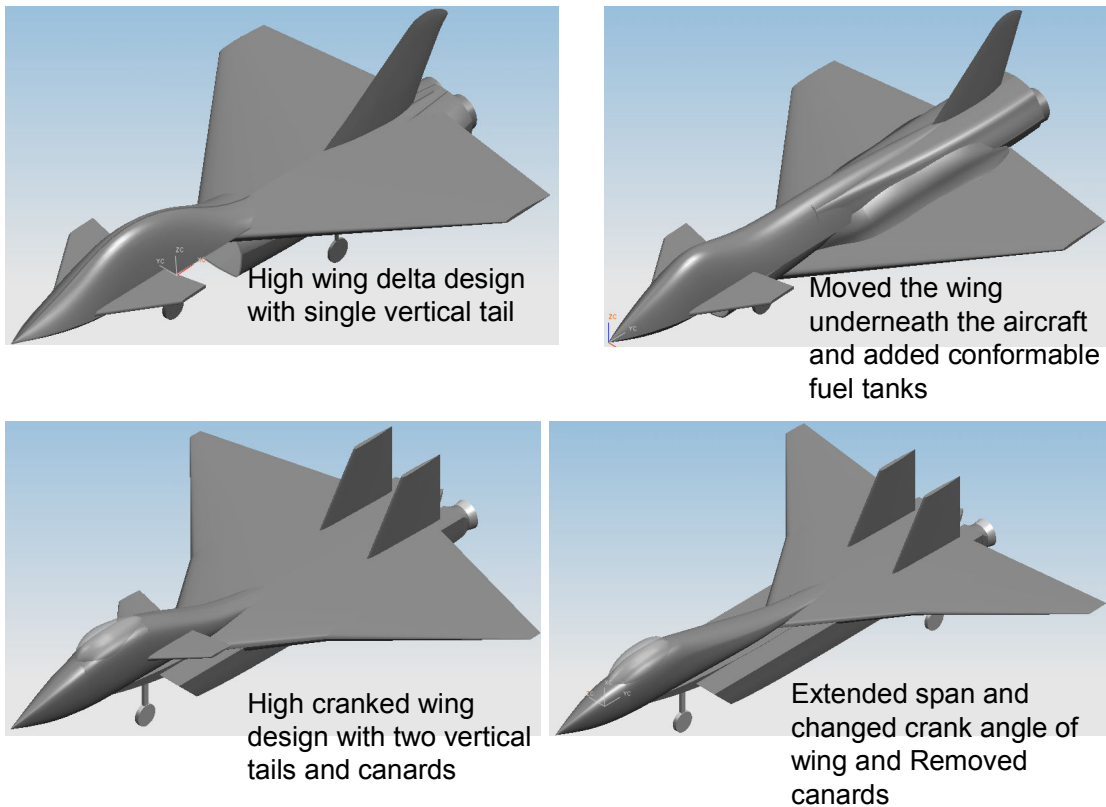


Figure 2.4. Initial changes made to the arrow wing and canard.

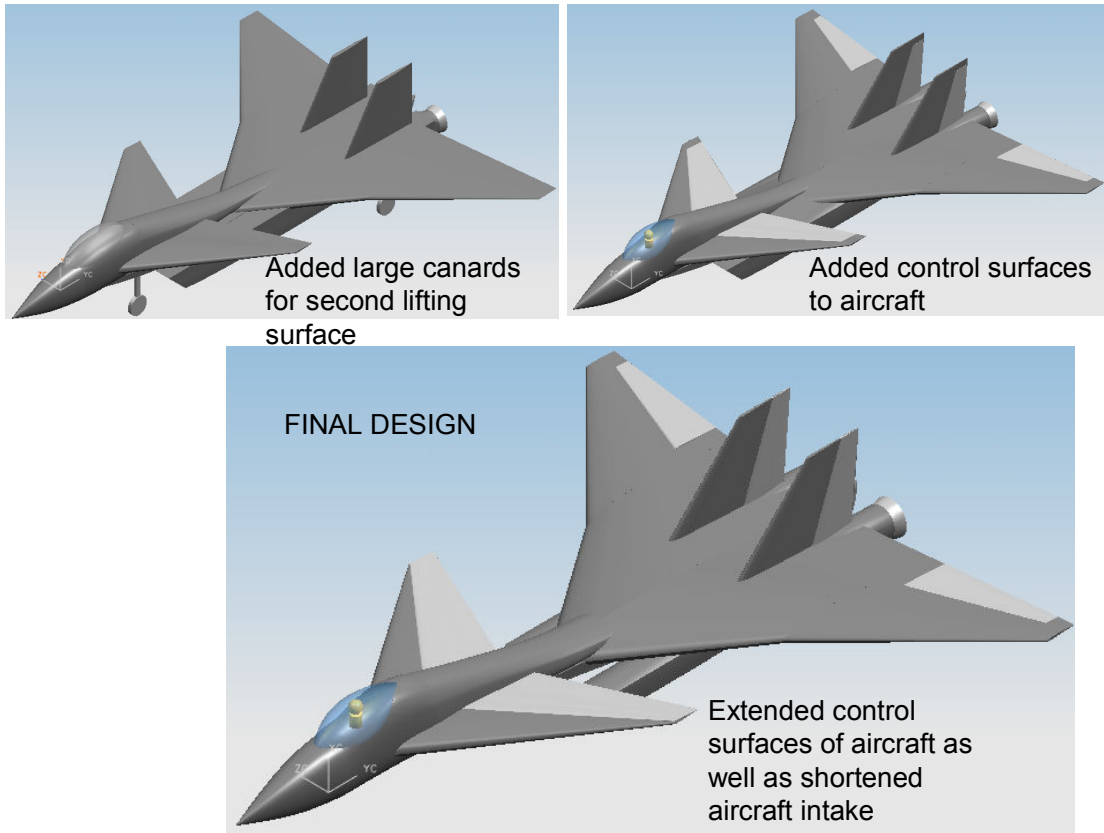
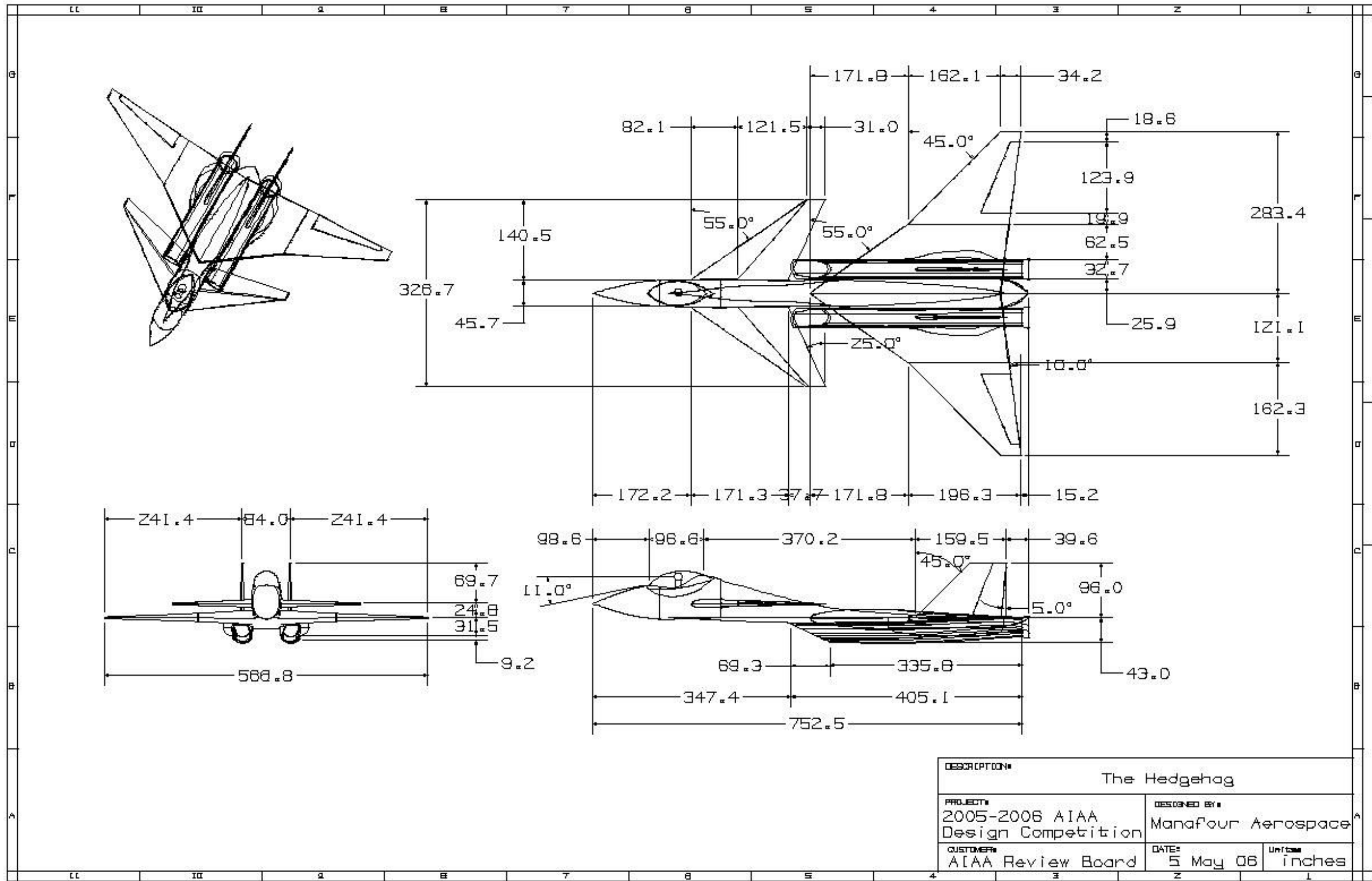


Figure 2.5. Final design progression of The *Hedgehog*.

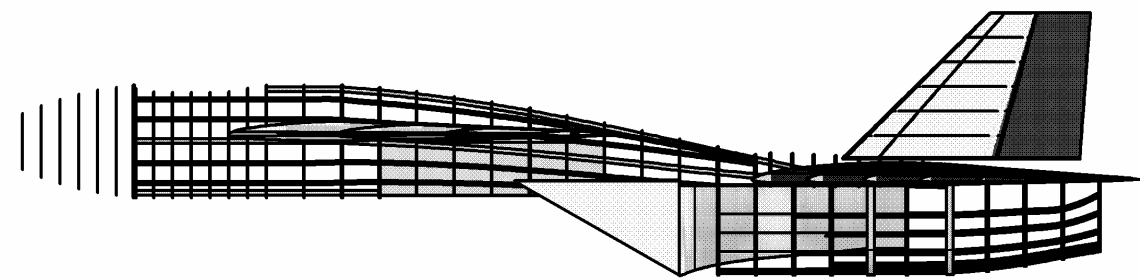
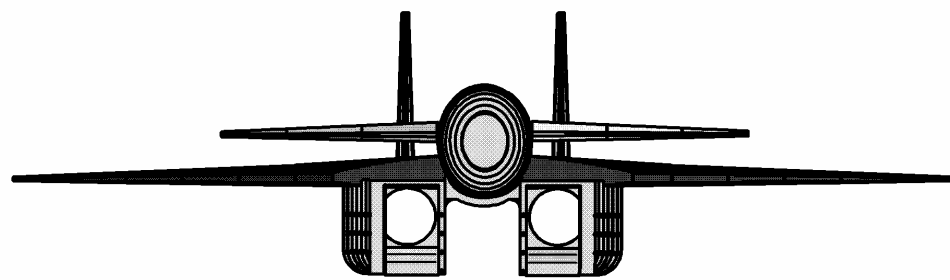
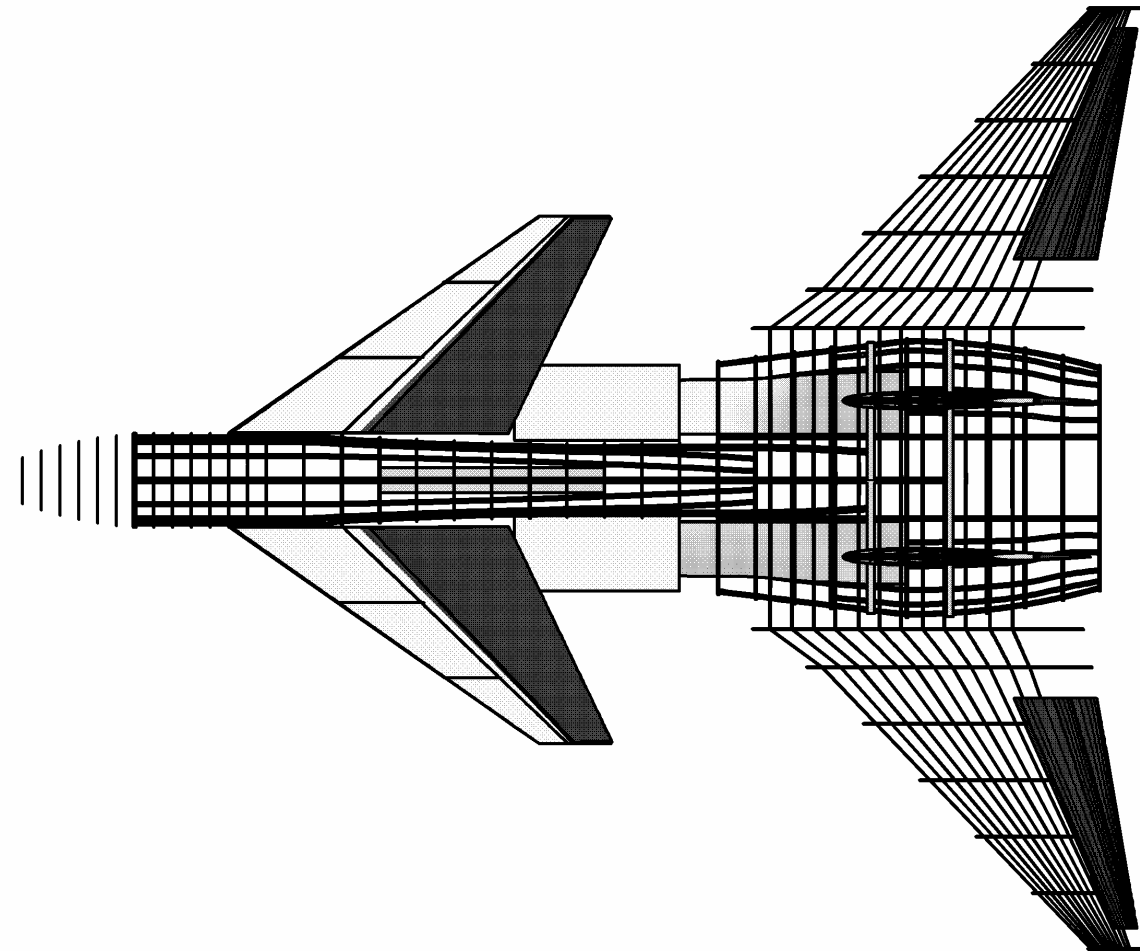
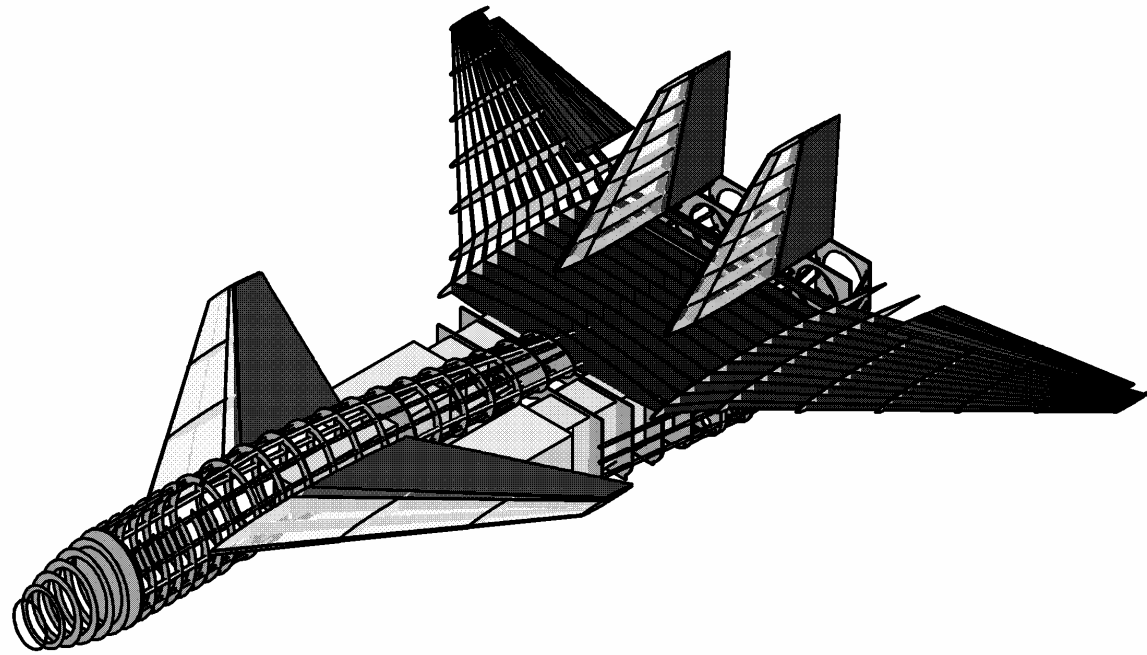
These changes were made to give the aircraft the best performance capabilities possible while meeting all the mission requirements and all the RFP requirements. These changes made way for the final design of The *Hedgehog*, which meets all RFP requirements and mission requirements for the 2005-2006 AIAA homeland defense interceptor.

More detailed, larger drawing can be seen below. Figure 2.6 is a three-view drawing of the *Hedgehog* with dimensions given in inches. Figures 2.7 through 2.9 are different views.

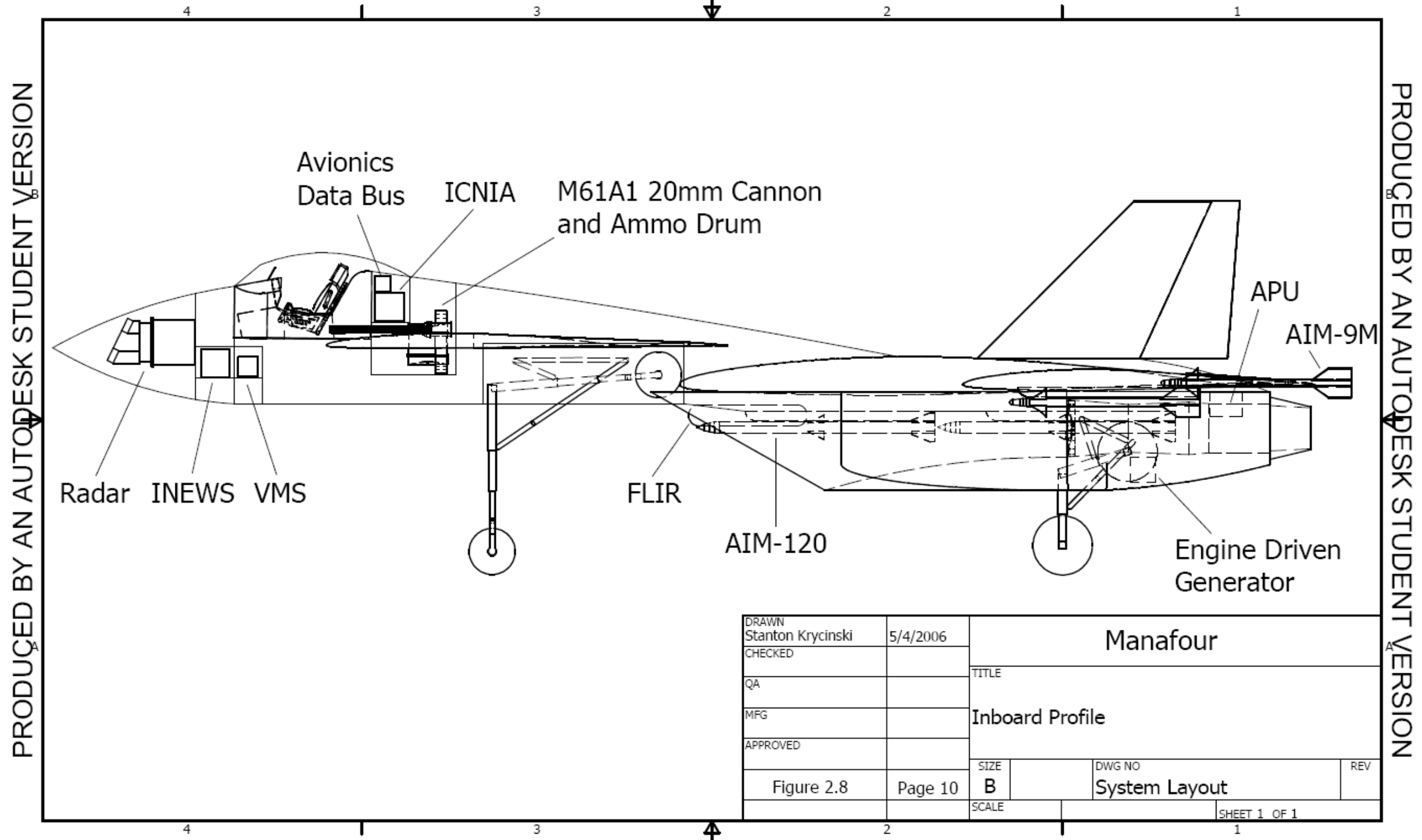


PRODUCED BY AN AUTODESK STUDENT VERSION

4	3	2	1
DRAWN Chris Bright	5/4/2006	Manafour Aerospace	
CHECKED		TITLE	
QA		Hedgehog Structural Drawing	
MFG Jena Rosebrock	5/4/2006	SIZE	DWG NO
APPROVED Jena Rosebrock	5/4/2006	B	structures_layout
Figure 2.7		SCALE	REV
Page 9			SHEET 1 OF 1



PRODUCED BY AN AUTODESK STUDENT VERSION



DRAWN Stanton Krycinski	5/4/2006	Manafour	
CHECKED		TITLE	
QA		Inboard Profile	
MFG			
APPROVED			
Figure 2.8	Page 10	SIZE B	DWG NO System Layout
		SCALE	REV
		SHEET 1 OF 1	

PRODUCED BY AN AUTODESK STUDENT VERSION

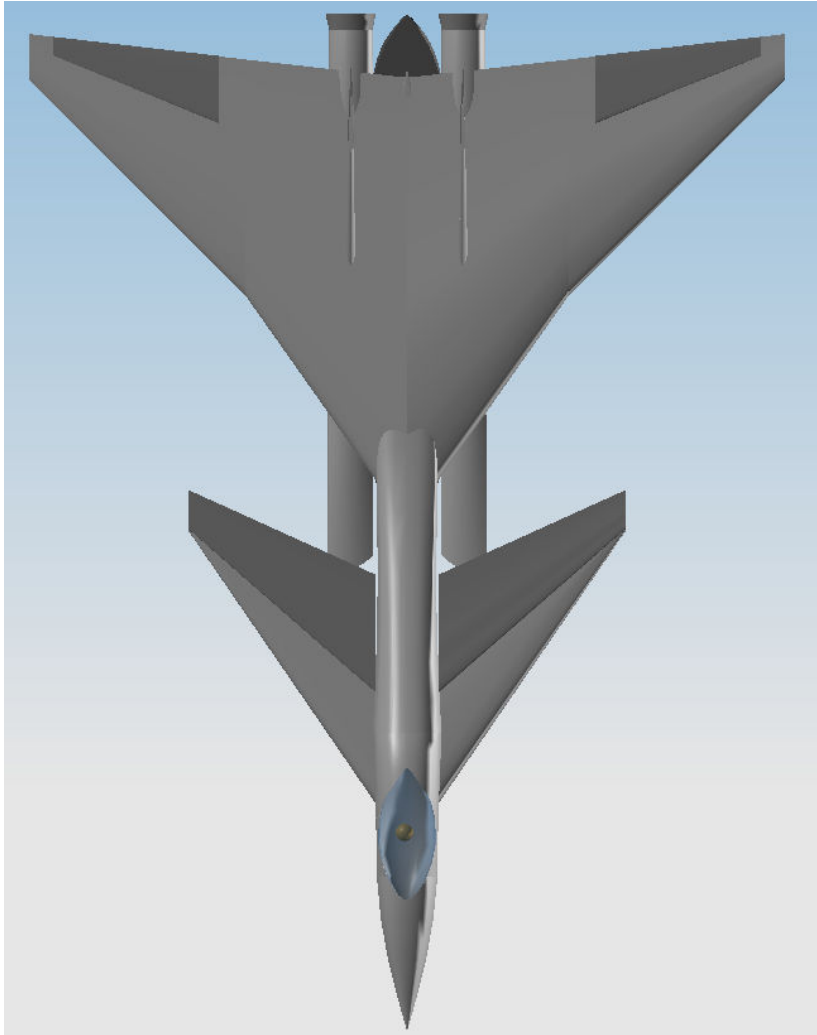


Figure 2.9. Top view of *Hedgehog*.

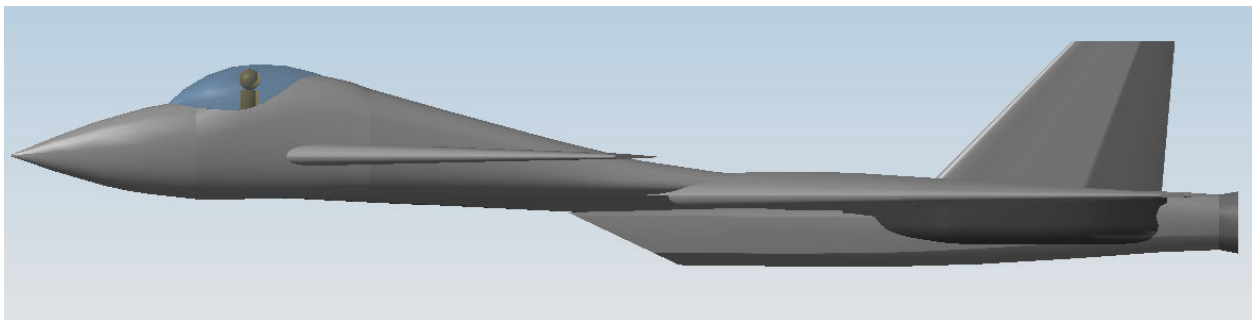


Figure 2.10. Side view of *Hegehog*.

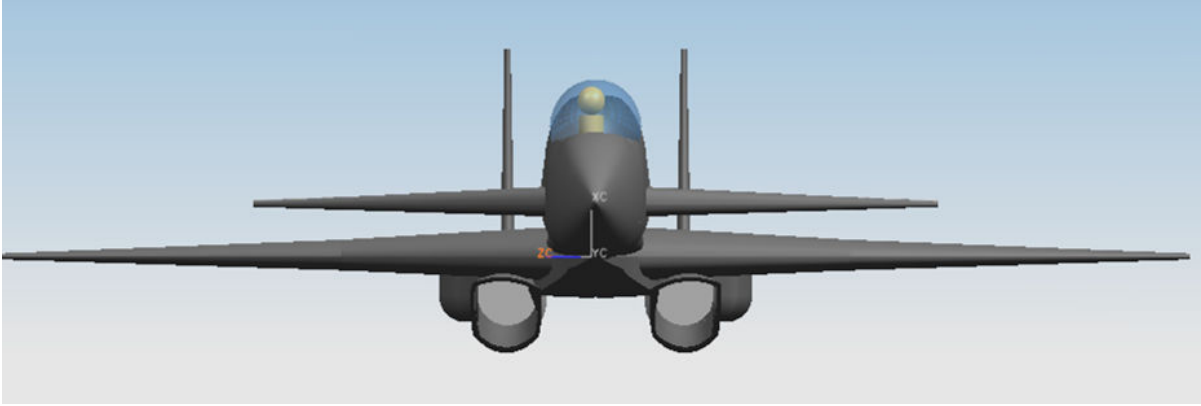


Figure 2.11. Front view of *Hedgehog*.

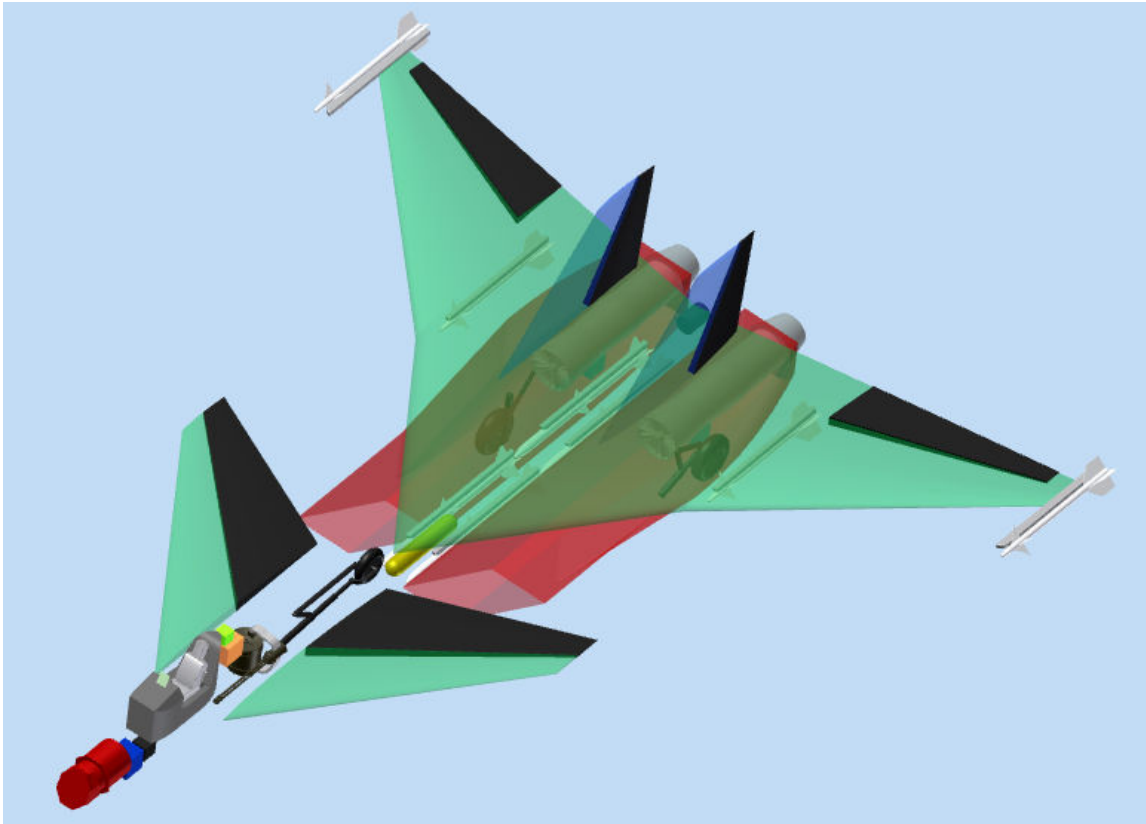


Figure 2.12. Isometric systems layout.

3. Mission and Performance Analysis

3.1 Mission

3.1.1 The Defensive Counter-Air Patrol Mission

There were three missions defined by the RFP which are used to design our plane. The most important in terms of design constraints is the Defensive Counter-Air Patrol Mission shown in Figure 3.1, and is defined further in Attachment 1 of Appendix A.

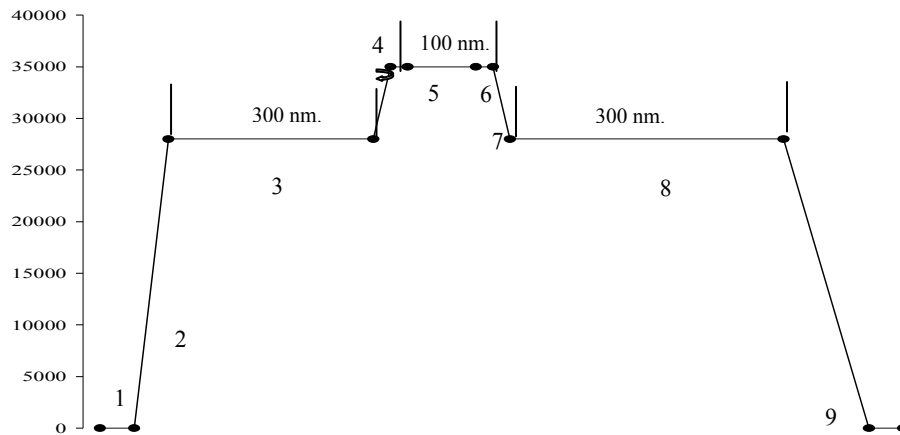


Figure 3.1. Defensive Counter-Air Patrol Mission Profile.

This mission is the main design mission in terms of determining the amount of fuel that is going to be needed because it requires a four hour loiter phase. The plane in this mission is to warm-up and take-off, and then it has to climb to the optimum cruise altitude, which for our initial calculations was determined to be approximately 28,000 ft. Then, it has to cruise out 300 nm at an optimum speed. Once the plane reaches its destination, it is to loiter at the optimum loiter speed at an altitude of 35,000 ft. At this point in the mission, a combat allowance is added. Included in the combat allowance is one sustained 360° turn at Mach 1.2 and one sustained 360° turn at Mach 0.9. During combat, all missiles are fired and the gun ammunition is retained. The plane then returns to optimum speed and altitude and cruises back 400 nm before descending to sea level and landing. There is also a requirement of retaining fuel reserve for 30 minutes at sea level speed for maximum endurance.

3.1.2 The Point Defense Intercept Mission

This is the second mission defined in the RFP and is most like a typical interceptor mission. The mission profile is shown in Figure 3.2, and is defined further in Attachment 2 of Appendix A.

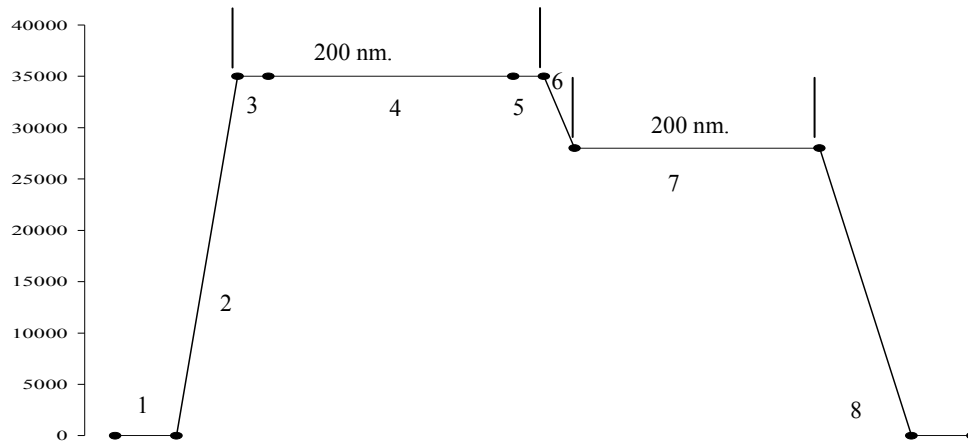


Figure 3.2. Point Defense Intercept Mission Profile.

This mission requires far less fuel than the other two which makes the design constraints far easier. Like the last mission, there is fuel required for warm-up and take-off. The plane then climbs to an altitude of 35,000 ft. and accelerates to maximum speed. Upon reaching altitude, it dashes out 200 nm at Mach 2.2. Once it reaches the destination, the same combat maneuvers as the previous mission are performed, and missiles are fired while gun ammunition is retained. The plane then climbs to the optimum altitude and cruises back at an optimum cruise speed 200 nm. Finally, the plane lands at sea level while retaining enough fuel for 30 minutes at sea level at the speed for maximum endurance.

3.1.3 The Intercept/Escort Mission

This is the third and final mission defined by the RFP. The minimum practical airspeed was determined to be Mach 0.5 for the escort mission. There is once again a heavy constraint of fuel, but it is not comparable to the first mission. This mission requires the same warm-up and take-off as the previous missions. Upon take-off, the plane then climbs to 35,000 ft and accelerates to its maximum speed of Mach 2.2. It then dashes out an undefined distance to meet up with another plane. It escorts this plane at a minimum practical airspeed for 300 nm while retaining all weapons. Upon completion of the escort portion of the mission, the plane returns to the best cruise speed and altitude and returns home. At this point, the aircraft lands with 30 minutes of reserve fuel at sea level.

The mission profile is shown in Figure 3.3, and is defined further in Attachment 3 of Appendix A.

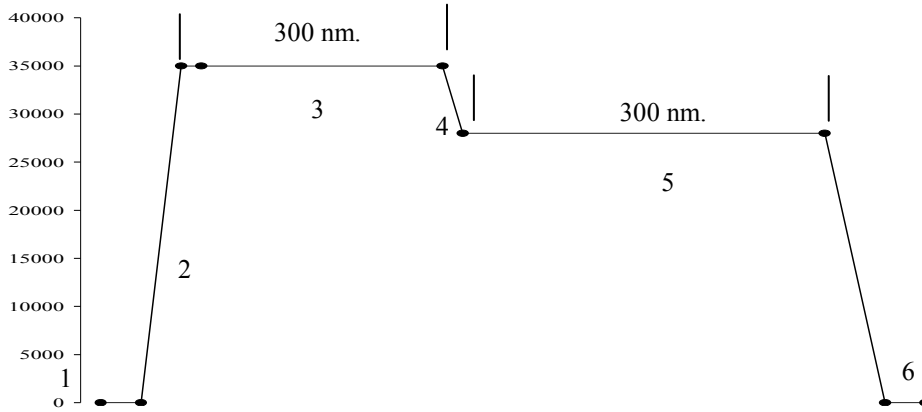


Figure 3.3. Intercept/Escort Mission Profile.

3.2 Other Design Considerations

In addition to the requirements set forth in the missions, the RFP also provides other minimum performance constraints. The most difficult of which is an $18^\circ/\text{sec}$ maximum instantaneous turn rate. This is a high value for the instantaneous turn rate based on other constraints in the RFP. To determine how this turn rate could be accomplished, possible plots of the instantaneous turn rate vs. Mach number were made for constant load factors and a constant value of $C_{L_{maxturn}} = 1.454$. The point at which the lines intersect is the maximum instantaneous turn rate for the parameters. This plot is shown in Figure 3.4 for the aircraft.

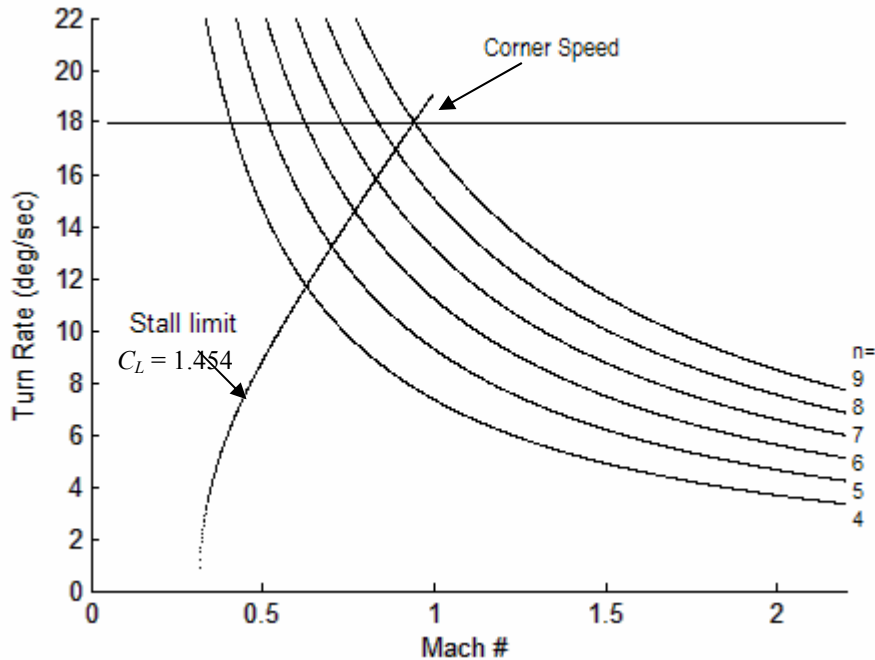


Figure 3.4. Instantaneous Turn Rate vs. Mach Number at 35,000 ft

In the above figure structural limit for the load factor has had to be increased from a maximum of $n = 7$ to $n = 9$. This allows for a lower value of $C_{L_{maximum}}$ and as modern technology has increased, a load factor of 9 is possible. Doing this gives a corner speed of $M = 0.94$. Though the load factor has been increased and will raise costs slightly, it allows for a simpler lifting system which keeps the cost low.

3.3 Initial Sizing

To begin the design process, initial weight had to be determined. To do this, fuel fractions for the each segment of the missions were determined based on historical data for similar configurations. This was done using methods from Raymer.⁴ Then as more calculations were made values for AR , C_{D0} , S , and T , these values were changed in the original program and further iterations were performed to determine the fuel weight of the configuration as it was. In the following tables, the fuel fractions based on the current fuel consumption for the AIAA provided engine deck and geometry of each configuration can be seen, as well as the initial take-off gross weight values.

Table 3-1 below shows the fuel fraction of each mission segment as well as the total fuel fraction and Take-Off Gross Weight for the Point Defense Intercept Mission. This later became the design mission for the configuration as it requires the most fuel, as well as a Mach 2.2 dash and a loiter of 4 hours. Notice that loiter segment of the mission is the one in which the most fuel is used.

Table 3-1. Fuel Fractions for the Defensive Counter-Air Patrol Mission

Defensive Counter-Air Patrol Mission		
Mission Segment		Fuel Fraction
Take-Off	1	0.97000
Climb	2	0.98500
Cruise	3	0.95617
Loiter	4	0.78180
Dash	5	0.99108
Combat	6	0.97923
Climb/Accelerate	7	0.98500
Cruise	8	0.94199
Descent/Landing	9	0.99500
Total		0.63994
TOGW = 52649 lb		

Table 3-2 shows the fuel fractions for each of the three configurations for the point defense intercept mission. This is the most typical mission for a defense interceptor. Due to the short range of the mission, it proved to have a much lower *TOGW* than either of the other two missions.

Table 3-2. Fuel Fractions for the Point Defense Intercept Mission

Point Defense Intercept Mission		
Mission Segment		Fuel Fraction
Take-Off	1	0.97000
Climb	2	0.98500
Accelerate	3	0.92720
Dash	4	0.98224
Combat	5	0.97923
Climb/Accelerate	6	0.98500
Cruise	7	0.97056
Descent/Landing	8	0.99500
Total		0.81052
TOGW = 21350 lb		

Table 5-3 shows the fuel fractions for each of the three configurations for the intercept/escort mission. In this mission, the slow flight speed during the escort segment is what consumes a majority of the fuel required.

Table 3-3. Fuel Fractions for the Intercept/Escort Mission

Intercept/Escort Mission		
Mission Segment		Fuel Fraction
Take-Off	1	0.97000
Climb	2	0.98500
Escort	3	0.82107
Climb/Accelerate	4	0.98500
Cruise	5	0.95482
Descent/Landing	6	0.99500
Total		0.73412
TOGW = 31230 lb		

For each of the weight fractions, historical values were used to determine an estimate of the gross take-off weight.⁴ This was then used to find the weight of the fuel for the mission as well as the empty weight of the plane. These values were then compared, and if the initial guess wasn't close enough to the calculated value of the weight, another run was iterated. This process was run until the weight converged to the value for *TOGW*.

Upon determining the *TOGW* of the configuration, it was determined that the *TOGW* for the defense counter-air patrol mission would be used to determine the design space for the aircraft. Using equations from Raymer⁴, the curves for supersonic cruise, subsonic cruise, take-off, landing, maximum loiter, and the 18°/sec turn were plotted on a *T/W* versus *W/S* graph to create the design space. However, for the configuration being considered, certain parameters such as take-off at sea level didn't show up in the design space. Below in Figure 5.5, this design space can be seen for this design.

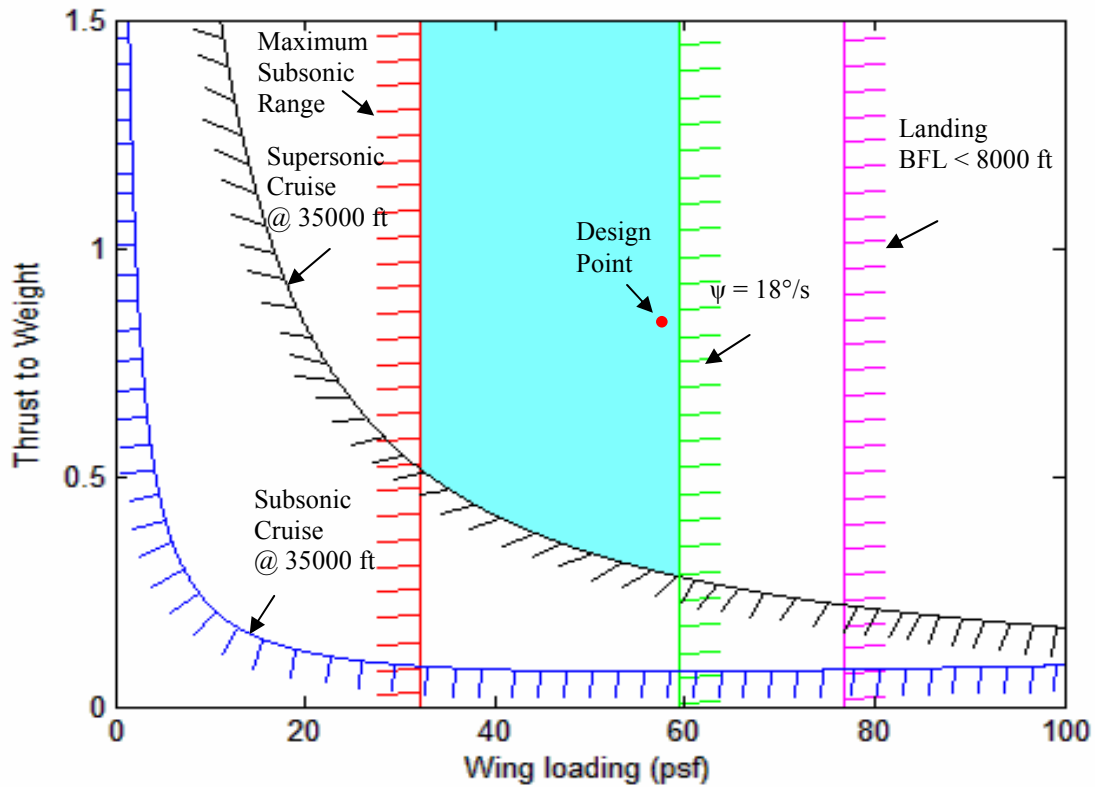


Figure 3.5. Design Space.

The final design has a wing loading of 58.63 psf and T/W of about 0.84 as seen above, which allows us nearly the highest possible wing loading for the configuration. This value is however slightly lower than the typical fighter (70- 80 psf), but with the constraint on the instantaneous turn it was as high as could be achieved.

3.4 Performance

3.4.1 Maximum Thrust Maneuvering Performance

The RFP calls for three diagrams, each showing maximum thrust maneuvering performance, at altitudes of 10000 ft, 30000 ft, and 50000 ft. as seen below in Figures 5.6, 5.7 and 5.8 respectively Using Raymer's model with the data provided in the engine deck, the figures were used in checking mission requirements, as well as other point performance requirements.⁴

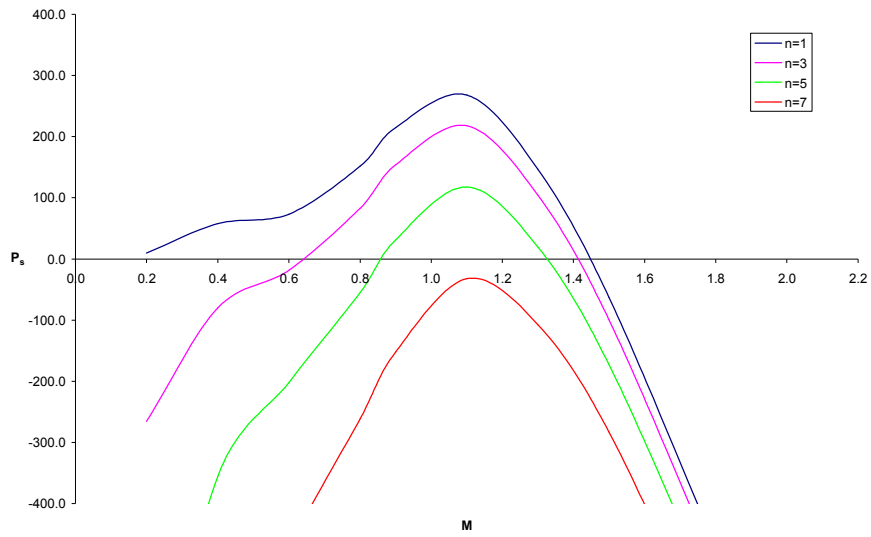


Figure 3.6. Maximum Thrust Maneuvering Performance at 10000 ft.

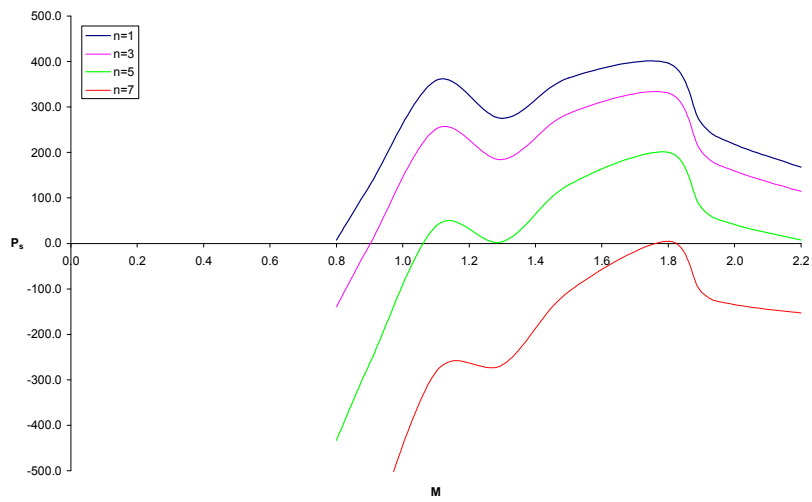


Figure 3.7. Maximum Thrust Maneuvering Performance at 30000 ft.

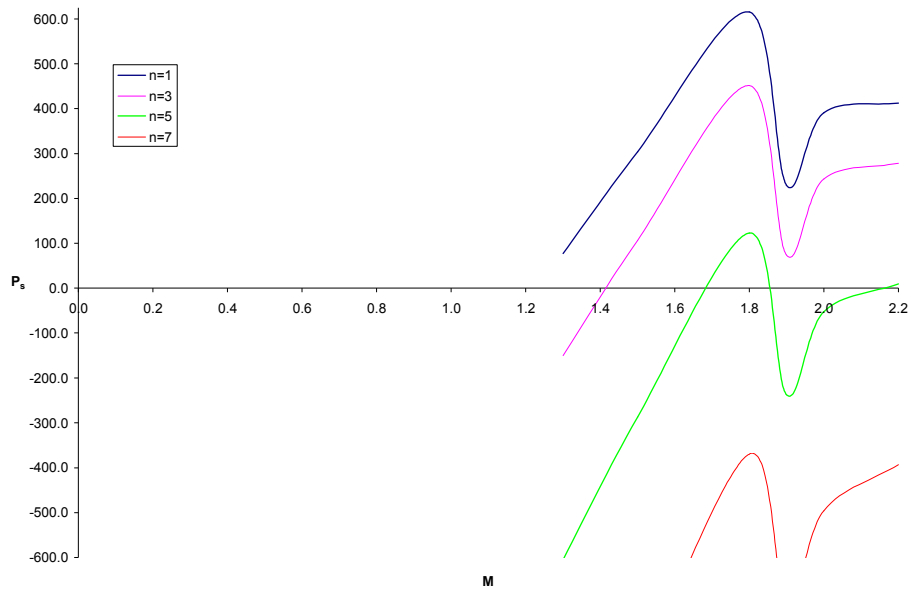


Figure 3.8. Maximum Thrust Maneuvering Performance at 50000 ft

As can be seen above, at maximum thrust, the limit would be $n = 9$, as for two of the three altitudes, there is enough power to maintain the maneuver with a load factor of 9 with the exception of the 50,000 ft case, however this is not a significant enough case to raise the load factor further. Another noticeable feature of the plots is the sudden crests and peaks. This is a common effect when using afterburners as they essentially create their own specific power curves within those for lesser load factors. These lower values for the load factor will not however impair the capability of the airplane to reach a load factor of $n = 9$ for the $18^\circ/\text{second}$ instantaneous turn, as that will not be performed with maximum thrust, both relieving stress in the structure as well as the performance.

3.4.2 Point Performance Requirements

Figure 3.9 below shows a plot of the 1-g Maximum Thrust Specific Excess Power Envelope. As shown the requirement of $M = 2.2$ at 35,000 ft is met both structurally and in terms of available power with this configuration. It should be noted however that the curve levels off near 50,000 ft. due to a lack of data provided in the engine deck.

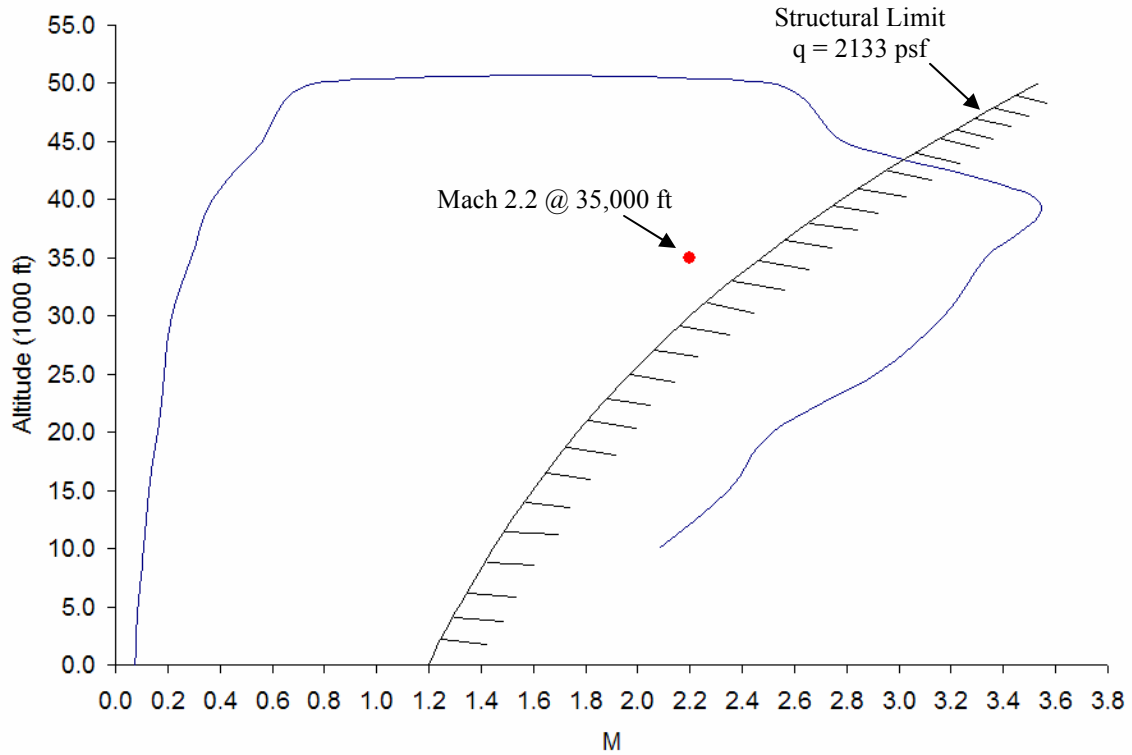


Figure 3.9 1-g Maximum Thrust Specific Excess Power Envelope

Other minimum requirements as specified in the RFP can be found in Appendix B. These requirements were met and in all cases exceeded as shown in Tables 3-4 through 3-7 below.

Table 3-4. 1-g Specific Excess Power - Military Thrust

Mach	Altitude (ft)	Ps Required (ft/s)	Ps Acquired (ft/s)
0.9	0	200.00	535.31
0.9	15,000	50.00	231.15

Table 3-5. 1-g Specific Excess Power - Maximum Thrust

Mach	Altitude (ft)	Ps Required (ft/s)	Ps Acquired (ft/s)
0.9	0	700.00	813.91
0.9	15,000	400.00	614.54

Table 3-6. 5-g Specific Excess Power - Maximum Thrust

Mach	Altitude (ft)	Ps Required (ft/s)	Ps Acquired (ft/s)
0.9	0	300.00	707.84
0.9	15,000	50.00	436.65

Table 3-7. Sustained Load Factor - Maximum Thrust

Mach	Altitude (ft)	Load Factor Required	Load Factor Acquired
0.9	15,000	5.0	4.93

3.4.3 Takeoff and Landing

The RFP specified for take-off and both take-off and landings for Standard conditions and Icy conditions. In addition calculations must be made at both sea-level and 4,000 ft. For all conditions we are working with an 8,000 ft balanced field length. ⁴ The values obtained using Raymer’s methods can be seen below in Table 3-4.

Table 3-8. Take-off and Landing Roll distance.

Conditions	Take-Off (ft)		Landing (ft)	
	Sea Level	4,000 ft MSL	Sea Level	4,000 ft MSL
Standard	828.01	932.30	1193.89	1344.26
Icy	841.15	947.10	1212.83	1365.60

It is obvious in the above table that the field length of 8,000 ft will not be of concern with this configuration.

4. Aerodynamics

4.1 Wing Geometry

Results from the mission analysis indicate that a reference area of 915 ft² is needed to successfully meet the RFP requirements. This reference area is split between the wing and lifting canard with the wing producing 76.5% of the lift. The cranked wing design allows the aircraft to sufficiently perform both the supersonic dash and loiter portions of the mission. The highly swept inner part of the wing decreases drag in the transonic and supersonic flight regimes. The moderately swept outer part of the wing lets the wing area and span increase to improve loiter performance without significantly increasing supersonic drag. Thus, the cranked wing is able to generate higher lift-to-drag ratios than a traditional delta wing interceptor design. Lift-to-drag ratio is especially important in the cruise and loiter phases of the mission because increasing lift-to-drag ratio increases aircraft endurance by decreasing fuel consumption. The high wing area is also necessary due to a significant portion of the fuel being stored in the wings. The wing geometry is summarized in Table 4-1 and shown in Figure 4.1.

Table 4-1. Homeland defense interceptor wing geometry parameters.

Span	50.07 ft
Area	700 ft ²
Leading Edge Sweep (inner)	55°
Leading Edge Sweep (outer)	45°
Trailing Edge Sweep	10°
Root Chord	27.726 ft
Tip Chord	2.809 ft
Mean Aerodynamic Chord	17.57 ft
Taper Ratio	0.101
Aspect Ratio	3.58

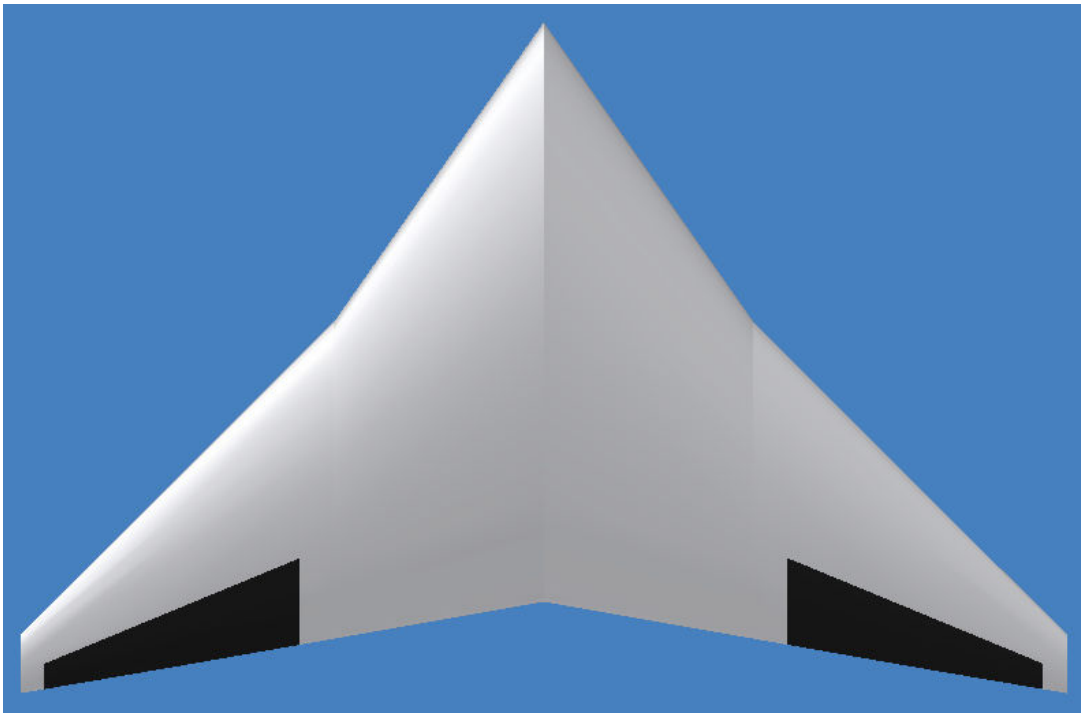
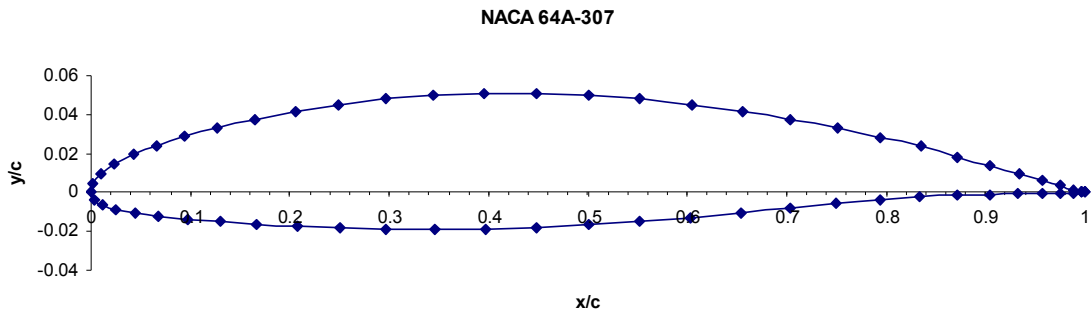


Figure 4.1. Homeland defense interceptor wing planform. Geometric parameters summarized in Table 4-1.

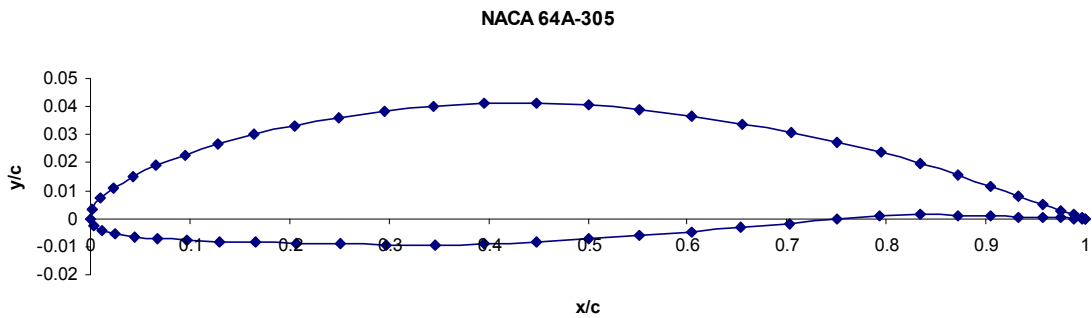
To reduce the amount of drag in the transonic and supersonic regimes, NACA 6-series airfoils similar to the ones used on the F-22 are implemented.⁵ The wing uses a NACA 64A-307 airfoil. This airfoil was selected to minimize thickness ratio while allowing enough space for wing structure and fuel. The NACA 64A-305 airfoil is used for the canard, and the NACA 64A-005 airfoil is used on the vertical tail. These airfoils have smaller thickness ratios than the wing airfoil because the canard and vertical tail only have to carry internal structure. The wing airfoil

has a thickness ratio of 7% of the chord, and the thickness ratio of the canard and vertical tail airfoils is 5% of the chord. The maximum thickness of all three airfoils is located at 40% of the chord. All airfoil coordinates were generated using JavaFoil.⁶ The aircraft is designed to cruise at a lift coefficient of 0.3. The selected airfoils are shown in Figure 4.2.

a)



b)



c)

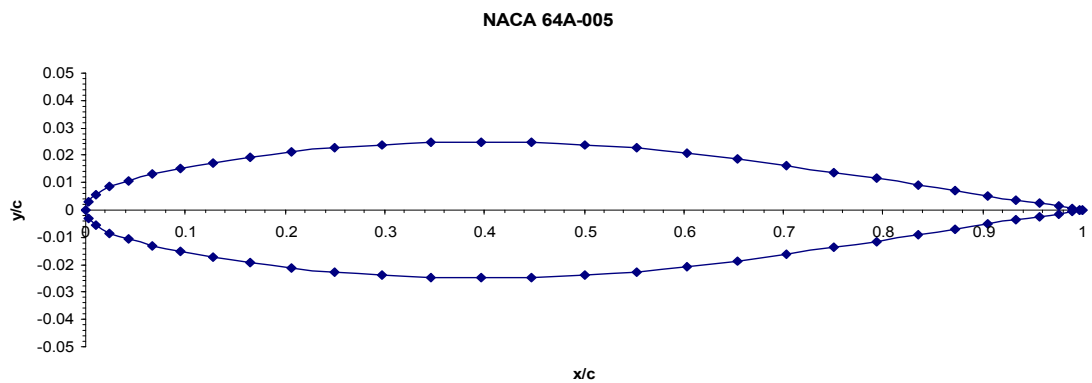


Figure 4.2. Airfoils used on homeland defense interceptor. a) NACA 64A-307 wing airfoil. b) NACA64A-305 canard airfoil. c) NACA 64A-005 vertical tail airfoil.

4.2 High-Lift Devices

Slotted flaps on the trailing edge of the wing will be used as both high-lift devices and roll control surfaces. These flaperons will increase $C_{L_{max}}$ so that the aircraft will be able to takeoff, land, and maneuver safely and effectively. They were sized from historical data found in Raymer⁴ and have a 65.942 ft² area. The flaperons encompass 48.85% of the wing span and 30% of the wing chord. The flapped area of the wing is 30.74% of the total wing area. According to the mission analysis, a $C_{L_{max}}$ of 1.4 is needed to meet the RFP's 18°/s instantaneous turn rate requirement at a load factor of 9. The flaperons are capable of generating the maximum lift coefficient required for this maneuver. The clean lift $C_{L_{max}}$ was estimated by comparison with similar aircraft configurations.⁷ The change in $C_{L_{max}}$ due to flap deflection was calculated using methods from Raymer.⁴ The effectiveness of the flaperons is shown in Table 4-2. The effect of the trailing edge devices on the lift curves is discussed in the following section, and can be seen Figure 4.1.

Table 4-2. Maximum lift coefficient at various flight conditions. $C_{L_{max}}$ determined from Hom et al.⁷ and Raymer.⁴

	$C_{L_{max}}$
Clean	1.1
Takeoff (flaperons deflected 30°)	1.385
Landing (flaperons deflected 60°)	1.454

4.3 Lift and Drag

NASA Langley's VLMpc code was used to determine the lifting characteristics of the canard and wing. This code was also used to calculate the induced drag in subsonic flight and aircraft neutral point. The aircraft's Oswald efficiency factor was found to be 0.796. The aircraft neutral point is located at 23.7% of the wing mean aerodynamic chord. The VLMpc code calculated the lift curve slope and zero-lift angle of attack at various flap deflections for the aircraft. Maximum lift coefficients were determined from Hom et al.⁷ and Raymer.⁴ This information was used to generate the lift curves in Figure 4.3.

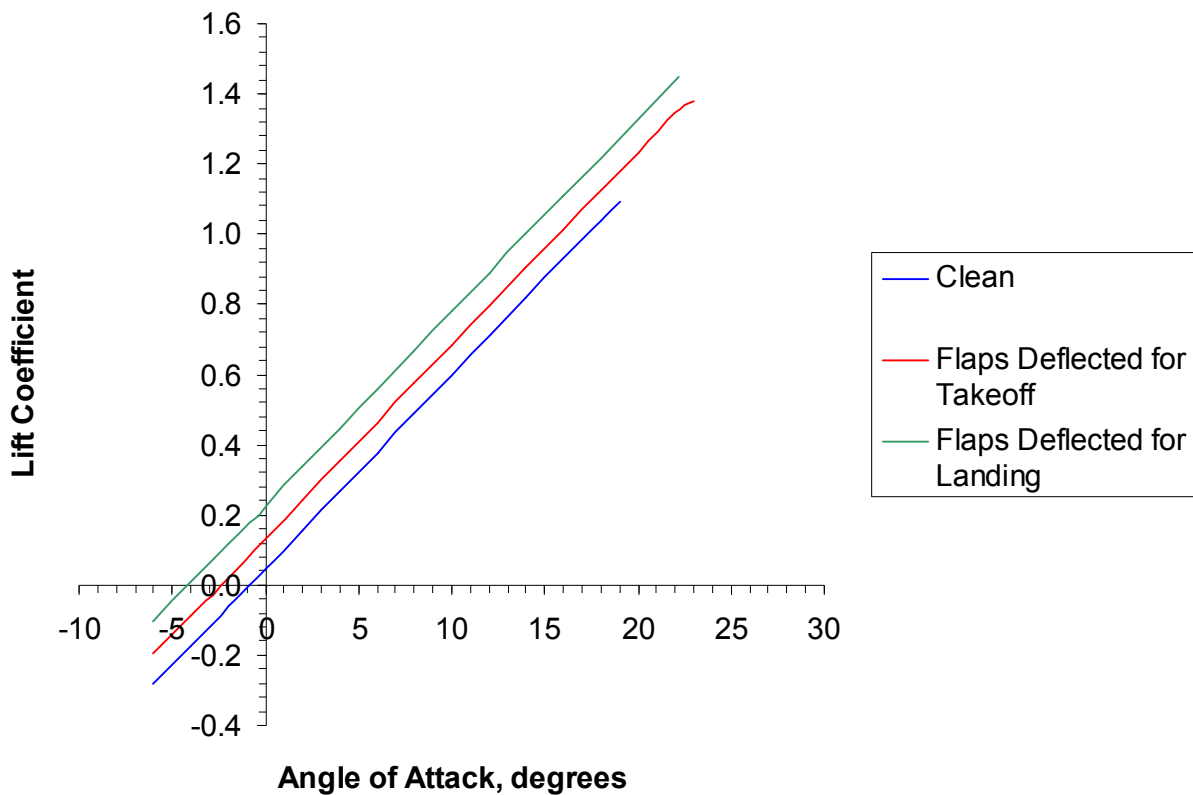


Figure 4.3. Homeland defense interceptor lift curves at various flap deflections. Lift curves go up to C_{Lmax} . Lift curve slopes and zero-lift angles of attack were determined from VLMpc. Maximum lift coefficients were calculated from Hom et al.⁷ and Raymer.⁴

Form and friction drag were found using the FRICTION program, and wave drag was determined using NASA's Harris Wave Drag code.⁸ The outputs from these two programs were combined to find the zero lift drag coefficient for each Mach number. These results are shown in Figure 4-4 and Table 4-3. The wave drag program's geometrical output and MATLAB were used to plot the aircraft area distribution seen in Figure 4-5. Furthermore, the drag results (including induced drag) were compared with the propulsion analysis to see if the aircraft is capable of dashing at Mach 2.2. The chosen propulsion system is able to complete the dash segment of the mission; however, afterburning must be used to reach supersonic speeds. The results from this analysis can be found in Table 4-4.

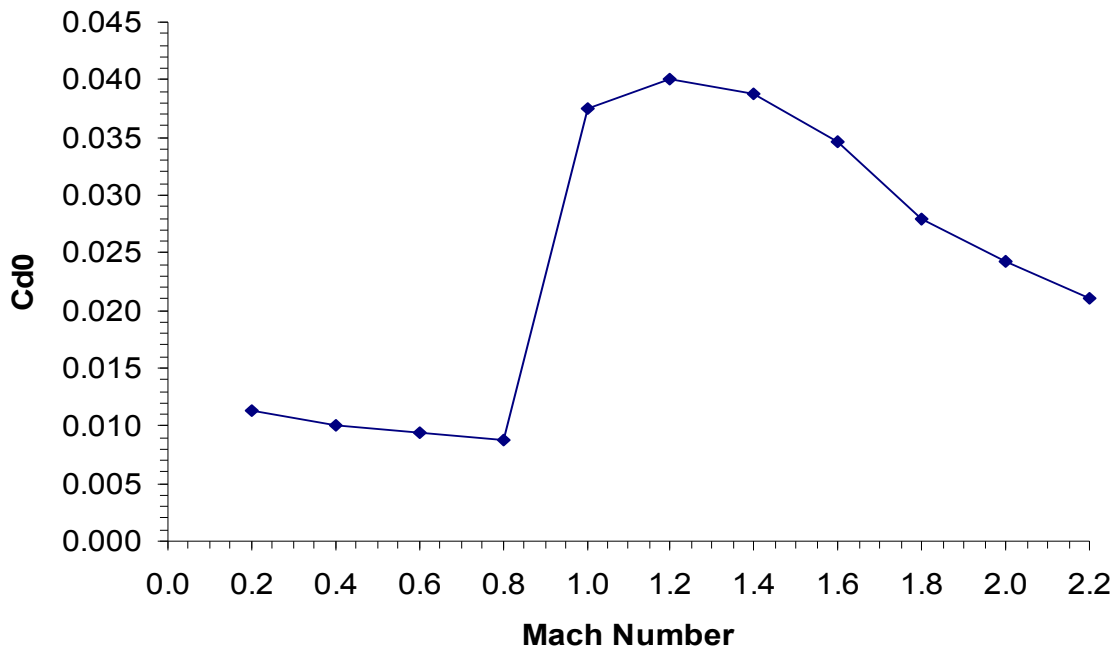


Figure 4.4. Homeland defense interceptor zero-lift drag coefficients at various Mach numbers. Drag coefficients calculated using FRICTION program and Harris Wave Drag code.⁸

Table 4-3. Homeland defense interceptor zero-lift drag build-up. Form and friction drag calculated using FRICTION program. Wave drag calculated using Harris Wave Drag code.⁸

Mach Number	Friction Drag	Form Drag	Wave Drag	Total Zero-lift Drag
0.2	0.00945	0.00191	0.00000	0.01136
0.4	0.00840	0.00170	0.00000	0.01010
0.6	0.00778	0.00157	0.00000	0.00935
0.8	0.00730	0.00147	0.00000	0.00877
1.0	0.00689	0.00139	0.02914	0.03742
1.2	0.00651	0.00131	0.03229	0.04011
1.4	0.00616	0.00124	0.03136	0.03876
1.6	0.00582	0.00117	0.02758	0.03457
1.8	0.00550	0.00111	0.02137	0.02798
2.0	0.00520	0.00105	0.01803	0.02428
2.2	0.00492	0.00099	0.01518	0.02109

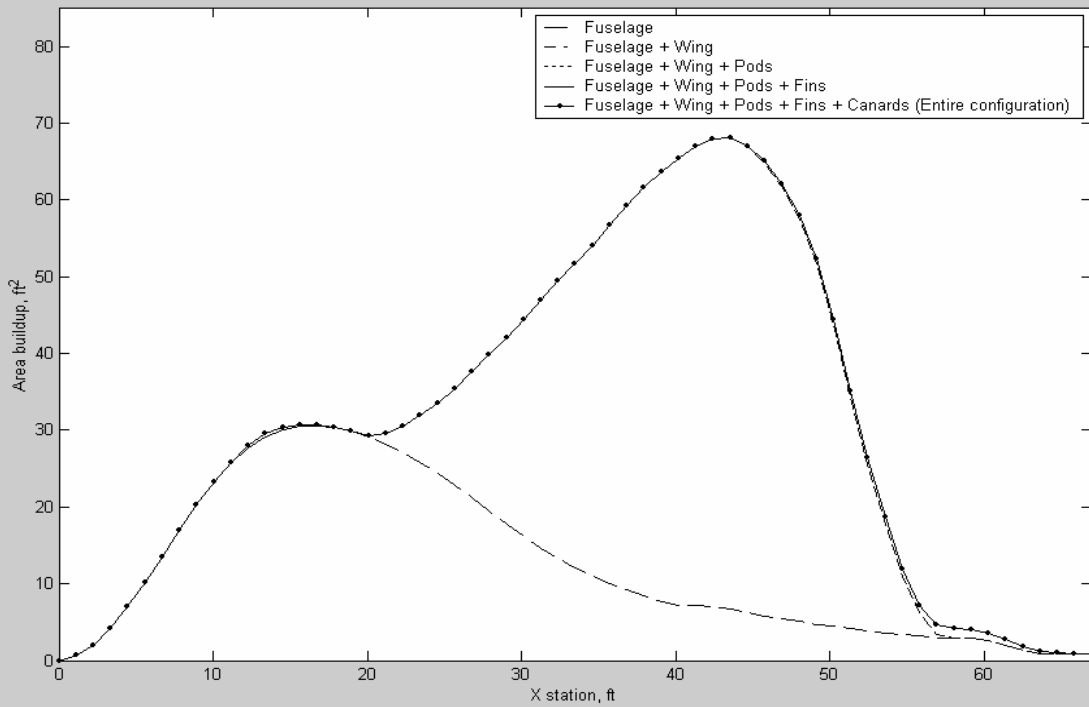


Figure 4.5. Homeland defense interceptor area distribution. The smooth area distribution minimizes the wave drag during the dash portion of the mission.

Table 4-4. Homeland defense interceptor thrust and drag analysis. Bold print denotes that afterburning is required to reach that particular Mach number.

Mach Number	D/q	T/q (not afterburning)	T/q (afterburning)
0.2	22.409	442.022	725.661
0.4	21.247	111.035	187.192
0.6	20.570	52.229	91.808
0.8	20.039	32.735	61.085
1.0	34.242	27.745	53.462
1.2	36.699	24.958	70.308
1.4	35.461	22.393	41.991
1.6	31.634	21.767	66.785
1.8	25.602	22.266	72.198
2.0	22.218	23.768	43.468
2.2	19.297	26.834	53.093

Drag polars (including trim drag) for the most important phases of the mission were calculated using methods from both Raymer⁴ and Etkin and Reid⁹. The control surface deflections necessary for trim are discussed in the Stability and Control section of this report. The takeoff and landing drag polars are shown in Figure 4.6. Due to the large control deflections (high trim drag) needed for both trim and maximum lift, the lowest L/D_{max} occurs at landing (L/D_{max} of 6.2 at C_L of 0.5). Conditions at takeoff are more favorable (L/D_{max} of 8.6 at C_L of 0.4) because the necessary control deflections are smaller. L/D_{max} must be maximized during the four hour loiter phase in order to decrease the fuel consumption. The loiter drag polar is shown in Figure 4.7. For the loiter segment, L/D_{max} was determined to be 11.8 at a C_L of 0.3. The L/D_{max} for the dash portion of the mission is relatively low due to the wave drag inherent in supersonic flight. The dash drag polar is shown in Figure 4.8. The dash phase features an L/D_{max} of 9.0 at a C_L of 0.4. Because one of the main design goals is to decrease wave drag, the maximum lift-to-drag ratio for the dash segment is relatively high compared to most supersonic aircraft.

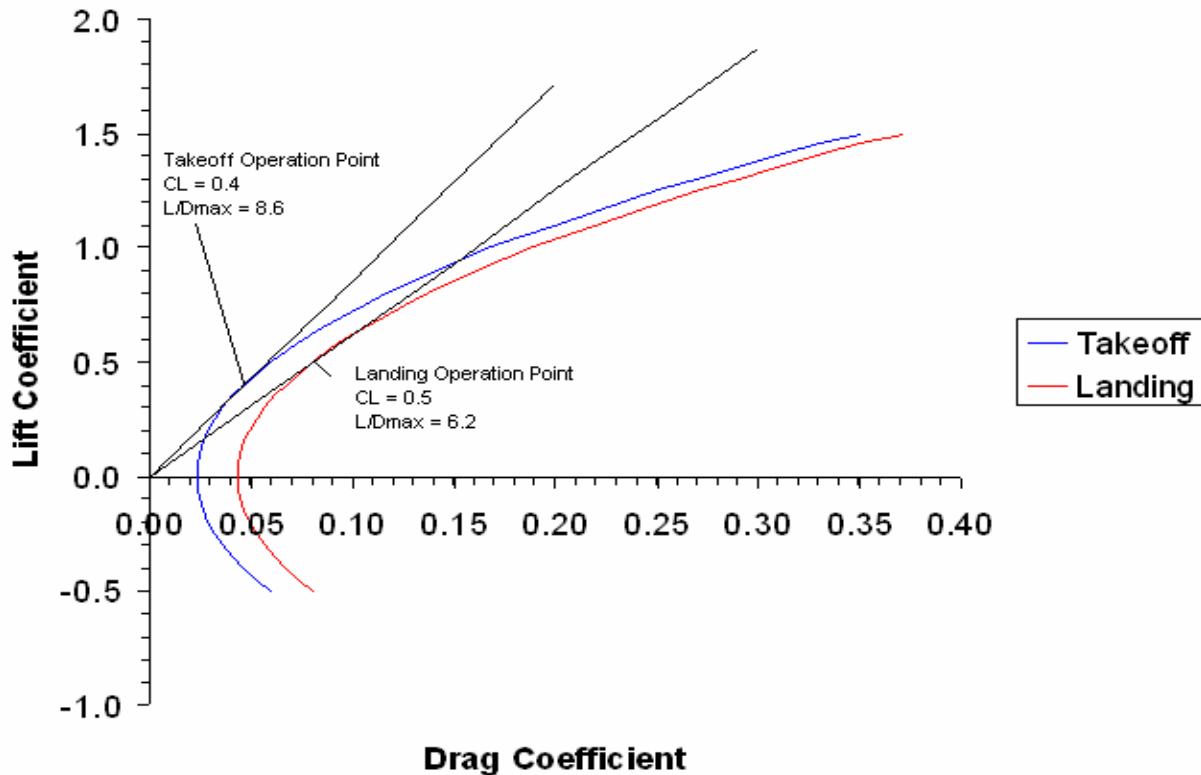


Figure 4.6. Takeoff and landing drag polar. Takeoff operation point occurs at $L/D_{max} = 8.6$ and $C_L = 0.4$. Landing operation point occurs at $L/D_{max} = 6.2$ and $C_L = 0.5$.

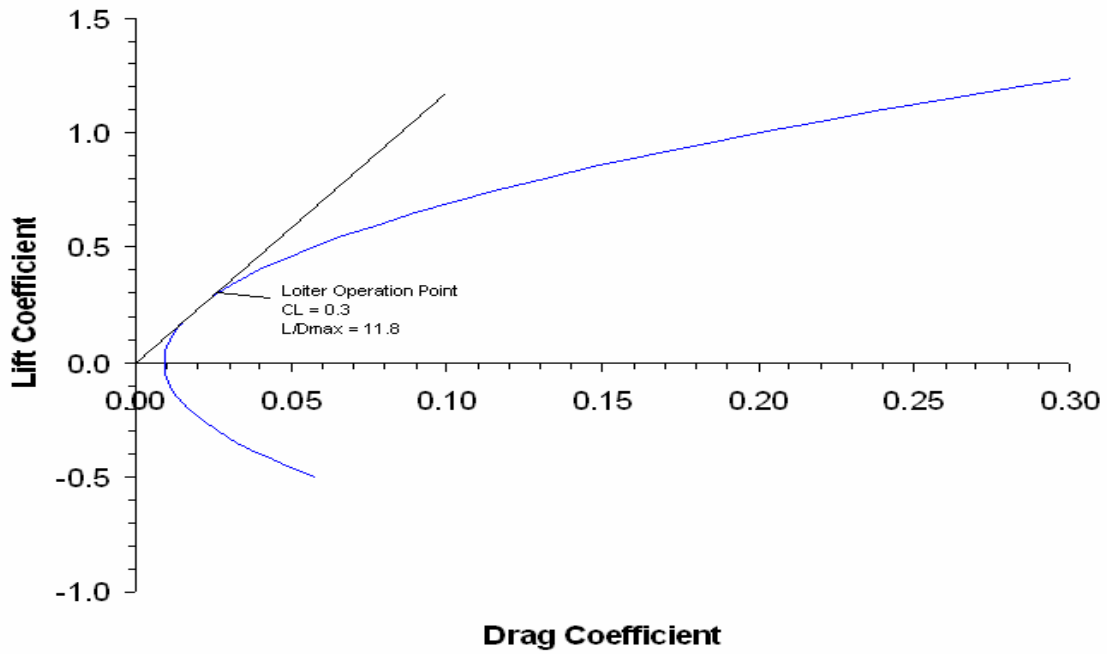


Figure 4.7. Loiter drag polar. Loiter operation point occurs at $L/D_{max} = 11.8$ and $C_L = 0.3$.

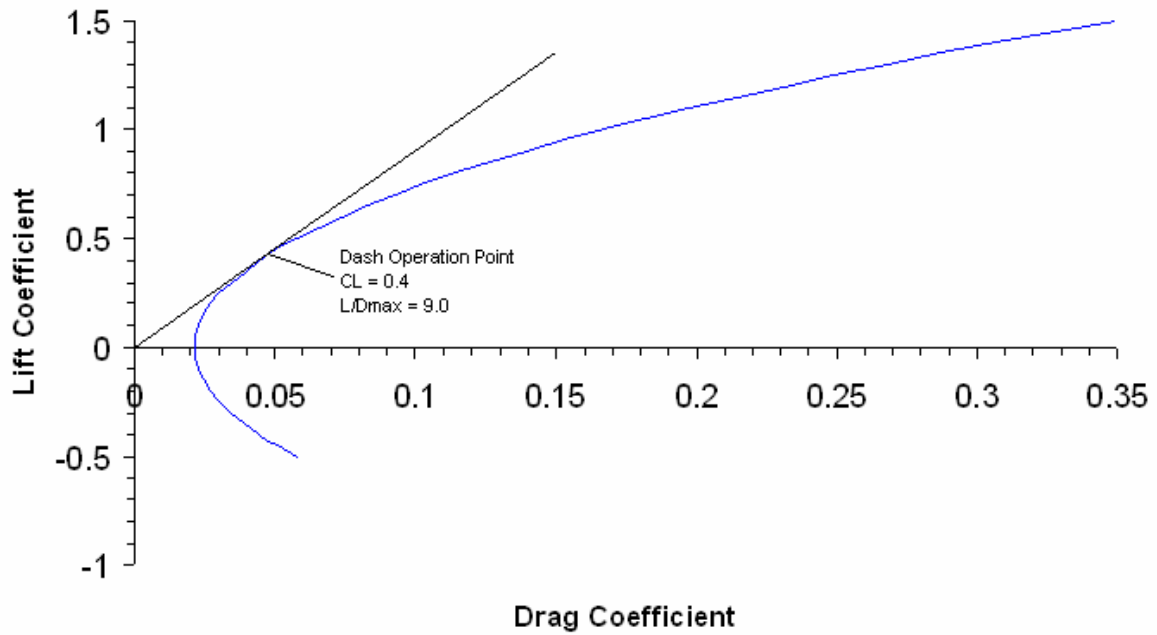


Figure 4.8. Dash drag polar. Dash operation point occurs at $L/D_{max} = 9.0$ and $C_L = 0.4$.

5. Propulsion

5.1 Research

Before any analysis was done on the F414 deck supplied by AIAA, other engines were investigated. The research covered engines built by General Electric, Pratt and Whitney, and Rolls Royce since these are the major companies that produce the engines used in most modern fighter and interceptor aircraft. One of the engines considered was also used for the B-1 Bomber. First, a summary of the General Electric aircraft engines will be presented. All of the data regarding General Electric aircraft engines was taken from General Electric's corporate website.¹⁰

The General Electric F101 seemed to be one of the best engines for the homeland defense interceptor (HDI). It was introduced in 1970 and used to power the B-1 Bomber. The F101 produces 28,000 lbs to 32,000 lbs of thrust at maximum power at sea level with a specific fuel consumption of 1.9 to 2.09 lb/hr/lb. The weight of the F101 ranged from 3,920 lbs to 4,400 lbs. The F101 produced 10,000 more pounds of thrust than the AIAA F414 at maximum power while having a greater TSFC. However, the F101 was over 1,300 lbs heavier.

Another engine that was researched was the General Electric F110. Some notable aircraft that are propelled by the F110 are the F-14, F-15, and F-16. The performance of the F110 is very similar to that of the F101. At maximum power the F110 produces 27,000 to 32,000 lbs of thrust with a *TSFC* of about 2.0 lb/hr/lb. The dry weight of the F110 is 4,400 lbs. The F110 produced significantly more thrust than the AIAA F414 with a higher *TSFC* and was still about 1,800 lbs heavier.

The research of General Electric engines continued with the F404 which can be found on the F/A-18 and the F-117A. With its 11,000 to 18,000 lbs of thrust at maximum power, the F404 produced significantly less thrust than the AIAA F414 and other General Electric engines. At 1.7 lb/hr/lb to 1.85 lb/hr/lb at maximum power, the *TSFC* of the F404 was still slightly greater than the *TSFC* of the AIAA F414 at maximum power. The dry weight of the F404 ranged from 2,195 lbs to 2,335 lbs, which was only about 300 lbs to 400 lbs lighter than the AIAA F414.

The last General Electric engine to be considered was the F118. The F118 is used to propel the B-2 and the U-2. At maximum power, it produces 17,000 lbs to 19,000 lbs of thrust. Since the F118 does not have an afterburner, its *TSFC* at maximum power is only 0.67 lb/hr/lb. Due to the low *TSFC*, the F118 may have been useful for the loiter portion of the HDI's mission, but it may not have been able to propel the HDI to Mach 2.2. The 3200 lb weight of the F118 also makes it 550 lbs heavier than the AIAA F414.

In addition to General Electric engines, Pratt and Whitney aircraft engines were also researched. All of the data regarding Pratt and Whitney engines was taken from Pratt and Whitney's corporate website.¹¹ Although Pratt and Whitney makes advanced engines for the Joint Strike Fighter and the F-22, little or no data on those engines was available. Research on the F117 was not pursued because it is a high bypass ratio turbofan engine and would likely perform poorly at supersonic speeds. The one Pratt and Whitney engine that may have been useful is the F100 which has been used on the F-16 and F-15. While no information regarding specific fuel consumption could be found, the F100 could produce 23,770 lbs to 29,160 lbs of thrust. This amount of thrust is greater than the maximum thrust of the AIAA F414, but without any insight into the dry weight or *TSFC* of the F100, it could not be compared to the AIAA F414.

Some research was also conducted to determine whether or not a Rolls Royce engine would be useful. All of the data presented in this paragraph was taken from Rolls Royce's corporate website.¹² One of the lightest engines, the Adour MK871, weighing in at 1299 lbs, produced 6000 lbs of thrust at maximum power. The slightly heavier Adour MK951 produced 6500 lbs of thrust. Neither of these engines was equipped with afterburners. While the weight of these engines was attractive, they did not produce enough thrust. Two other engines, the Adour MK106 and Adour MK811, weighed 1784 lbs and 1633 lbs respectively. They both produced about 8400 lbs of thrust at maximum power. While both the MK106 and MK811 were equipped with afterburners, neither produced sufficient thrust. The Rolls Royce EJ200 weighed 2180 lbs and produced 20,000 lbs of thrust. This engine came close to matching the performance of the AIAA F414. One main problem with the Rolls Royce engines was that no *TSFC* data could be found.

Of all the engines studied, the AIAA F414 was selected for use with the HDI. One of the main reasons for this choice was the lack of data available for other engines. Attempts to find an engine deck or enough information to calculate an engine deck all failed. However, the AIAA F414 does have good performance characteristics. It weighs 2651 lbs, produces 22,250 lbs of uninstalled thrust at maximum power, and has an installed *TSFC* of 1.32 lb/hr/lb at maximum power. As stated previously, these characteristics measure well compared to other engines produced by major aerospace companies. The table below summarizes the information presented above.

Table 5-1. This table summarizes the research presented above. The AIAA F414 was selected for use with the HDI due to its low *TSFC* and high thrust.

Engine	Dry Weight (lb)	TSFC at Max Thrust (lb/hr/lb)	Max Thrust at Sea Level (lb)
General Electric			
F101-GE-100	3920	2.06	28000
F118-GE-100	3200	0.67	19000
F404/RM12	2325	1.78	18100
F404-GE-102	2282	1.74	17700
TF34-GE-100	1440	0.371	9065
TF34-GE-400A	1478	0.363	9275
Pratt and Whitney			
F100	3740		23770 to 29160
F117	7100		41700
Rolls Royce			
EJ200	2180		20000
RB199-104	2151		16400
Adour MK951	1345		6500
Adour MK871/F405	1299		6000
Adour MK106	1784		8430
Adour MK811	1633		8400
AIAA F414	2651	1.32	21049

5.2 Inlet Design

It was important to keep installed thrust as high as possible while keeping the inlet as simple as possible. Any overly-complex inlet configurations could drive up the cost of the overall aircraft. However, good pressure recovery was also necessary. A simple normal shock inlet would have the most straightforward configuration but it would yield terrible pressure recovery at high Mach numbers. An internal compression inlet would yield excellent pressure recovery at high Mach numbers and have a relatively simple design but to start the inlet the aircraft would have to exceed the desired Mach number; in this case 2.2. Also, once the inlet was started, any variation in the operating conditions of the engine could cause an unstart. The type of inlet selected was a 2-dimensional, external compression ramp inlet similar to the type used on the F-14 and F-15. This type of inlet is the most mechanically complex of all the inlets considered but the advantages outweigh the complexity. The desired Mach number does not have to be exceeded to start the inlet, unstart is not a problem, and it can be designed to yield good pressure recovery.

To begin the design of the inlet, pressure recoveries were calculated for various amounts of flow deflection. Obviously, the less the flow is deflected, the weaker the oblique shock and the better the pressure recovery but only

deflecting the flow by 1 degree would require too many ramps to make the flow subsonic. To solve the problem, a MatLab program was written to calculate the pressure recovery over a system of shocks. The flow deflection angle and the free stream Mach number were held constant. The program iterated until oblique shocks were no longer possible and then calculated the pressure drop over a final normal shock. Then the pressure drop over the entire system of shocks was calculated. The equations used were taken from a propulsion text book by Hill and Peterson.¹³ The product of the stagnation pressure ratios across each individual shock is the stagnation pressure ratio for the overall inlet. As stated previously, the MatLab program written for this calculation held the flow deflection angle constant and performed oblique shock calculations iteratively until oblique shocks were no longer possible. It then performed a normal shock calculation and calculated the stagnation pressure ratio across the whole system of shocks. The output of the program is shown in Figure 5.1 below which shows the pressure recovery over a system of shocks. The peaky behavior of the plot is due to the varying Mach number upstream of the normal shock, thus causing varying pressure recoveries over the final shock.

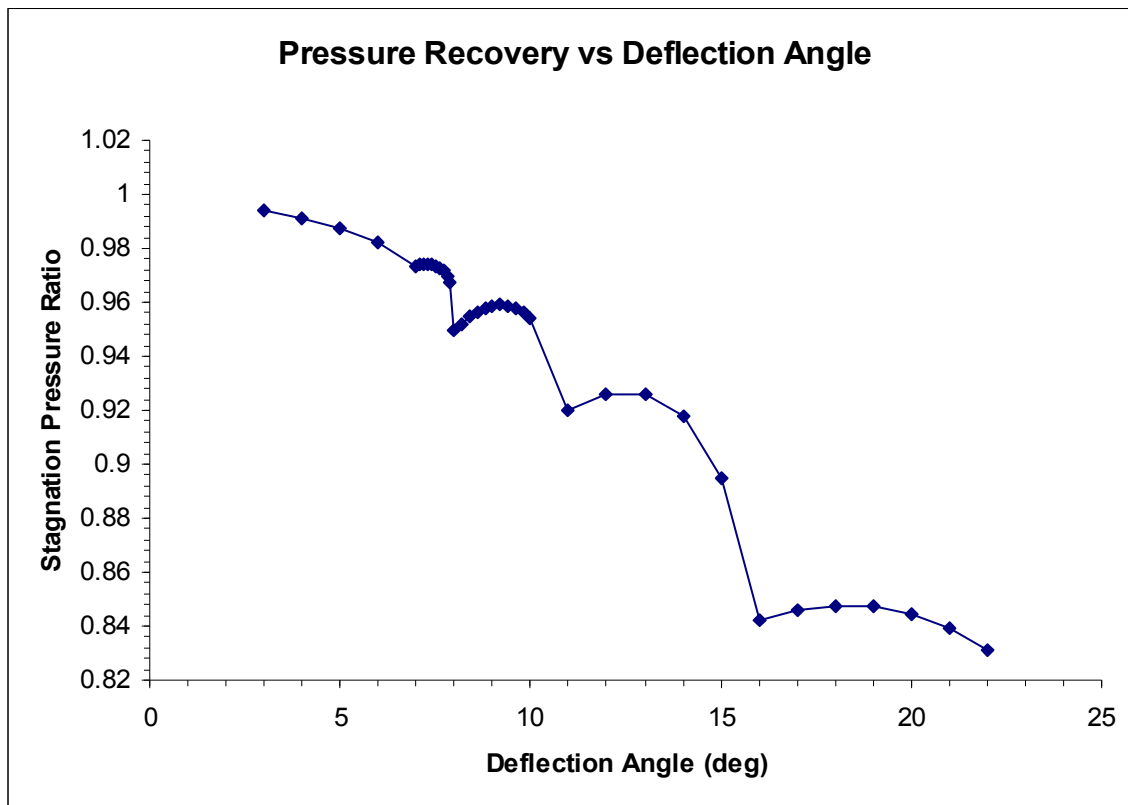


Figure 5.1. Inlet pressure recovery versus flow deflection angle with a free stream Mach number of 2.2. The best deflection angle to use is 7 degrees because it yields the pressure recovery shown at the top of the first peak. For lower deflection angles, too many ramps are required. For higher deflection angles, the pressure recovery drops dramatically.

From the results of these calculations, a deflection angle of 7 degrees was chosen. This deflection angle would require 4 oblique shocks and 1 normal shock, thus the inlet has 4 deflection ramps. All four ramps are movable, which will maintain good pressure recovery at lower Mach numbers and also maintain the shock-on-cowl condition. The shock-on-cowl condition is when all of the shocks in the inlet converge on the cowl. The overall pressure recovery for this inlet and a free stream Mach number of 2.2 is 97%.

All 4 ramps are not necessary for every free stream Mach number. Only 3 ramps are needed for free stream Mach numbers from 1.8 to 2.0 and only 1 ramp is needed for Mach 1.5. From Mach 1.0 to Mach 1.3, no ramps are necessary and the only shock present is a normal shock.

To properly find the necessary inlet dimensions, the mass flow rate of air required by the engine at each flight condition must be known or calculated. All attempts to find a method of calculating mass flow rate failed so another method was used. A correctly functioning inlet should decelerate the flow to approximately Mach 0.4 at the front face of the engine. The area of the front face of the engine was known and the Mach number just downstream of the inlet was also known. So area relations for an isentropic flow were used to find the necessary inlet area. The flow inside the duct is not isentropic but only 4% stagnation pressure is lost in the duct so the entropy change is not very significant. Also, to compensate for neglecting the entropy change and to allow for some auxiliary airflow, the diameter of the duct at the front face of the engine is slightly larger than the diameter of the engine. The diameter of the duct at the front face of the engine is 45 inches and the diameter of the engine is 35 inches. Equations 5.1 and 5.2 were used to find the necessary inlet area for each free stream Mach number.

$$\frac{A}{A^*} = \frac{1}{M} \left[\frac{2}{\gamma + 1} \left(1 + \frac{\gamma - 1}{2} M^2 \right) \right]^{\frac{\gamma + 1}{2(\gamma - 1)}} \quad (5.1)$$

$$A_{Inlet} = A_{Duct} \frac{A^*}{A_{Duct}} \frac{A_{Inlet}}{A^*} \quad (5.2)$$

Equation 5.1 was taken from a propulsion text book by Hill and Peterson.¹³ In equation 5.2 A_{Inlet} is the area of the inlet just downstream of the normal shock and A_{Duct} is the area of the duct at the front face of the engine. The actual size of the inlet is greater than A_{Inlet} because the deflection ramps partially block the flow. A drawing of the inlet is shown in Figure 5.2 below. For a free stream Mach number of 2.2, the required inlet area normal to the normal shock is 7.09 ft².

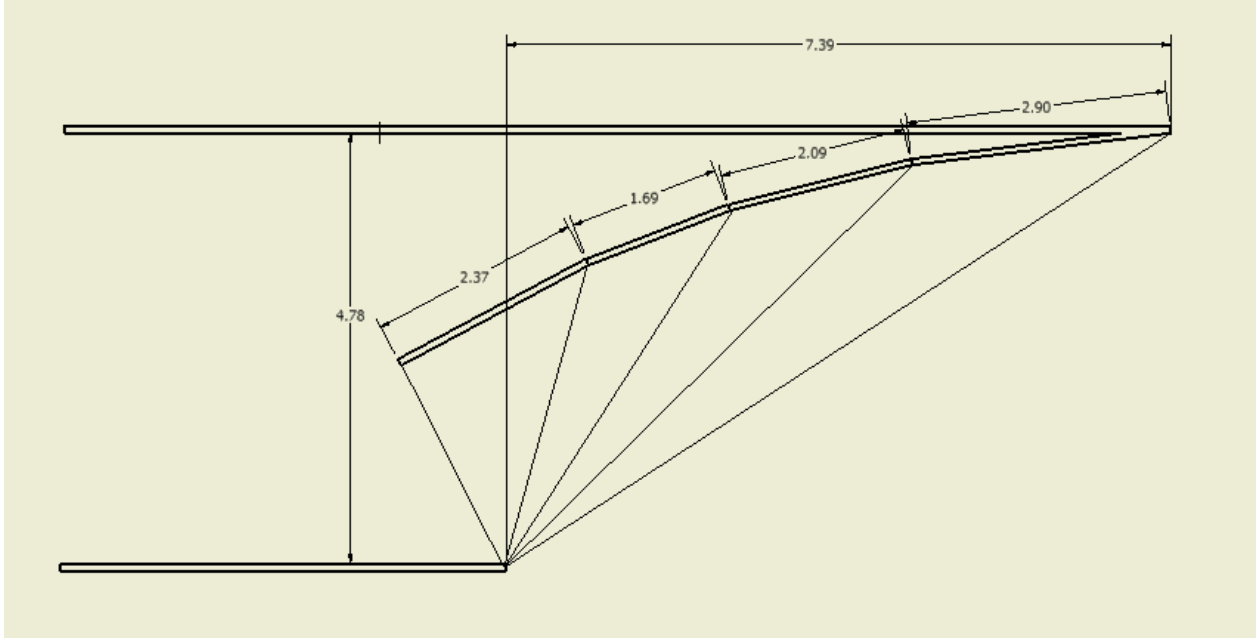


Figure 5.2. Side view sketch of inlet with dimensions and shocks shown for a free stream Mach number of 2.2.

5.3 Installed Thrust

Installed thrust depends heavily on pressure recovery. Another area where pressure recovery is important is in the duct between the inlet and the engine. The ducts were kept as straight as possible to maximize pressure recovery. An aircraft design text book written by Raymer⁴ suggested that for a straight duct, the pressure recovery was approximately 96%. With the pressure recovery in the duct and the inlet known, the installed thrust could be calculated according to the equations below taken from Raymer.⁴

$$\left(\frac{P}{P_0}\right)_{ref} = 1 - 0.075(M_\infty - 1)^{1.35} \quad (5.3)$$

$$C_{ram} = 1.35 - 0.15(M_\infty - 1) \quad (5.4)$$

Equations 5.3 and 5.4 apply to supersonic free stream Mach numbers (M_∞). For subsonic flight, $(P/P_0)_{ref}$ is 1 and C_{ram} is 1.35. Equations 5.5 and 5.6 are used to determine the installed thrust.

$$\%T_{Loss} = C_{ram} \left[\left(\frac{P}{P_0}\right)_{ref} - \left(\frac{P}{P_0}\right)_{actual} \right] \times 100 \quad (5.5)$$

$$T_{Installed} = T_{Uninstalled} \left(1 - \frac{\%T_{Loss}}{100} \right) \quad (5.6)$$

A requirement stated in the RFP is that the engines must generate 50 kW of power for the aircraft's systems. Since the aircraft will have 2 engines, 25 kW of power (18439 ft-lb/sec) must be drawn from each engine. The thrust lost due to this auxiliary power generation was calculated using equation 5.7.

$$T_{Lost} = \frac{Power}{Velocity} \quad (5.7)$$

Equation 5.7 does not give reasonable results for zero velocity. But when the aircraft is not moving, the suction of the engine induces a velocity in the inlet so the thrust lost at zero velocity is not infinity. The net usable thrust is

$$T_{Installed} - T_{Lost}$$

To aid in the aerodynamic design of the aircraft, a plot of the maximum allowable D/q was created from the engine deck data. Some of the data points in the engine deck were deleted because they did not make sense. For example, at Mach 2.2 at 30000 ft, the thrust listed on the engine deck was 42565.5 lbs; almost double the maximum uninstalled thrust of the engine. Due to the removal of some data points, the curve on the D/q plot is rough so a trend line was added to help define the upper limit on drag. The plot is shown below in Figure 5.3.

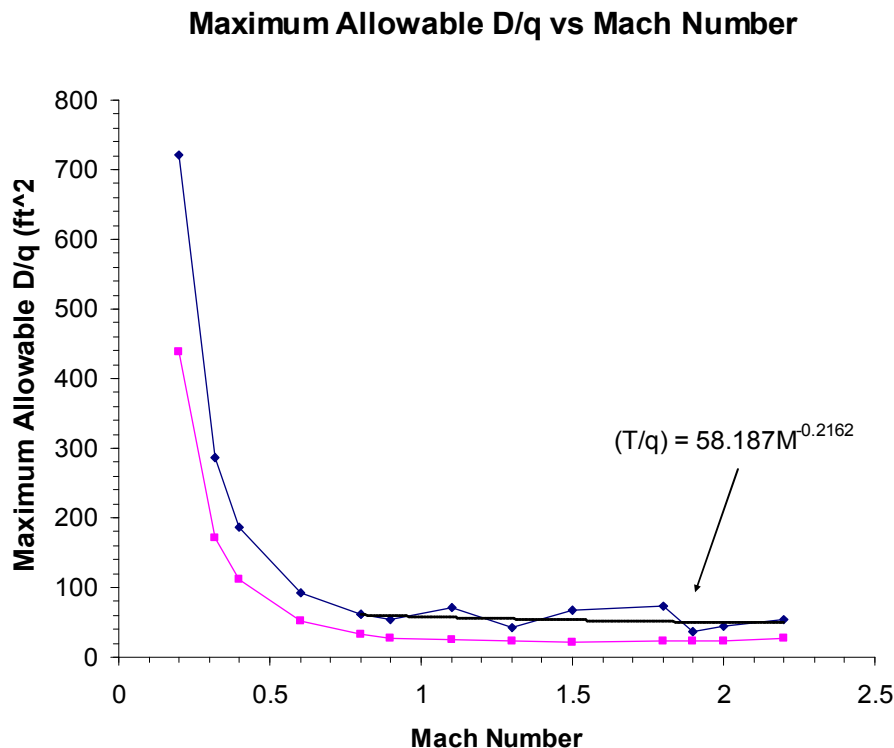


Figure 5.3. Maximum allowable D/q based on the net available thrust from 2 engines. The dark blue line represents the maximum T/q with afterburning. The pink line represents the maximum T/q without afterburning. The black line is a trend line that was added due to the roughness of the T/q afterburning line.

5.4 General Configuration Comments

This aircraft has 2 AIAA F414 engines. Each engine has its own inlet. The type of inlet used for this aircraft is a 2-dimensional ramp inlet. The inlet has 4 ramps, 1 fixed and 3 movable. The inlets are located on each side of the aircraft below the wings and canards. The inlets were placed in an undisturbed flow so a boundary layer diverter was not necessary. Also, some boundary layer suction is used on the deflection ramps. The ducts between the inlets and the engines were kept as straight as possible to minimize pressure loss. Since nothing was known about the flow conditions at the exit of the engine, trade-off studies could not be performed to determine whether a converging exhaust nozzle or a converging-diverging exhaust nozzle should be used. For the sake of simplicity and cost, converging exhaust nozzles are used on this aircraft.

6. Materials

6.1 Material Selection

The materials on the *Hedgehog* are a careful blend of strength and minimum cost. With a 52,000lb aircraft capable of maneuvers at 9 g's, the structural requirements dictate a material with a very high strength to weight ratio such as composites. The general considerations guiding material selection on the *Hedgehog* listed in order of importance are:

- 1) Strength to weight ratio
- 2) Cost
- 3) Manufacturing
- 4) Availability

Two types of materials are used, metal alloys and composites. The metals will be used in low load areas where large amounts of material are required such as frames, bulkheads, ribs and the fuselage skin. This is due to the higher availability of metals compared to composites, as well as easing manufacturing costs. Composites are used in the high load areas in the wings, control surfaces, and longerons.

6.2 Composites

Initially thermosets, thermoplastics and metal matrix composites (MMC) are considered for the high load areas such as spars and bulkheads, but MMCs are abandoned due to an unfavorable cost, availability and ease of manufacturing compared to typical metals. Instead of using MMCs, aluminum 7075 was also considered for low

stress areas. High stress areas require materials such as fiber based composites with either a thermoplastic or thermoset matrix.

The wing of the aircraft needs very high strength components, so varieties of composites are considered. The materials considered for the spar are listed in Table 6-1. This list shows for components like the wing skin materials such as Kevlar and Spectra based composites are not suitable for the high sustained temperatures during supersonic flight. The skin is made out of Hexcel with a high temp thermoplastic matrix with a honeycomb core. The thermoplastic Celazole® Polybenzimidazole or PBI, is used as the matrix material in high heat areas because it can withstand 580°F for over 20000 hours before degrading.¹⁴ The material properties can be seen in Table 6-2. The wing spars use Spectra 1000 as the fiber as it has a higher specific strength compared to Hexcel, and the material is not subjected to the high temperatures. Hexcel’s excellent thermal properties are not required. The matrix material for the Spectra 1000 parts is RTP 3000, a low temperature matrix material that has a mold temperature below the critical temperature of 147°C of Spectra 1000. The spars also contain a honeycomb core to prevent buckling of the load carrying Spectra by increasing the stiffness and increasing the strength. The core increases the strength up to 9 times the strength of the panel and up to 37 times the stiffness, if the core is 4 times the plate’s thickness.¹⁵ The honeycomb used is an aluminum based material because it has the highest strength to weight ratio.¹⁵

Other areas that use composites are the longerons and control surfaces. The forward fuselage longerons are made of Spectra fibers and the rear longerons are made of Hexcel. The Hexcel is required for the rear longerons as they undergo the heat produced by the engine. The control surfaces are made of a Hexcel based skin, and have a honeycomb core.

To assemble the composite sections, thermoplastic flanges will be attached to the bulkheads. The thermoplastic of flange and adjoining piece can then be heated locally to bond the flange and adjoining piece together.

Table 6-1. Composite Comparisons.

MATERIAL	DENSITY	MAX TENSILE STENGTH	MAX TEMP
Hexcel Carbon Fiber AS4C ¹⁵	.0643lb/in ³	602000 psi	
Honeywell Spectra 10000 ¹⁴	.0351lb/in ³	435000 psi	147°C
Dupont Kevlar ¹⁴	.0521lb/in ³	435000 psi	149°C
Thornel T-300 PAN ¹⁴	.0636lb/in ³	529000 psi	
SGL SIGRAFIL C S009 ¹⁴	.0651lb/in ³	522000 psi	

Table 6-2. Thermoplastics used and their properties.

MATRIX MATERIAL	DENSITY	MAX TENSILE STENGTH	MAX TEMP	MOLD TEMP
Celazole® Polybenzimidazole PBI ¹⁴	0.047 lb/in ³	23200 psi	310°C	
RTP 3000 ¹⁴	.0303 lb/in ³	3500 psi	250°C	93.3°C

6.3 Metals

Metals such as aluminum are a staple in aircraft structures. Aluminum is a material with a strength to weight ratio better than steel and is much cheaper than composites. Stainless steel is a very high strength material and has very good high temperature properties, so it will be used around the engine to shield the composite longerons from the extreme engine heat. Different aluminums were compared for use and are listed in Table 6-3. This chart shows that aluminum lithium is lighter than typical 7075 aluminum and will therefore be used in the high load bulkheads where the weight savings over aluminum 7075 would be the greatest. Aluminum lithium is also used for the skin of the fuselage, canard, and tails for the same reason. Aluminum 7075 is used in the frames because cost difference for the weight saved is not great enough to be cost effective.

Table 6-3 Aluminum alloy comparisons.

MATERIAL	DENSITY	MAX STRENGTH	MAX TEMP
AL-li 8090-T511	.0918lb/in ³	74000psi (65300psi yield)	600°C
AL-li 2090-T86 1 ¹⁴	.0936lb/in ³	79800psi (75400psi yield)	560°C
AL 7075-T73 ¹⁴	.102lb/in ³	73200psi (63100psi yield)	477°C

7. Structures

7.1 Loads

The structure of the aircraft needs to withstand not only the maximum load generated by the wing and canard, but also must be able to take gust loads as well as not yield at the limiting aero loads. Typical loads on military fighters are +7gs and -3gs. To achieve the 18 deg/sec instantaneous turn, the aircraft undergoes a 9g load. This turn fixes the maximum sustained load at 9gs. The factor of safety is 1.5, so the limit loads are 13.5gs and -4.5gs.

A V-n diagram was constructed, as seen in Figure 7.1. This diagram shows the maximum aerodynamic g loads, the FAR gust requirements, and the structural limits. The maximum dive speed is assumed to be the maximum speed. The blue lines represent the gust FAR gust requirements for supersonic aircraft.⁴

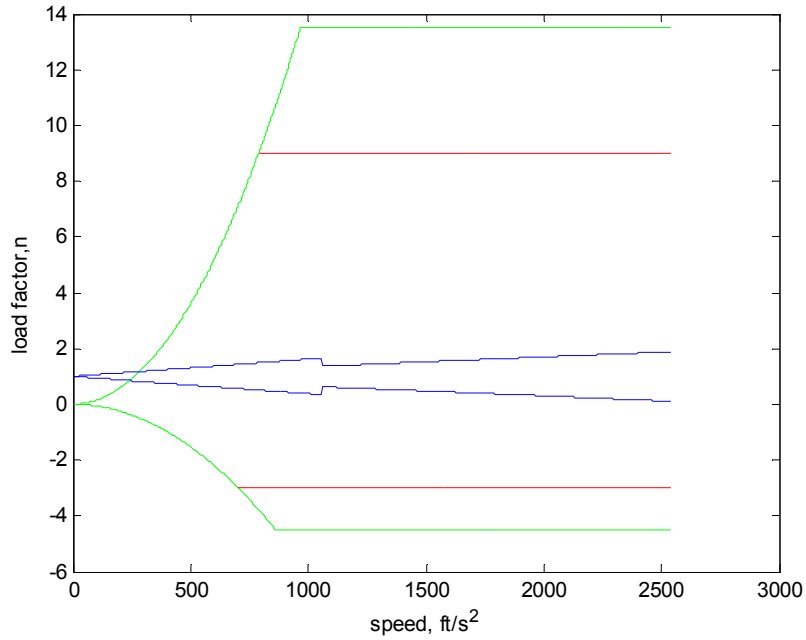
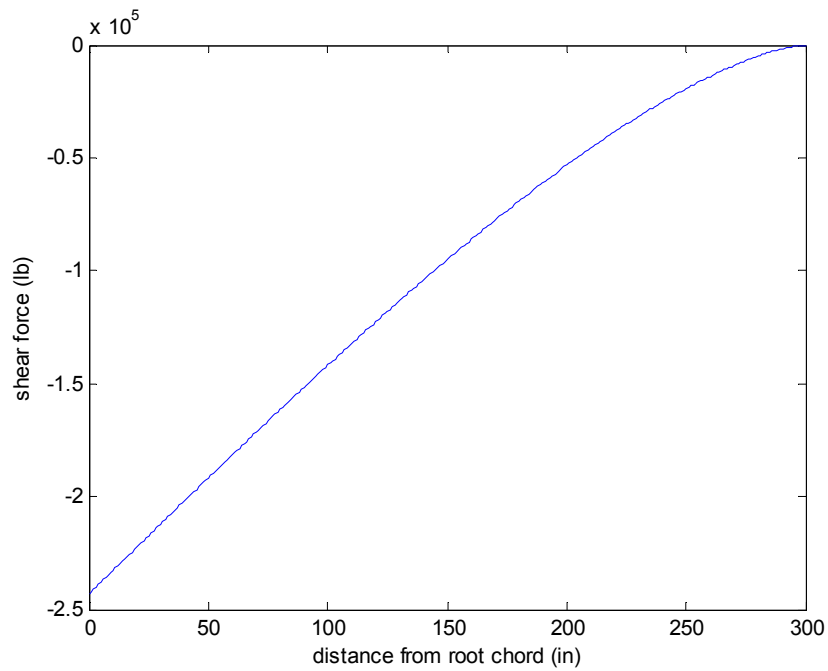


Figure 7.1. Structural V-n diagram.

The wing only takes 76% of the load, and the resulting shear and bending moments of the wing are present in Figures 7.2 and 7.3. This shows the need for the high strength materials as well as multiple spars to distribute the loads.



Figures 7.2. Shear Diagram.

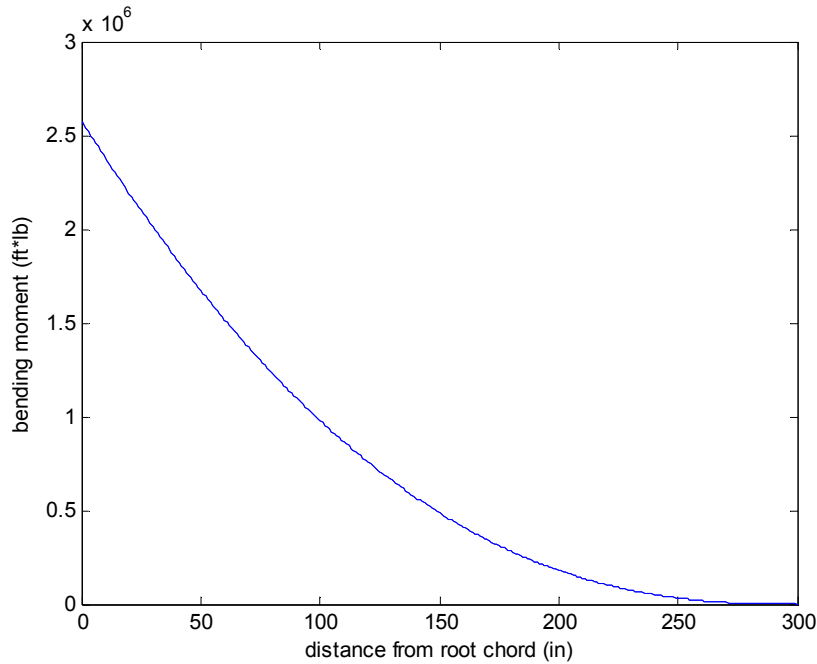


Figure 7.3. Bending Moment Diagram.

7.2 Wings

The wing consists of 12 small spars at the root. This helps to distribute the loads and provides failure resistance due to damage to a single spar. The rear 3 spars end at the transition of the leading edge from 55 degrees to 45 degrees because of the control surfaces. The first spar is located at 15% of the chord length behind the leading edge, the last is located 85% of the chord length, and the other 10 spars are evenly distributed between the first and last spars. There is a carryover box that runs from the outside of one engine pod to the other. The spar cross section is made of 2 composite C channels with honeycomb core and Spectra spar caps as shown in Figure 7.4.

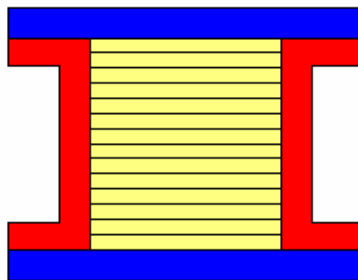


Figure 7.4. Honeycomb spar construction.

The first ribs are located at the edges of the engine pod. Another rib is located at the transition from the inboard section of the wing to the outboard section and also serves as the mounting point for an AIM9 missile. The

outboard section has a rib spacing of 3ft. The last rib is also carries an AIM9 missile. All the ribs will be divided into 12 sections, to allow the spars to pass between each section. The leading edge of the wing is made of Aluminum lithium and is split into segments, an inboard section and outboard section. A complete structural drawing of the wings can be seen in Figure 7.5 and Figure 7.7.

7.3 Canard and Tail

The tail and canard will have 2 spars and a rib spacing of 3 ft. The fixed section of the canard has 2 spars. The front spar is located at 20% of the chord behind the leading ledge at the root and 25% of the chord edge at the tip. The rear spar is located at 40% of the chord behind the leading edge at the root and tip. The control surfaces have 2 ribs located at the edges of the control surface and a spar behind the hinge location, Figure 7.5 and Figure 7.7.

7.4 Fuselage

The fuselage is made of a total of 13 bulkheads, 4 longerons and 8 large stringers in the forward section, 5 longerons and 16 large stringers in the aft fuselage section, and frames every 2 feet. The forward section's longerons are placed on the top, bottom and sides, while 2 stringers are located between each longeron. These longerons run from the front bulkhead of the plane to the first weapons bulkhead. The aft section of the fuselage has four of the longerons placed in the outer corners of the engine pod assembly, while one runs through the center section of the rear fuselage and is an extension of the bottom longeron in the forward fuselage section. Table 7-1 describes the purpose of each of the bulkheads. The fuselage is shown in Figure 7.6 and Figure 7.7.

Table 7-1. Bulkhead Functions.

Bulkhead Number	Function
1	Radar Mount
2	Front Pressure Bulkhead
3	Rear Pressure Bulkhead and Canard Mount
4	Gun and Canard Hinge Mount
5	Landing Gear Hinge Mount
6	Front Fuselage to Engine Pods
7	Weapons
8	Front Spar
9	Spar
10	Front Tail Spar Rear Weapons
11	Rear Landing Gear Spar
12	Rear Tail Front Engine Mount
13	Rear Engine Mount

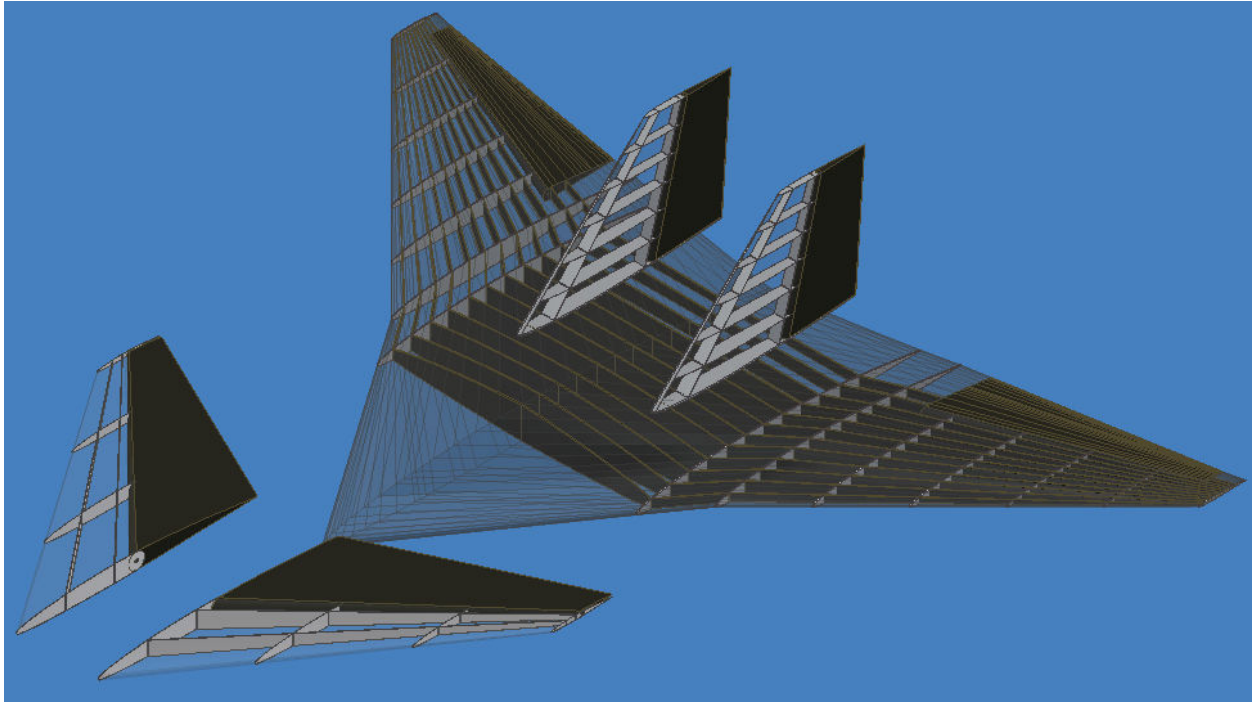


Figure7.5. Structural drawing of the wing, canard and vertical tails.

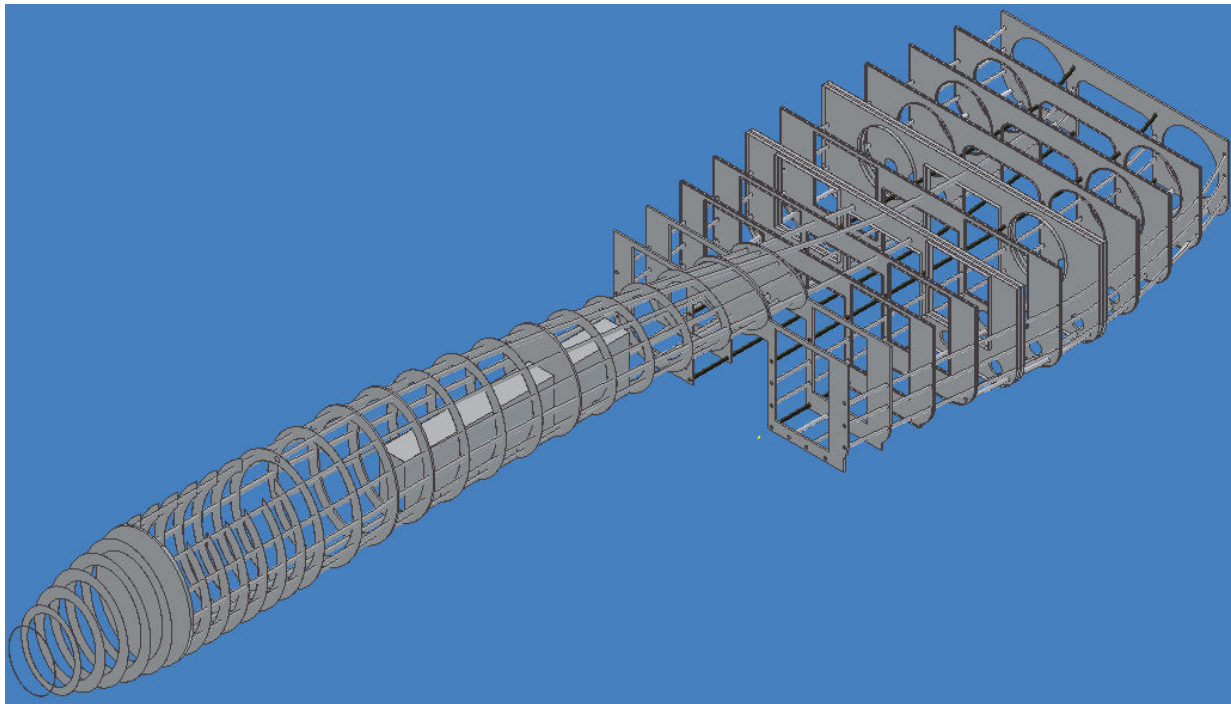


Figure 7.6. Structural drawing of the fuselage.

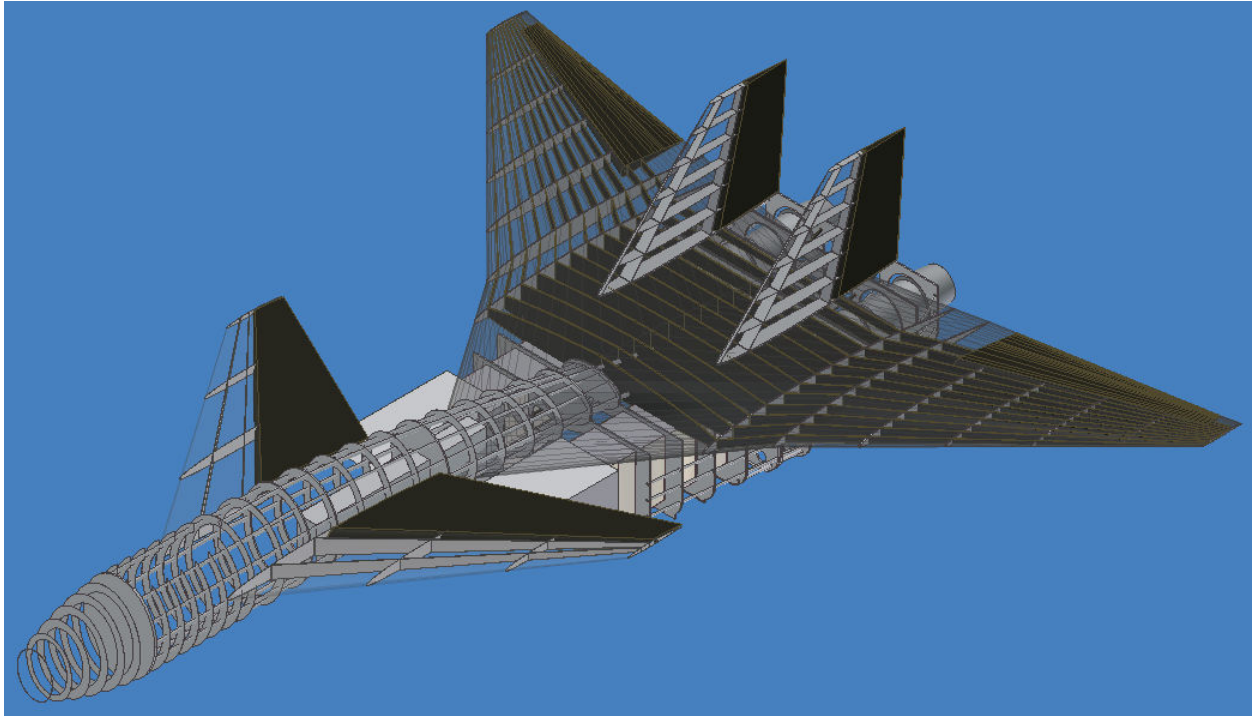


Figure 7.7. Structural drawing of all components and control surfaces.

8. Weights and Balance

8.1 Structural Weight

For weight predictions, historical scaling factors are used to calculate the weight of each component of the aircraft. This method accounts for the size and geometry of the aircraft in order to find the weight of the empty structure. A table of scaling factors and multipliers is shown below.

Table 8-1. Table of scaling factors, multipliers and approximate locations for calculating empty structural weight.⁴

	lb/ft ²	Multiplier	Location
Wing	9	$S_{\text{exposed planform}}$.4 MAC
Horizontal Tail	4	$S_{\text{exposed planform}}$.4 MAC
Vertical Tail	5.3	$S_{\text{exposed planform}}$.4 MAC
Fuselage	4.8	$S_{\text{wetted area}}$.45 length
Landing Gear	0.03	TOGW	
Installed Engine	1.3	Engine Weight	
“All-Else Empty”	0.17	TOGW	.45 length

From this simple formula, an Excel Spreadsheet is developed to do calculations with the above inputs for each of the components. The maximum take off ground weight was assumed to be the weight predicted in the

mission analysis. Beyond the structure and fuel of the aircraft, there are other systems and items that need to be included in the aircraft. The notably heavy systems include the ICNIA and INEWS, each weighing 100 lb, the electrical systems, weighing 300 lb, the ejection seat, weighing 160 lb, and the active array radar, weighing 450 lb. The ejection seat and active array radar will be significant for calculating the center of gravity because they add 600 lb near the nose of the aircraft. Weapons also pose large weights. For the “Defensive Counter-Air Patrol Mission,” two Sidewinders, 2 AMRAAMs, and the 20 mm cannon will need to be attached to the aircraft. For a table of weights for the government furnished equipment, refer to Appendix C.

Table 8-2. Table of weights for each aircraft components.

Component	Weight	X_{cg} (from nose, ft)	Z_{cg} (ft)
Wing	7139.3	53.1	0.0
Vertical Tail	805.6	57.1	4.5
Fuselage	3590.4	32.0	3.0
Landing Gear - Nose	255.8	50.4	-1.0
Landing Gear - Main	1449.6	50.4	-1.0
Installed Engine	6892.6	57.8	0.0
Systems	8268.8	29.4	0.1
2 AMRAAM	654.0	55.0	-1.0
2 Sidewinders	382.0	47.0	0.0
Cannon	575.0	9.0	3.0
Canard	1202.6	28.3	1.0

As a result the total empty weight is 30,179 lbs with a center of gravity at 70.4% of the total aircraft length or 12% of the mean aerodynamic chord. The vertical center of gravity is located at 3.4 inches above the center of the wing. The maximum take off weight is 52,649 lbs which accounts for additional weight from the fuel and the weapons. Fully loaded, the center of gravity is at 76.6% of the total length or 34% of the mean aerodynamic chord.

8.2 Fuel Weight and Corresponding Cg Shift

The fuel weight is another element with significant contribution to the weight. The fuel weight is calculated by using the mission analysis which predicted the take off ground weight and fuel fractions for each leg of the mission. The predicted fuel weights for each mission are presented in Table 8-3.

Table 8-3. Fuel weights predicted by mission analysis for each mission.

	Fuel Weight (lb)
Defensive Counter-Air Patrol Mission	21,433
Point Defense Intercept Mission	4,393
Intercept/Escort Mission	9,028

With the addition of the fuel, the aft *cg* is determined and in combination with the fuel fractions from the mission analysis, there is a shift in center of gravity which is plotted with the *cg* in percent of length of the total aircraft and also the weight as a function of *MAC* in Figures 8.1 through 8.6.

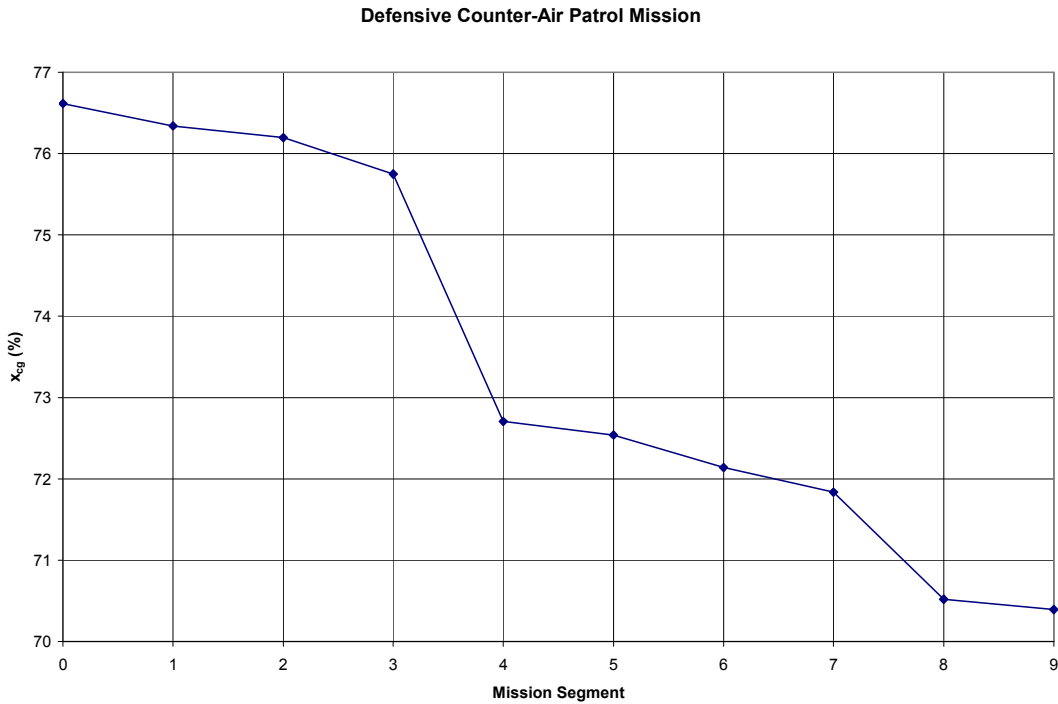


Figure 8.1. Plot of *cg* location during the Defensive-Air Patrol Mission

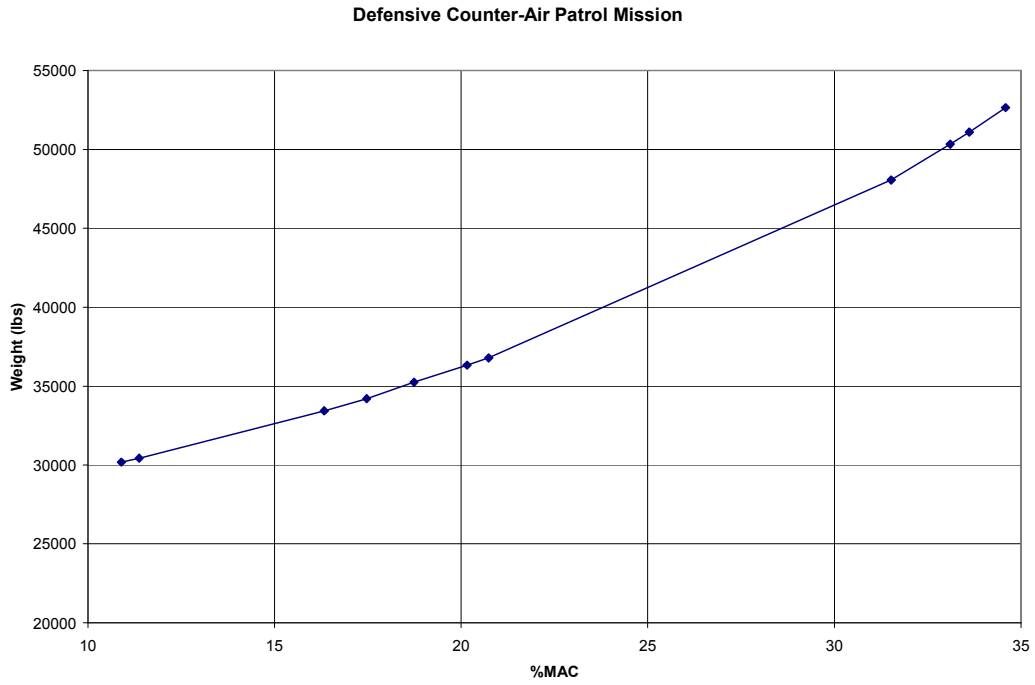


Figure 8.2. Plot of cg location as a function of *MAC* during the Intercept/Escort Mission.

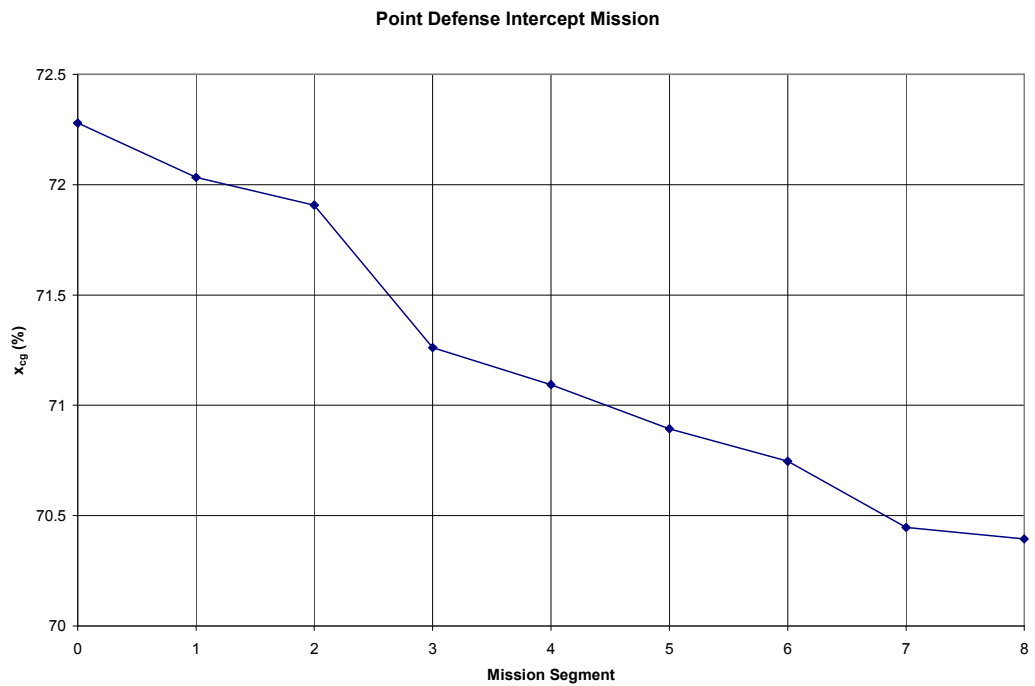


Figure 8.3. Plot of cg location during the Point Defense Intercept Mission.

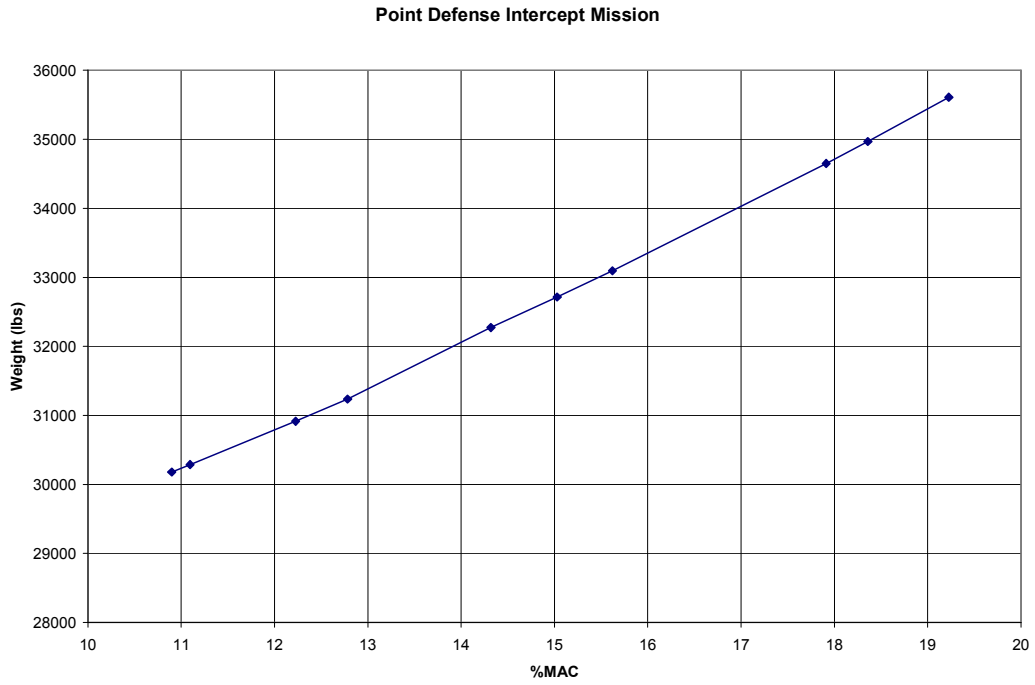


Figure 8.4. Plot of cg location as a function of MAC during the Point Defense Intercept Mission.

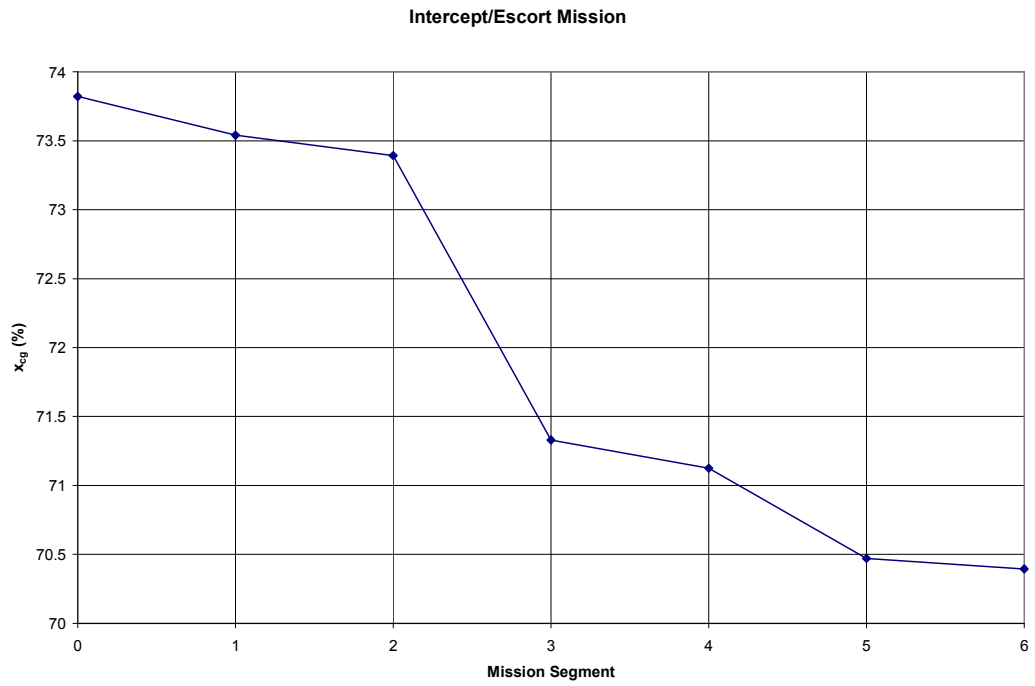


Figure 8.5. Plot of cg location during the Intercept/Escort Mission.

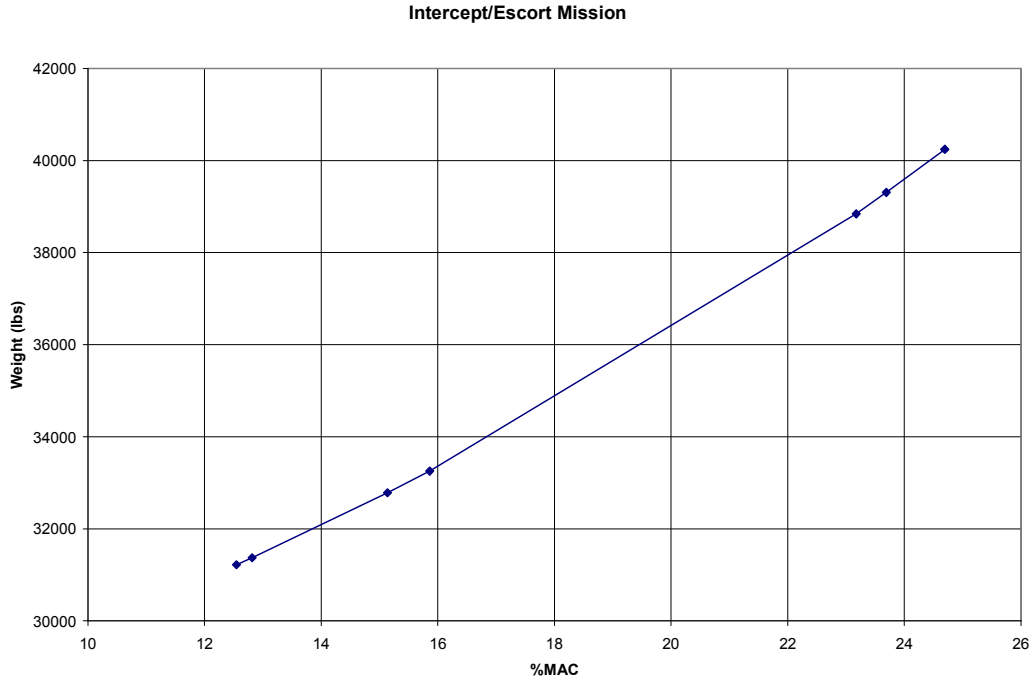


Figure 8.6. Plot of cg location as a function of *MAC* during the Intercept/Escort Mission.

8.3 Mass Moments of Inertia

Similar to the weight calculations, historical data was used to calculate the mass moments of inertia.¹⁸ Using the length, the span, take off weight, empty weight, and configuration the moments are calculated using the following equations. The axis were taken so that I_{xz} would equal zero.

$$I_{xx} = \frac{b^2 W_{TO} R_x^2}{4g} \quad (8.1)$$

with $R_x = 0.251$

$$I_{yy} = \frac{L^2 W_{TO} R_y^2}{4g} \quad (8.2)$$

with $R_y = 0.368$

$$I_{zz} = \frac{\left(\frac{b+L}{2}\right)^2 W_{TO} R_z^2}{4g} \quad (8.3)$$

with $R_z = 0.482$

The resulting mass moments of inertia were calculated as $I_{xx} = 64,433 \text{ slug-ft}^2$, $I_{yy} = 226,125 \text{ slug-ft}^2$, and $I_{zz} = 308,283 \text{ slug-ft}^2$.

9. Stability and Control

9.1 Canard and vertical tail sizing

The horizontal stabilizer concept is a lifting canard that is design to carry 23.5% of the total aircraft lift. The canard was sized using the X-plot shown in Figure 9.1.

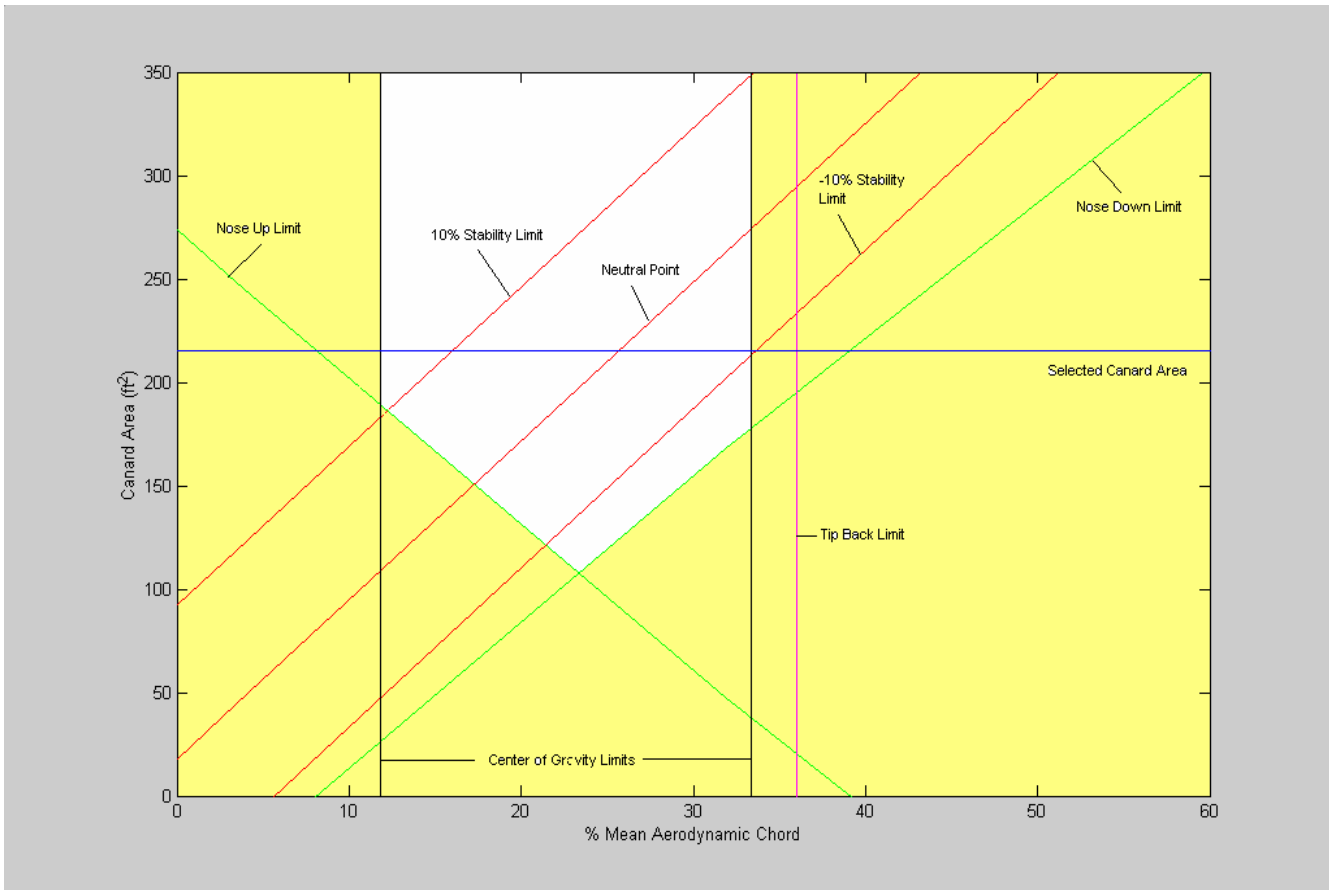


Figure 9.1. X-plot used to size canard. White region denotes canard areas capable of completing mission. A canard area of 215 ft² was selected for the homeland defense interceptor.

NASA Langley's VLMpc code was used to find the neutral point at 23.7% of the wing mean aerodynamic chord. Both the nose up and nose down criteria were calculated using methods from Roskam.¹⁹ The canard was sized specifically for the Defensive Counter-Air Patrol mission because it had the greatest cg shift. However, the cg shift for this mission is so large that the aircraft is unable to meet the $\pm 10\%$ static margin requirement for the RFP. The canard area was chosen so that the static margin was -10% at takeoff. This corresponds to a canard area of 215 ft².

At landing, the aircraft has a +12% static margin. The aircraft is better off being too stable after completing the bulk of the mission (loiter, dash, combat) than starting out too unstable. The remainder of the canard geometry was determined from similar existing designs. A summary of the canard geometry is shown in Table 9-1.

Table 9-1. Canard geometry parameters.

Span	23 ft
Area	215 ft ²
Leading Edge Sweep	55°
Trailing Edge Sweep	25°
Root Chord	14.878 ft
Tip Chord	3.817 ft
Mean Aerodynamic Chord	10.434 ft
Taper Ratio	0.257
Aspect Ratio	2.46

The aircraft uses a conventional vertical tail design. The vertical tail was sized using tail volume coefficients from Raymer.⁴ Other tail geometrical parameters were determined from similar aircraft designs. The vertical tail geometry is summarized in Table 9-2.

Table 9-2. Vertical tail geometry parameters.

Half-Span	8 ft
Area	144 ft ²
Leading Edge Sweep	45°
Trailing Edge Sweep	85°
Root Chord	12.65 ft
Tip Chord	5.35 ft
Taper Ratio	0.423
Aspect Ratio	1.78

Planviews of the canard and vertical tail geometry are shown in the following section.

9.2 Control surfaces and trim

The aircraft uses an elevator on the trailing edge of the canard for pitch control, as seen in Figure 9-2. The elevator has an area of 102.4 ft², and it covers 100% of the canard span and 50% of the canard chord. The large elevator area is necessary since the moment arm for the canard is smaller than the moment arm for a traditional aft horizontal tail. Most similar aircraft designs use all-moving canards rather than trailing edge devices. However, trailing edge devices are superior for this particular design for two reasons. First, the canard will be mounted behind

the canard and firing above it, all-moving canards would interfere with this process. Also, because of the shape of the fuselage, an all moving canard would not remain in contact with the fuselage when deflected.

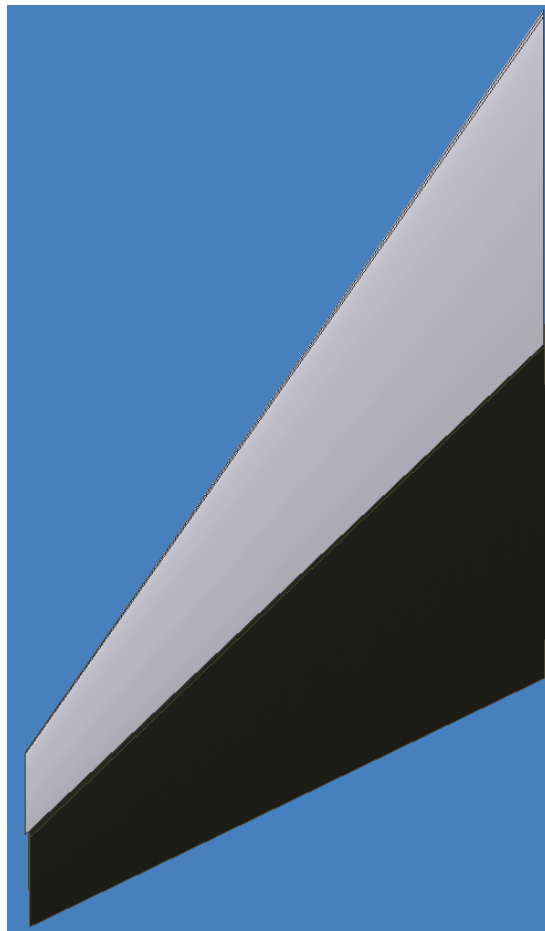


Figure 9.2. Top view of the canard showing the elevator in black.

Yaw moment is generated by flaps on the vertical tail, seen in Figure 9.3. The rudder has an area is 65.9 ft^2 which is 9.4% of the vertical tail span and 35% of the vertical tail chord. All control surfaces were sized using historical data from Raymer.⁴

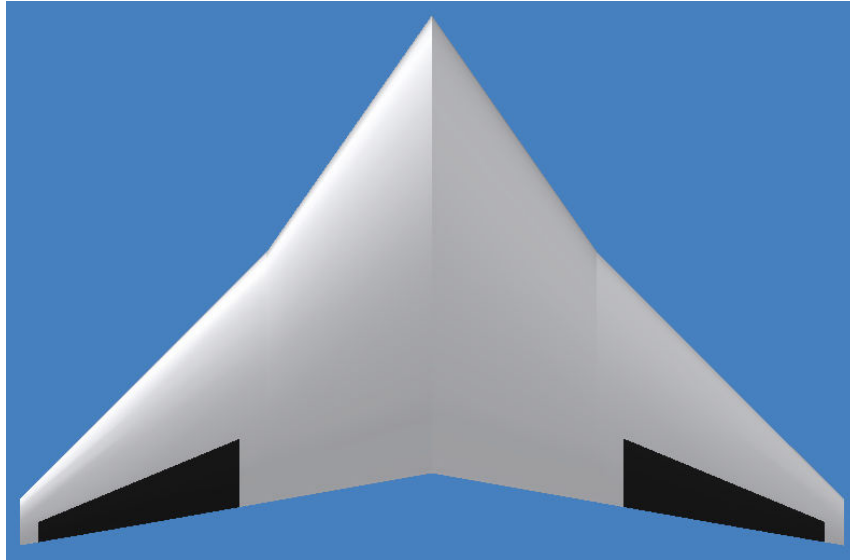


Figure 9.3. Top view of the wing showing the flaperons in black.

Yaw moment is generated by a rudder on the vertical tail, seen in Figure 9.4. The rudder has an area of 45.8 ft². The rudder covers 100% of the vertical tail span and 35% of the vertical tail chord. All control surfaces were sized using historical data from Raymer.⁴

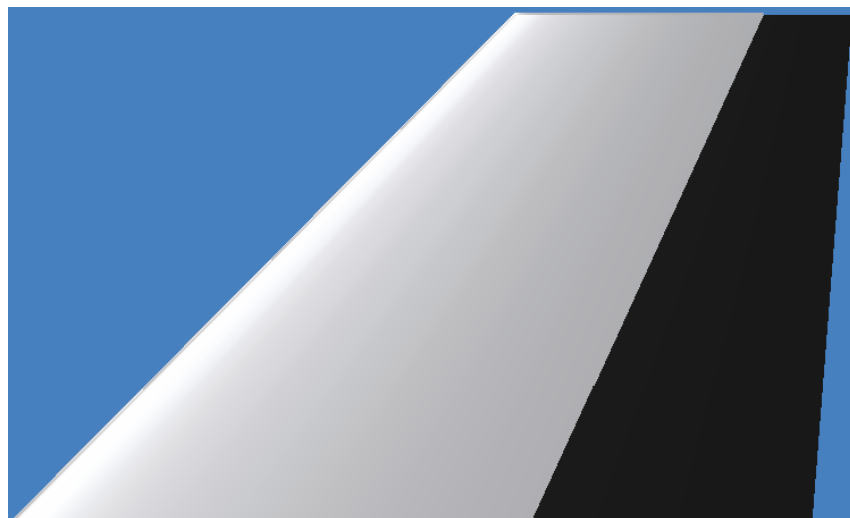


Figure 9.4. Side view of the vertical tail with the rudder shown in black.

The elevator is able to effectively trim the aircraft in all mission phases. Trim analysis was done using both JKayVLM and the Air Force's Digital DATCOM. Takeoff and landing respectively require 14.5° and 17.3° elevator deflections. Cruise and loiter respectively require 8.8° and 10.5° elevator deflections. The dashing portion of the mission requires a 15.1° elevator deflection.

9.3 Stability and control derivatives and flying qualities

The aircraft stability and control derivatives were calculated using the Air Force's Digital DATCOM.⁸ These derivatives were calculated for the most critical portions of the Defensive Counter-Air Patrol mission and were used to determine aircraft stability and flying qualities. The DATCOM analysis was performed at the conditions shown in Table 9-3. The results from the DATCOM analysis are summarized in Table 9-4.

Table 9-3. Flight conditions used in Digital DATCOM analysis to find stability and control derivatives.

	Takeoff	Cruise	Loiter	Dash	Landing
Mach Number	0.15	0.75	0.75	2.20	0.25
Altitude (ft)	sea level	28,000	35,000	35,000	sea level
C.G. (% of m.a.c.)	33.4	30.3	21.0	20.3	11.8

Table 9-4. Homeland defense interceptor stability and control derivatives. Stability and control derivatives calculated using USAF Digital DATCOM.

	Takeoff	Cruise	Loiter	Dash	Landing
$C_{L\alpha}$	3.14284	3.15765	3.13893	2.618921	3.08921
$C_{M\alpha}$	0.311047	0.20828	-0.085947	-0.25453	-0.36766
C_M/C_L	0.09897	0.06596	-0.027381	-0.09364	-0.11902
C_{Lq}	9.7593	10.54717	8.66923	6.81394	8.5923
C_{Mq}	-4.92183	-5.29058	-4.36412	-4.46193	-4.48291
$C_{L\delta e}$	1.31593	1.37125	1.29032	1.19381	1.28342
$C_{M\delta e}$	-0.75912	-0.76139	-0.71203	-0.69104	-0.72301
$C_{L\delta a}$	-0.2859	-0.2859	-0.2859	-0.2318	-0.2859
$C_{N\delta a}$	-0.00359	-0.00359	-0.00359	-0.00288	-0.00359
$C_{Y\delta r}$	0.15253	0.15334	0.15121	0.09987	0.15145
$C_{L\delta r}$	0.01753	0.01703	0.008295	0.007103	0.007932
$C_{N\delta r}$	-0.03729	-0.03645	-0.037154	-0.03402	-0.03702
$C_{Y\beta}$	-0.25701	-0.26139	-0.252134	-0.00112	-0.2491
$C_{N\beta}$	0.02413	0.02473	0.023997	0.001795	0.02439
$C_{L\beta}$	-0.02301	-0.02314	-0.0228193	-0.01012	-0.02282
C_{Yr}	0.1396	0.1456	0.1387	0.11839	0.1382
C_{Nr}	-0.03773	-0.03788	-0.036392	-0.03231	-0.03618
C_{Lr}	0.01423	0.01469	0.01399	-0.01272	0.01402
C_{Lp}	-0.31839	-0.37307	-0.291032	-0.24103	-0.28993
C_{Np}	-0.09313	-0.09583	-0.092214	-0.08771	-0.09194

The aircraft is longitudinally unstable during takeoff and cruise. A computerized flight control system will be necessary to aid the pilot during these phases. By the beginning of the loiter segment, the aircraft becomes stable. As discussed previously, the aircraft actually becomes too stable (by the RFP's standards) at landing. Longitudinal

stability analysis is shown for each mission in Table 9-5. The pitch stiffness CN_{β} is positive during each mission segment which means that the aircraft exhibits directional stability. The negative CL_{β} during each phase shows that a restoring moment keeps the aircraft stable in roll. Because the aircraft has no dihedral, this effect is most likely generated by the design's high wing sweep. It is also important to note that all of the control surfaces become less effective during the supersonic dash portion of the mission

Table 9-5. Static margin at crucial points in flight envelope.

	Defensive Counter-Air Patrol Mission	Point Defense Intercept Mission	Intercept/Escort Mission
Takeoff	-0.09897	0.04332	-0.02896
Cruise	-0.06596		
Loiter	0.02738		
Dash	0.09364	0.08088	0.0769
Escort			0.08544
Return Cruise	0.11446	0.10422	0.11617
Landing	0.11902	0.11902	0.11902

The flying qualities were calculated using methods from both Roskam¹⁹ and Etkin and Reid.⁹ The aircraft is designed to have the highest level (Level 1) flight qualities. The aircraft successfully meets the flying qualities designated by MIL-F-8785C. Flying quality analysis is summarized in Table 9-6. (Class A and C) and Table 9-7. (Class B).

Table 9-6. Level 1 flying qualities (Class A and C).

Class A and C Flying Qualities				
	Minimum	Maximum	Takeoff	Landing
$\zeta_{S.P.}$	0.35	1.3	0.956	0.957
$\omega_{S.P.}$	0.28	3.6	0.426	0.428
ζ_{Ph}	0.04		0.614	0.617
$\zeta_{D.R.}$	0.19		0.203	0.204
ω_{Sp}	0.4		0.457	0.459
$T_{1/2Sp}$ (sec)	12		7.58	7.62
T_r		1	0.897	0.873
T_{30° (sec)		1.1	0.998	1.003

Table 9-7. Level 1 flying qualities (Class B).

Class B Flying Qualities					
	Minimum	Maximum	Cruise	Loiter	Dash
$\zeta_{S.P.}$	0.3	2	1.253	1.126	0.891
$\omega_{S.P.}$	0.085	3.6	0.791	0.784	0.519
ζ_{Ph}	0.04		0.419	0.399	0.062
$\zeta_{D.R.}$	0.08		0.279	0.267	0.112
ω_{Sp}	1		0.936	0.922	1.037
$T_{1/2Sp}$ (sec)	20		8.354	8.325	15.185
T_r		1.4	0.713	0.697	1.368
t_{30° (sec)		1.1	0.879	0.873	1.091

10. Systems and Avionics

The systems and avionics are essential components of any aircraft. These components provide the aircraft the ability to function properly and to communicate with the pilot. The systems of a fighter aircraft are particularly important due to the type of missions involved in defense. The aircraft needs to identify, track, and act upon any possible hostile threats. This information needs to be communicated effectively to the pilot in a precise and timely manner. The aircraft also needs a mechanism to protect the aircraft from any possible attacks. This is accomplished with set of complex systems that provide the necessary information and response needed to be a dominant role in modern military defense.

10.1 Integrated Avionics

The avionics used in this aircraft are completely integrated and controlled by one unit. This gives an advantage over separately installed systems. There is no need for separate controls for each component of the avionics, which is beneficial to the cost and weight of the aircraft, and frees any interior volume in the aircraft that can house other components and fuel. The integration of the avionics also provides enhanced situation assessment of the surrounding environment of the aircraft and is communicated more effectively to the pilot through the use of a computer controlled program. The integrated avionics include an Integrated Electronic Warfare System (INEWS), an Active Array Radar, and an Infrared Search and Tracking System (IRSTS). These systems are all controlled by a Common Integrated Processor (CIP).

10.2 Common Integrated Processor

The CIP is the control unit of the integrated avionics and is provided by Raytheon. This unit supports all of the signal and data processing from all avionics. It has the ability to control “mission processing and sensor fusion; radar signal and data processing; integrated electronic warfare processing; and integrated communications, navigation,

and identification processing applications.”²⁰ The CIP is a collection of 66 modular slots that allow for future upgrades and has the power of two Cray supercomputers. The CIP has a general purpose processing capacity of up to 2000 million instructions per second and a signal processing capacity of up to 50 billion operations per second.²¹

The INEWS shown in Figure 10.1 is the Advanced Self-Protection Integrated Suite (ASPIS) provided by Raytheon. The ASPIS includes a Threat Warning System, DRFM-Based Jammer, and a Countermeasures Dispenser System. The Threat Warning System is model AN/ALR-93(V) manufactured by Northrop Grumman. The DRFM-Based Jammer is model AN/ALQ-187 manufactured by Raytheon. The Countermeasures Dispenser System is model ALE-47 manufactured by BAE Systems.



Figure 10.1. Integrated Electronic Warfare System. ASPIS. Warning system, Jammer, Countermeasures.²²

The ALR-93 provides threat radar detection, identification and warning in dense signal environments. It also controls the countermeasures deployment of the suite. The ALQ-187 has the ability to “counter modern pulse, pulse Doppler, and continuous wave threats in a dense signal environment, including surface-to-air and air-to-air as well as anti-aircraft artillery.”²¹ The ALQ-187 also has the benefit to provide coverage forward and aft of the aircraft. The ALE-47 Countermeasures Dispenser System is the last line of defense for the aircraft. The system “provides an integrated, threat adaptive, reprogrammable, dependable, computer-controlled capability for dispensing” countermeasures.²¹ It also has the ability to release the correct type and amount of countermeasure.²¹

10.3 Fire Control Systems

The fire control systems include an Active Array Radar, shown in Figure 10.2, and an IRSTS, shown in Figure 10.3. Both of these systems are provided by Raytheon. The Active Electronically Scanned Array Radar (AESA) is model AN/APG-79, and the Advanced Targeting Forward-Looking Infrared Pod (ATFLIR) is model AN/ASQ-228.

The AESA radar system provides simultaneous detection and tracking of ground vehicles and other aircraft. It has the ability to actively scan the surrounding environment at “nearly the speed of light.”²³ Two important benefits of this particular radar system is the use of commercial off-the-shelf (COTS) components and no maintenance for an estimated 10 to 20 years.



Figure 10.2. AESA. Active Array Radar, AESA-79 provided by Raytheon.²³

The ATFLIR provides the aircraft with precision targeting and tracking of both ground vehicles and other aircraft. It has long range capabilities of up to 40 nautical miles, and high altitude capabilities up to 50,000 feet. This model houses all its components into a single pod and uses COTS components, which provides for easier maintenance and repairs.^{23, 24}



Figure 10.3. ATFLIR. Forward Looking Infrared Radar provided by Raytheon.²⁴

10.4 Cockpit Layout and Instrumentation

The cockpit instrumentation used in this aircraft is based off the F-22 Raptor instrumentation layout in order to take full advantage of the integrated avionic system. The layout of the panel is shown in Figure 10.4. It is an all digital design that includes a Head-Up Display (HUD), Integrated Control Panel (ICP), two Up-Front Displays, a single primary Multifunction Display (MFD), and three secondary MFDs. All the information of the avionics is displayed on six Liquid Crystal Displays (LCD) that provide the benefit of lower power consumption and less size and weight than traditional Cathode-Ray Tube (CRT) displays.²⁵

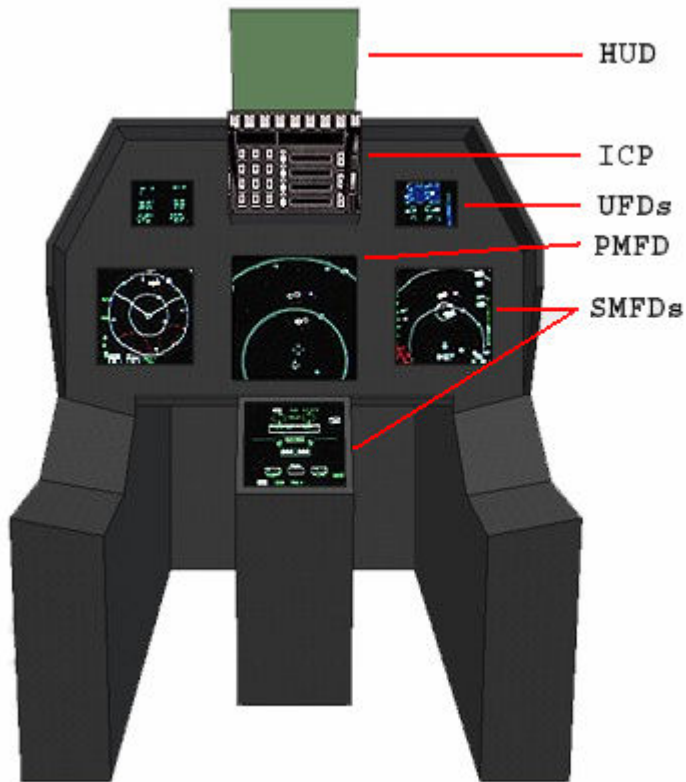


Figure 10.4. Cockpit Instrument Panel. Layout of displays.

The HUD is manufactured by GEC-Marconi and is the primary flight instrument for the pilot. This display uses the same tactical symbols as the Head-Down Displays (HDD). The ICP is located below the HUD and provides the pilot with manual data entry capability including communications, navigation, and auto-pilot functions. There are two Up-Front Displays (UFD) located on either side of the ICP. The UFDs display “Integrated Caution/Advisory/Warning (ICAW) data and communications/ navigation/ identification (CNI) data and serves as the Stand-by Flight instrumentation Group and Fuel Quantity Indicator (SFG/FQI).”²⁵ The SFG is used for displaying an artificial horizon to fly the aircraft. Located in the center of the instrument panel is the primary MFD which displays navigation and situation assessment. The three secondary MFDs located on either side and below the primary MFD display tactical and non-tactical information.²⁵

Another important component of the cockpit is the Advanced Concept Ejection Seat (ACES). The ACES was developed in the 1970’s to provide a universal ejection seat for U.S. fighter aircraft. The ACES II is a third-generation model and operates in three modes. Mode 1 is for low speed/low altitude conditions up to a speed of 250 knots. In Mode 1 the parachute is inflated in less than two seconds. Mode 2 is capable of deploying the parachute in

less than 6 seconds and is rated up to the maximum speed of 600 KEAS. Mode 3 is for high speed/high altitude conditions in which parachute inflation occurs when either Mode 1 or Mode 2 is reached.²⁶



Figure 10.5. ACES II Ejection Seat.²⁶

10.5 Additional Equipment

There are two gas generation systems included in this aircraft. The two systems include an Onboard Oxygen Generation System (OBOGS) and an Onboard Inert Gas Generation System (OBIGGS). Both of these systems are manufactured by Carleton Life Support Systems. The OBOGS is model OC1077 and provides onboard oxygen to the cockpit. The OBIGGS is model NC1029 and is used to prevent fuel tank ignition by injecting the fuel tank with nitrogen-enriched gas to reduce the oxygen level.^{27, 28}

10.6 Cockpit Layout

Figure 10.6 shows a basic layout of the cockpit and the position of the pilot. The cockpit is roughly nine feet long with a canopy less than two feet high. It has an over nose angle of 11 degrees, a grazing angle of 30 degrees, and a seat-back angle of 30 degrees. The space behind the pilot's ejection seat is the location of the avionics equipment bay. This area also includes room for the 20 mm cannon and ammo drum.

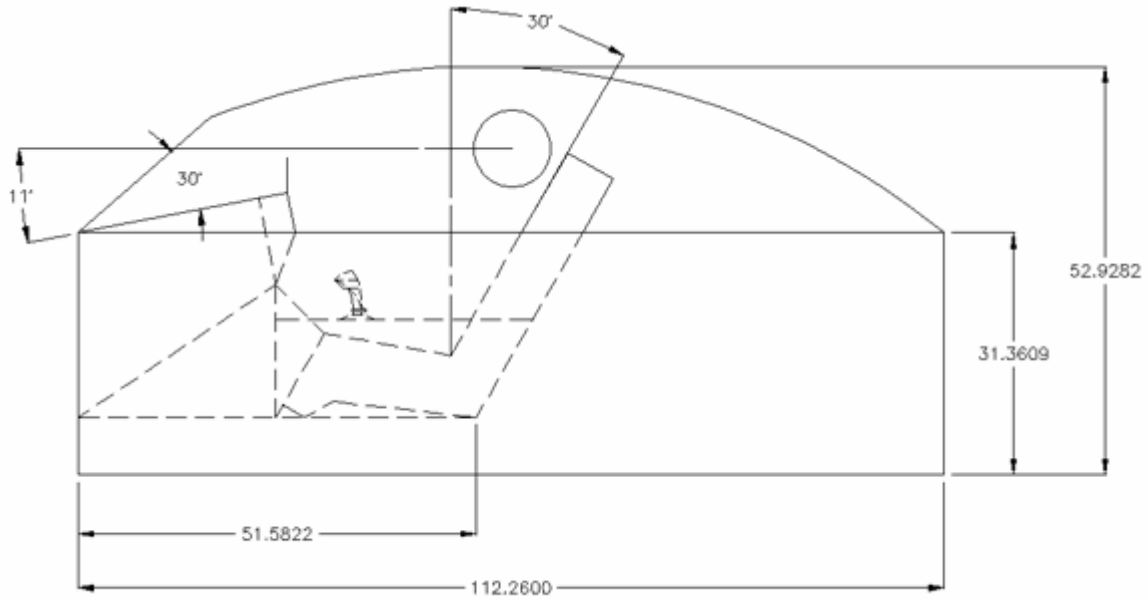


Figure 10.6. Cockpit Layout. View of pilot position in cockpit; dimensions in inches.

10.7 Landing Gear Location and Sizing

Equations and guidelines for the landing gear location and size were obtained from Raymer and Roskam.^{4,30} The aft x_{cg} and z_{cg} locations of the aircraft are 47.5 ft. from the nose, and 0.51 ft. above the wing centerline. To keep the angle from the main gear static position to the z_{cg} greater than the tipback angle, the main gear must be located 2.87 ft. aft of the x_{cg} . The tipback angle is 17 degrees, and the aircraft will sit 40 in. from the ground in its static position. The minimum static load on the nose gear is 10 percent of the total weight of the aircraft to account for proper steering capabilities, which puts the nose gear 28.7 ft. forward of the main landing gears. Figure 10.7 shows the side view, and a view from above the fuselage. The main landing gears are spaced 13 ft. apart with an overturn angle of 57 degrees.

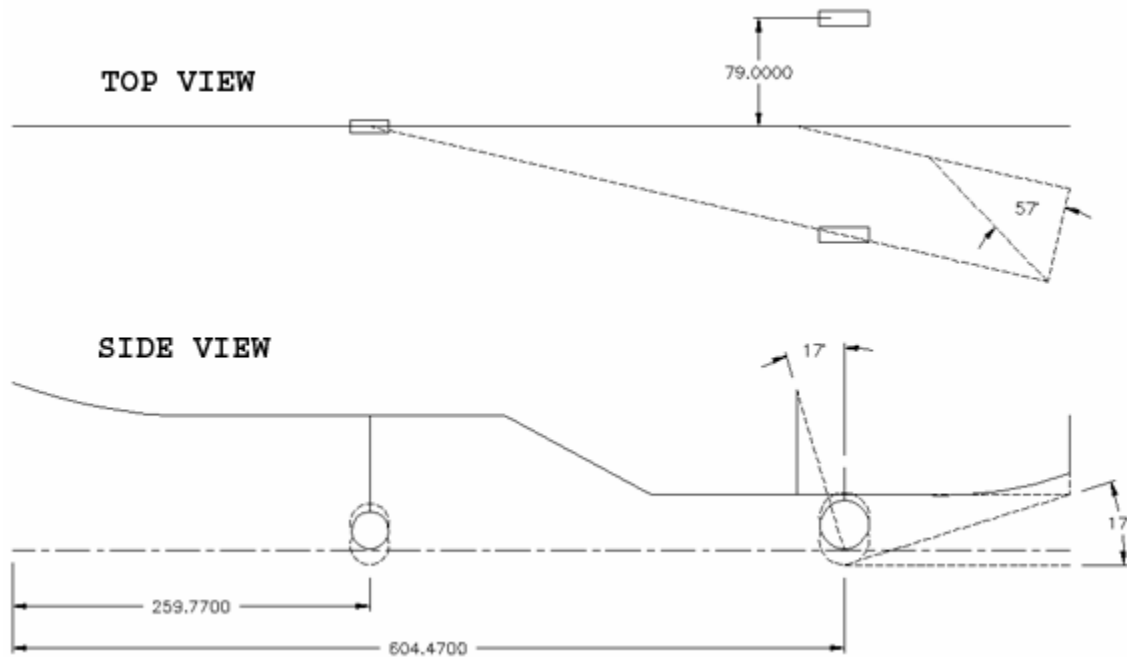


Figure 10.7. Landing Gear Layout. Top and bottom view shown; dimensions in inches.

To find suitable tire sizes the guidelines in Roskam were used.³⁰ The locations of the landing gears were used to find the maximum static loads that must be carried by the tires. The static loads were used to size the tires because they are typically listed by their maximum static loads. Using a 25 percent increase in maximum static loads to account for any future additions to the plane, the maximum static load for each main tire is 29615 lbs. and 15516 lbs. for the nose tire. These load calculations are 18 percent higher than what is necessary for FAR 25 qualification.³⁰ The tire chosen for the main gear is a 36x11 in. Type VII tire. It is capable of carrying a maximum static load of 31500 lbs., and it has an unloaded inflation pressure of 290 psi, a maximum speed of 200 mph, and is MIL qualified. The tire chosen for the nose gear is a 28x9 in. New Design tire. It is capable of a maximum static load of 18100 lbs., and it has an unloaded inflation pressure of 280 psi, a maximum speed of 200 mph, and is MIL qualified. The shocks used in the aircraft are oleoneumatic shock struts, which are typically for modern fighter aircraft. The data listed for the tires, along with the maximum static load calculations and landing gear locations, were used to size the oleoneumatic shock stroke and total strut length, and diameters. The stroke of the shock strut is 16.5 in for both rear and nose gears. The outer diameter of the oleoneumatic shock strut for the main gears is 5.65 in, and the inner diameter is 4.34 in. The nose gear outer diameter is 4.23 in and the inner diameter is 3.25 in. The total length of the shock strut, including the fixed portion, is 2.5 times the stroke.⁴

10.8 Systems Layout

The systems layout was created using a computer aided design (CAD) model using Autodesk Inventor to better visualize the locations of each component. A CAD model of the internal structures, shown in Figure 10.10, was superimposed with the systems CAD model to place the systems in locations where there is available space and structure support. Figure 10.8 shows a profile view of the layout. The integrated avionics and data bus are located in an avionics equipment bay behind the cockpit. The nose of the aircraft will hinge to the side to expose the radar dome for servicing and maintenance. An equipment bay door behind the radar will provide access to the INEWS and Vehicle Management System (VMS). The M61A1 cannon is located behind the avionics equipment bay and is recessed into the fuselage, with the ammo drum centered in the fuselage. The location of the cannon was inspired by the General Dynamics F-16. Initially the nose gear retracted forward before determining that the cannon would prevent it from retracting completely.

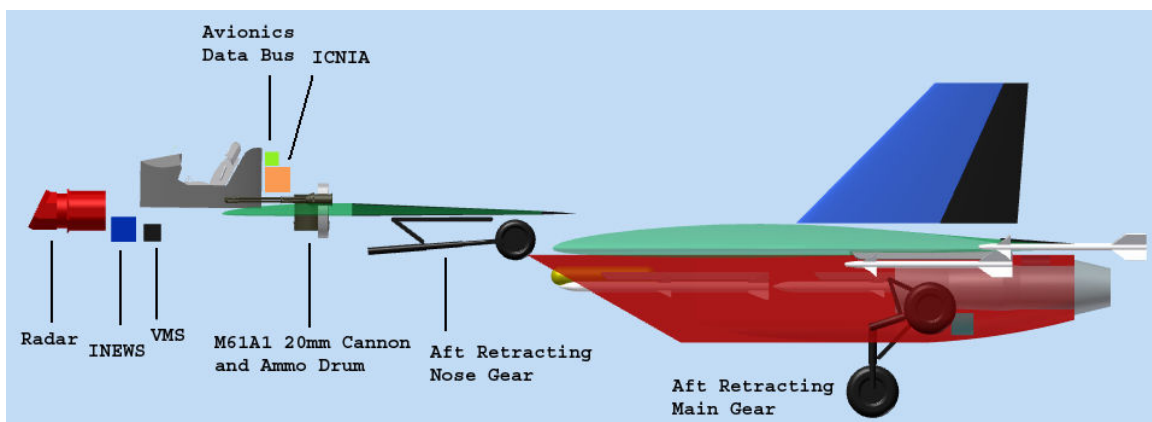


Figure 10.8. Systems Profile View. Layout of avionics and cannon.

Figure 10.9 is a view from the bottom of the fuselage. This view shows the fully loaded missiles capability. There is an AIM-9M Sidewinder located at each wing tip, and in the middle of the wing. There can be a large drag penalty for weapons externally mounted on pylons underneath the wing.⁴ Therefore, during the Mach 2.2 dash requirement the AIM-9M missiles are located on the wing tips to reduce drag penalties. The AIM-120 AMRAAM missiles are conformable to the fuselage between the two inlets to reduce drag as well. The FLIR pod is conformable to the bottom of the fuselage similar to the AIM-120s. This provides a straight line view from the pod forward. The auxiliary power unit (APU) is located in a small pod in the rear of the plane, and the engine driven generators are located below the engines. A pod on each side of the inlets is necessary to accommodate the rear landing gear in its retracted position.

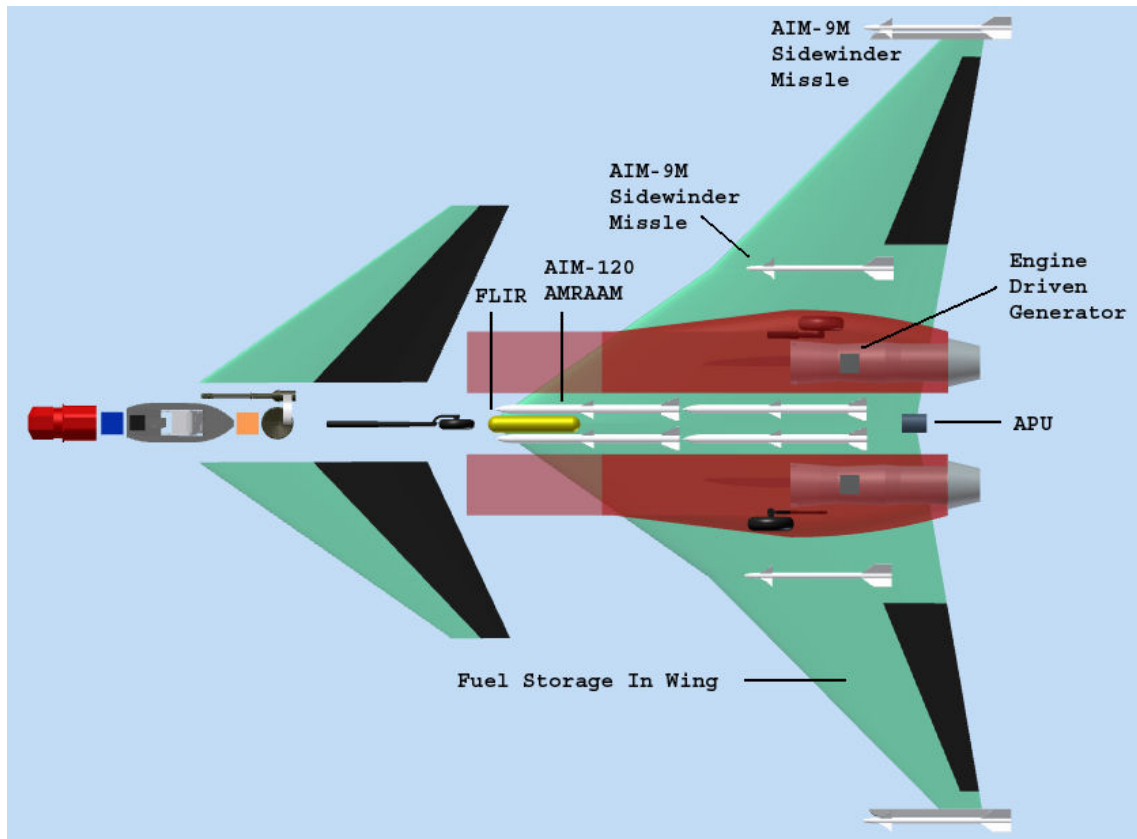


Figure 10.9. Systems Bottom View. Layout of missiles, FLIR, APU, generators.

During the Defensive Counter-Air Patrol mission, the airplane will require an estimated 415 cubic feet of fuel to complete the entire mission. Due to the large area of the wing, throughout final design of the plane the wing was considered the primary location of the fuel storage. To ensure there was sufficient volume to store the fuel in the wing, a CAD model of the wing was produced in Autodesk Inventor, and the volume was calculated as 575 cubic feet. The structure of the wing and the control surfaces on the wing were also modeled, and has a volume of 40 cubic feet and 15 cubic feet respectively. The volume of the wing's skin was also taken into consideration. A conservative estimate of useable volume for fuel storage in wing is 430 cubic feet, which is enough to complete the Defensive Counter-Air Patrol mission, with 15 cubic feet for time during unexpected landing conditions. The fuel storage is shown in Figure 10.11 in yellow.

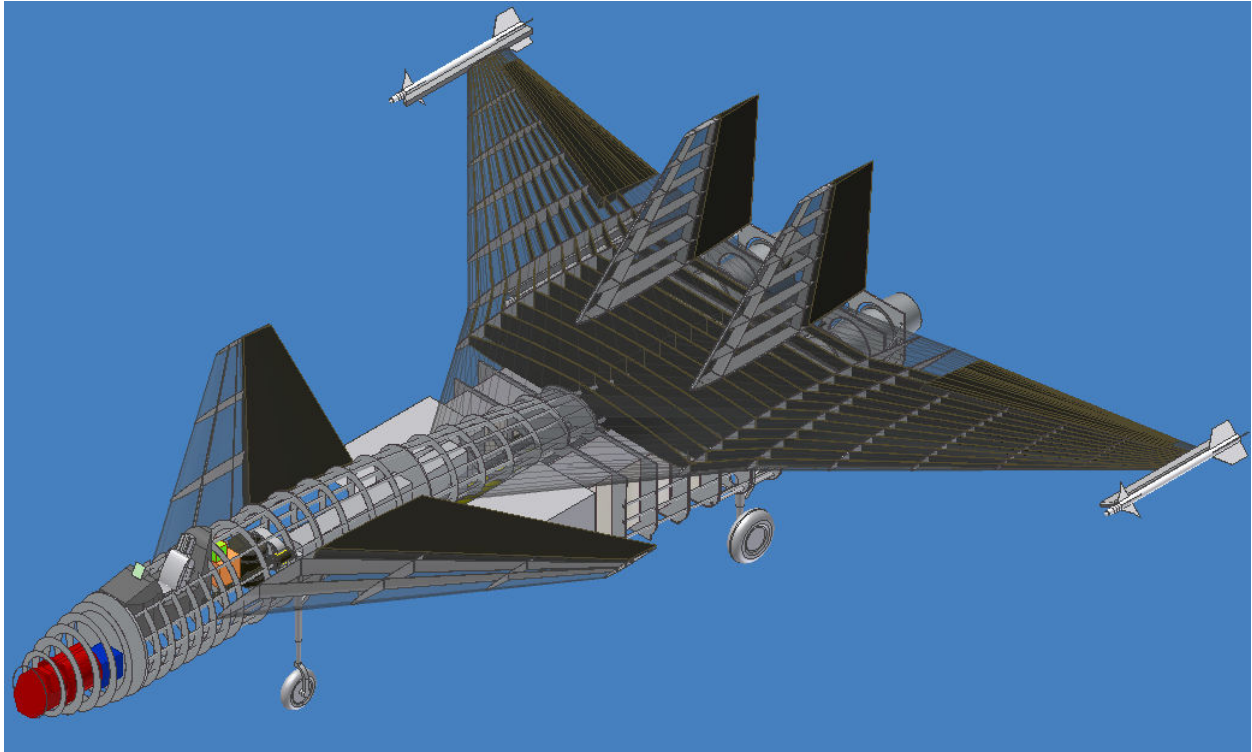


Figure 10.10. Structural drawing with systems integrated.

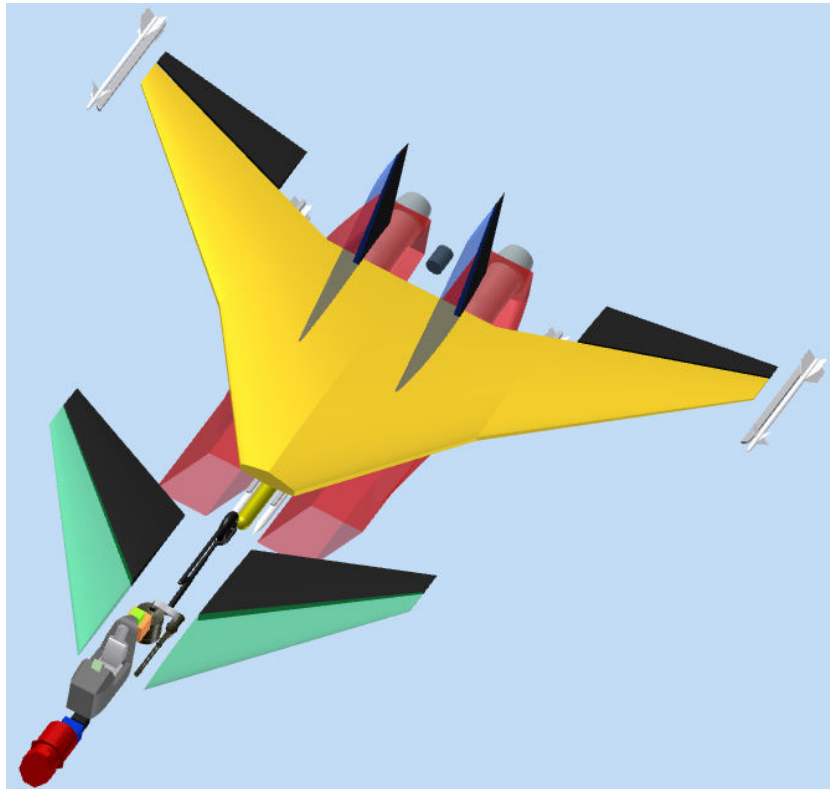


Figure 10.11. Fuel Storage. Fuel tank shown in yellow; approximately 430 cubic feet.

Figure 10.12 is a diagram of the actuator layout. Each control surface will be deflected using a dual-tandem electrohydrostatic actuator (EHA). The EHA is fully packaged hydraulic actuator with its own hydraulic pump, and electric motor. This reduces the amount of weight and volume consumed by a central hydraulic system that includes hydraulic lines throughout the plane to provide power to the actuators. The hydraulic lines of a central hydraulic system are susceptible to enemy fire and structural damage, which can lead to failure to control the aircraft. The EHA's compact design decreases this vulnerability. Each actuator package also provides easy access for servicing and maintenance. Early designs of EHA's were typically avoided in supersonic aircraft due to overheating caused by the high power output required by the actuator. Improvements to EHAs have now been proven effective in modern fighter aircraft. Dual-tandem electrohydrostatic actuators are currently being used in the Lockheed Martin F-35 aircraft, and are designed by MOOG Inc.³¹ Each actuator will be signaled electronically through a fly-by-wire flight control system. For increased safety the actuators will have 4 redundant electrical signals, providing fail-operate/fail-safe capability.³² Each signal will be separate from the other to reduce any interference. This allows for two electrical failures and one hydraulic failure while maintaining full functionality of the actuator.

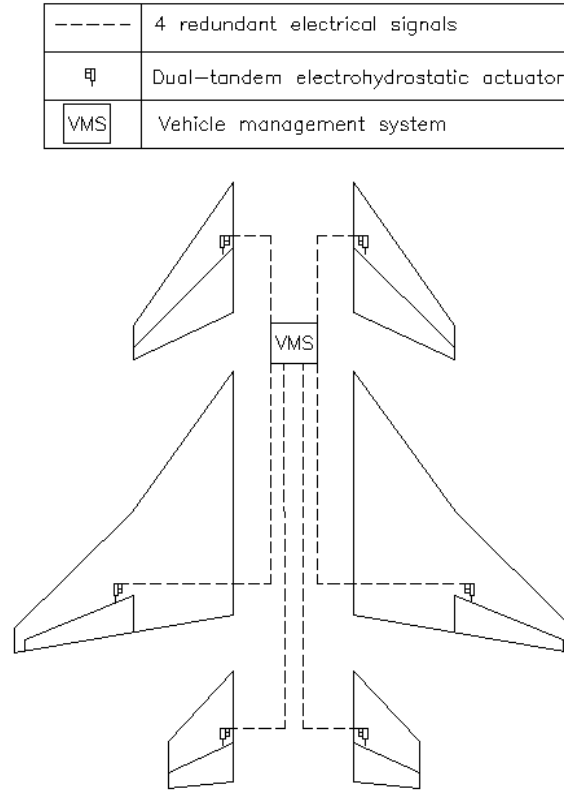


Figure 10.12. Actuator Diagram. Top-down schematic of electrical actuator system.

11. Cost Analysis

One key requirement in the RFP was the minimization of cost, with a flyaway cost of only \$15 million for a 1000 aircraft buy, and at all other times minimizing the lifecycle cost wherever possible. To do this, there were three key areas that were examined. Research, Development, Test, and Evaluation (*RD&E*), Flyaway or Production cost, and Operations and Maintenance (O&M).

It is important that both the size and complexity of the aircraft were taken into consideration as these are factors that can drive the cost of development as well as maintenance up. Another key factor in the evaluation of the cost was the size of the production run. For this the cost was analyzed for a production run of 100, 500, and 1000 units, with the 1000 unit production run being the focus of the \$15 million flyaway cost limit.

11.1 Research Development Test and Evaluation

RD&E was estimated using a conceptual approach for cost analysis from Raymer⁴ known as “DAPCA IV,” or the Development and Procurement Cost of Aircraft Model. This model shows a significant decrease in the cost per unit as the production run is increased. As can be seen in figure 11.1 below, the cost of a 1000 aircraft buy per unit is nearly $\frac{1}{4}$ of the cost per unit of a 100 aircraft buy.

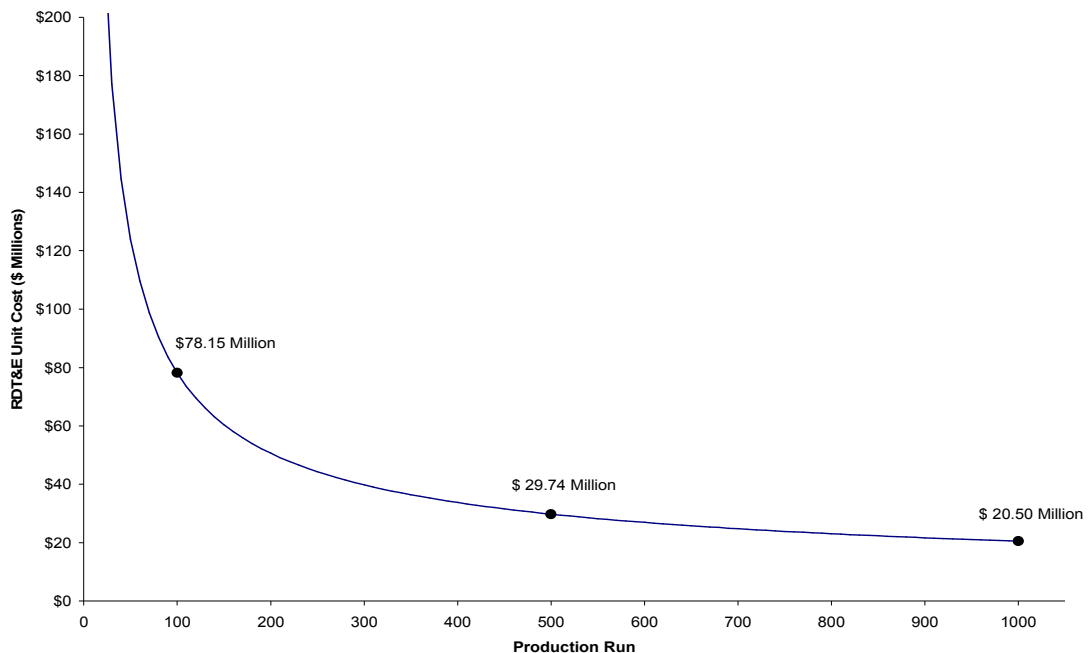


Figure 11.1. *RD&E* Cost Estimation for Production Run

This cost can be expected to decline with time as well as with larger aircraft buys. As seen in Figure 11.2, with just a 95% learning curve, the time to produce additional units decreases as more units are produced.

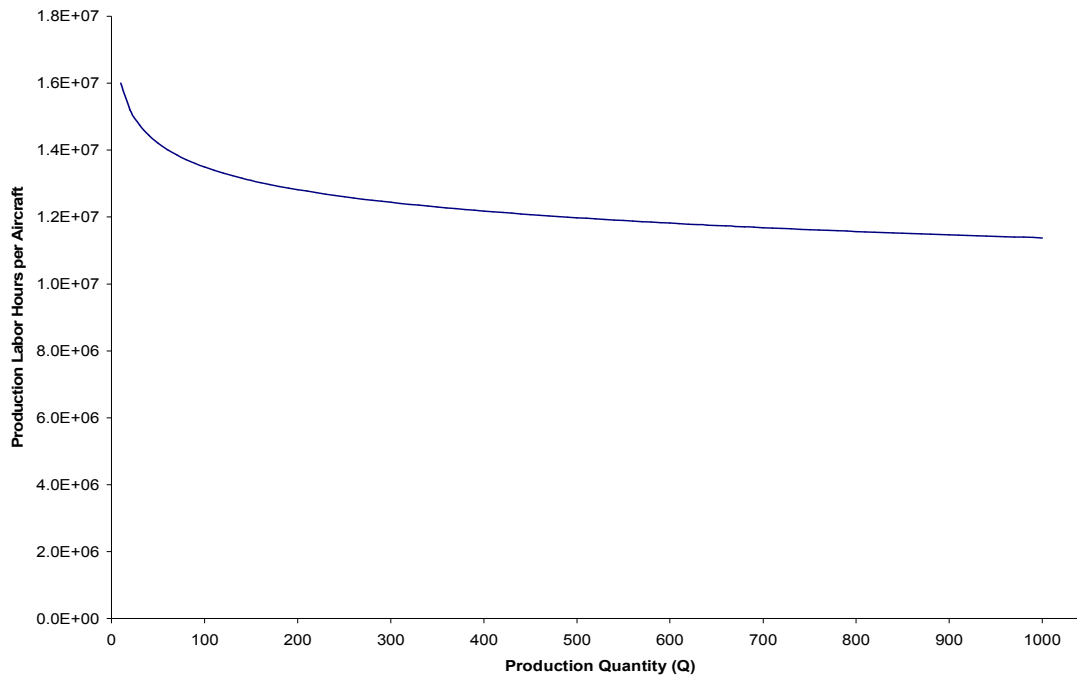


Figure 11.2. Production Learning Curve of 95%

11.2 Flyaway Cost

The flyaway cost consists of the cost of the airframe, the engine, and the avionics, and the labor necessary to manufacture the aircraft and engines. The flyaway cost for a 1000 aircraft buy for this aircraft came out to be \$14.06 million in 2005 US currency as shown in Figure 11.3, which is just below the \$15 million requirement specified in the RFP.³³

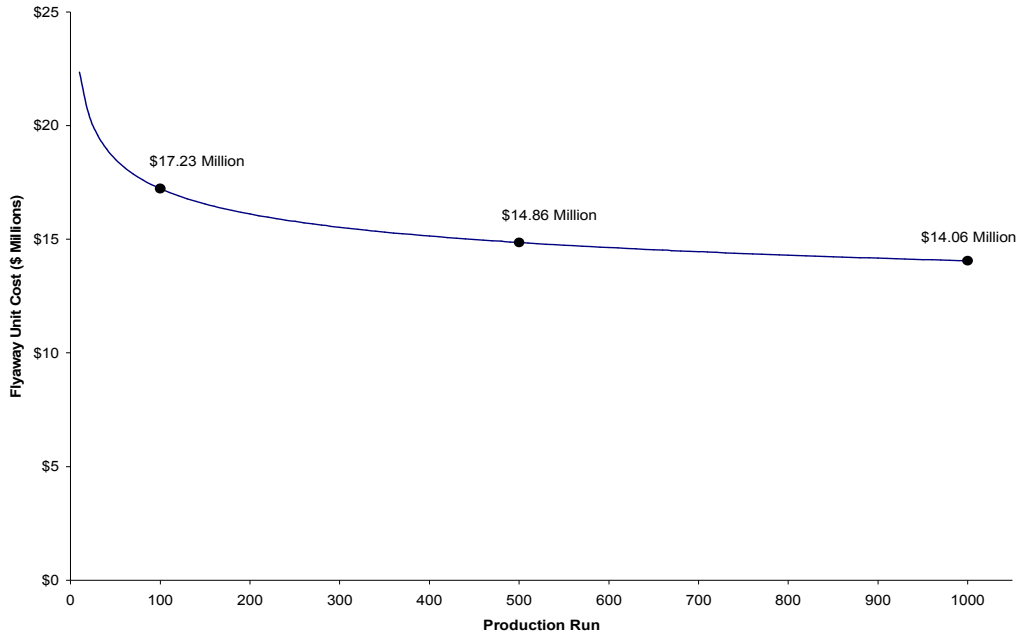


Figure 11.3. Flyaway Cost Estimation for Production Run

As can be seen in the two plots above the total cost of the aircraft without maintenance or operating costs is fairly minimal when compared to other fighters currently in service.

11.3 Operations and Maintenance Costs

The third and final part of the cost analysis is the operations and maintenance costs. These are determined based on how the airplane will be used, as this is a design for use in military service, the cost is fairly high as servicing the airplane is of utmost importance to both the pilot and those on the ground crew. This section of the cost however can be broken up into four other subcategories including fuel and oil costs, crew salaries, maintenance worker salaries, and maintenance expenses. For this design, the totals for a 1000 airplane buy over the course of one year can be seen in Table 11-1 below.

Table 11-1. Operations and Maintenance Cost Breakdown for each Section.

Section	Totals/Unit/yr (1000 unit production run)	% of Total
Fuel	\$12,919,995.00	13.23%
Maintenance Crew Salary	\$30,146,655.00	30.87%
Maintenance	\$43,066,650.00	44.10%
Crew (ground & flight)	\$11,534,151.24	11.81%
Total	\$97,667,451.24	100.00%

As can be see above, the majority of the cost is going towards the actual maintenance of the aircraft itself, be it materials or crew salaries. This is a fairly typical breakdown for a military class airplane.

11.4 Total Cost

The design as it stands right now has a very low overall cost and with a flyaway cost of less than \$15 million is needless to say a cost effective and efficient replacement for aircraft that will be coming out of service in the next 15 years. Table 11-2 Shows the total breakdown of all three portions of the cost of this aircraft and is supplemented with a visual representation in Figure 11.4 below the table.

Table 11-2. Total Initial Cost Breakdown for each Section.

Section	Totals/Unit/yr (1000 unit production run)	% of Total
RDT&E	\$20,500,674.32	15.50%
Flyaway	\$14,055,968.76	10.63%
Fuel	\$12,919,995.00	9.77%
Maintenance Crew Salary	\$30,146,655.00	22.80%
Maintenance	\$43,066,650.00	32.57%
Crew (ground & flight)	\$11,534,151.24	8.72%
Total	\$132,224,094.31	100.00%

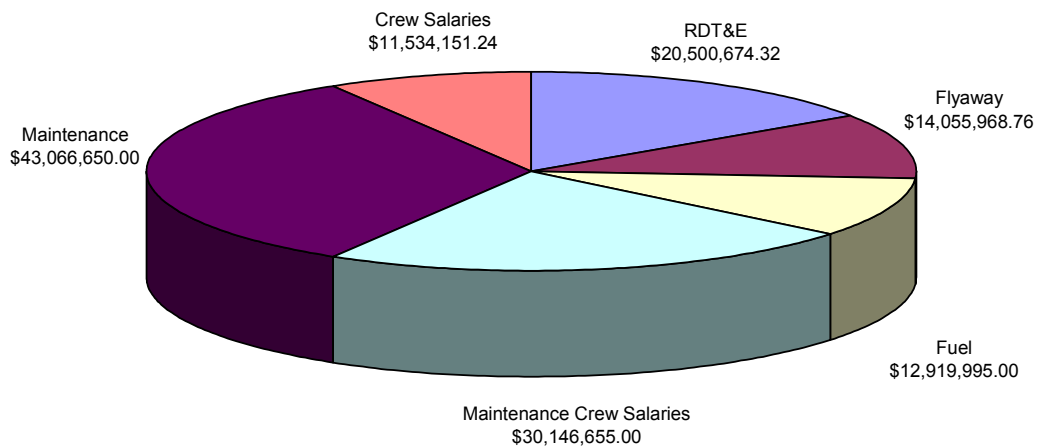


Figure 11.4. Total Cost Breakdown for a 1000 Airplane Buy

In this figure it is evident that the Operations and Maintenance makes up nearly 75% of the total cost of the aircraft, this is due largely to constant inspection and work of the ground and maintenance crews.

11.5 Life-Cycle Cost

For military aircraft the life-cycle cost includes the three segments that were just discussed. Though there will be a slight reduction in the *RDT&E* cost as the years go by, there will be a steady increase in maintenance cost due partially to inflation, but also in part to the additional maintenance needed as the plane gets older. Figure 11.5 below shows us this increase as a function of years passing. In addition Figure 11.6 shows the breakdown of the individual sections of the costs after 5, 10 and 20 years.

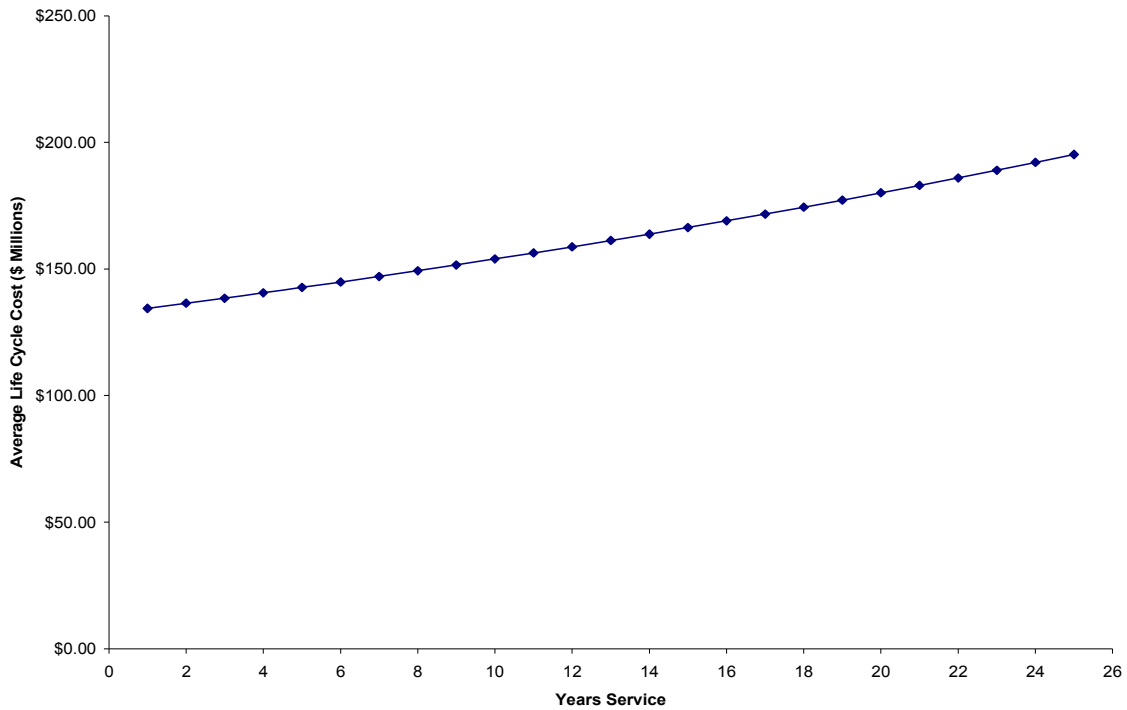


Figure 11.5. Average Life-Cycle Cost for a 1000 Airplane Buy

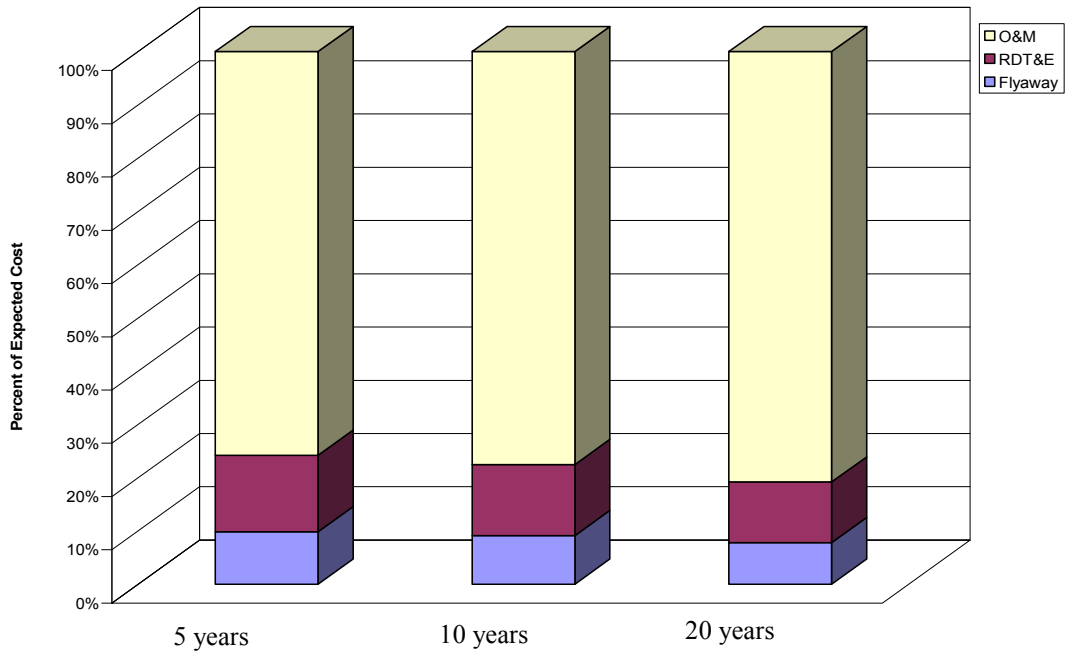
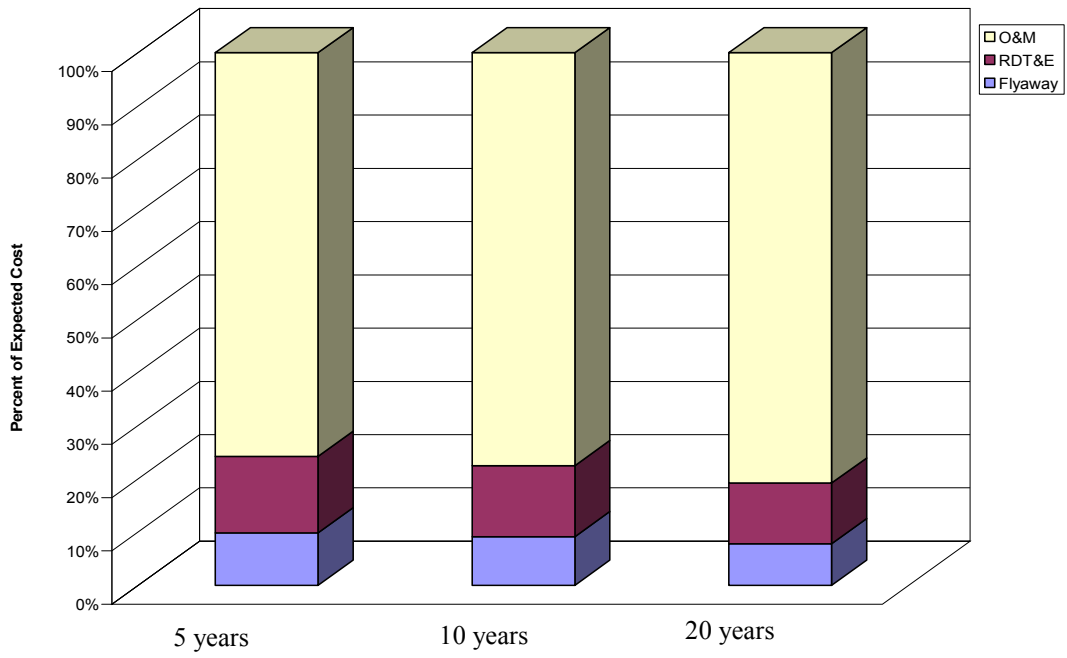


Figure 11.6. Average Life-Cycle Cost Breakdown for a 1000 Airplane Buy

12. Conclusion

The RFP for the homeland defense interceptor defined numerous performance and mission requirements that were difficult to meet. The ability to dash at Mach 2.2 and loiter for 4 hours in the same mission is a strenuous task for any aircraft to perform. Three initial concepts were considered and the final concept chosen was a cranked arrow and canard configuration. From that initial concept, the Hedgehog was developed.

Mission and performance analysis defined the constraints on the design. To attain the 18 degree per second turn at a reasonable C_{Lmax} the maximum load factor for the Hedgehog had to be increased from 7 to 9. The DCAP mission defined the TOGW. The loiter and dash portions of those missions also defined the wing geometry and size. All of the mission and performance requirements were combined to create a constraint diagram. The Hedgehog falls within all of the constraints with a thrust to weight ratio of 0.84 and a wing loading of 58.63 psf. Taking the engine and airframe into consideration showed that the Hedgehog has plenty of excess power at altitudes up to 50000 ft and exceeds the excess power requirements defined in the RFP.

The materials and structures that make up the Hedgehog allow it to sustain the immense loads that will be placed on it while performing its mission. A large portion of the aircraft is made up of light-weight and cost effective composites that have a high strength to weight ratio. The airframe is strong and efficient. The structures inside the wing are extremely durable and have a high strength while occupying only a small portion of the volume inside the wing. This efficient design allows all of the fuel to be stored in the wings, eliminating the need for external fuel tanks.

In addition to an efficient design, the Hedgehog is also well equipped. The hardware inside the aircraft is the best hardware available for the missions the Hedgehog must perform. The Hedgehog can carry all of the weapons required by the RFP and can operate those weapons to win any battle swiftly and decisively. In addition, the design is very damage tolerant. The pilot can maintain control of the Hedgehog in the event of up to two electrical failures and one hydraulic failure.

The Hedgehog is a superior interceptor. It is able to perform every mission in the RFP and exceeds the performance requirements. The design of the Hedgehog is strong, damage tolerant, efficient, and cost effective. For a 1000 unit buy, the flyway cost is under \$15 million. The Hedgehog is a superior interceptor and is more than capable of maintaining security in the United States.

Appendix A: Mission Requirements¹

Attachment 1

Defensive Counter-Air Patrol Mission

Configuration: (2) AIM-120 + (2) AIM-9 + M61A1 gun with 500 rounds 20mm ammunition

Phase Description

- 1 Take-off and acceleration allowance (computed at sea level. 59° F).
 - a. Fuel allowance for warm-up
 - b. Fuel to accelerate to climb speed at maximum thrust (no distance credit)
 - 2 Climb from sea level to optimum cruise altitude
 - 3 Cruise out 300 nm at optimum speed and altitude
 - 4 Combat air patrol 4 hours at best loiter speed and 35,000 ft
 - 5 Dash 100 nm at maximum speed at 35,000 ft
 - 6 Combat allowance: Fuel required to perform the following maneuvers at 35,000 ft with maximum thrust and fuel flow.
 - a. One sustained 360° turn ($P_s = 0$) at Mach = 1.2
 - b. One sustained 360° turn ($P_s = 0$) at Mach = 0.9After maneuvers, fire all missiles and retain gun ammunition.
 - 7 Climb/accelerate to optimum speed and altitude
 - 8 Cruise back 400 nm at optimum speed and altitude
 - 9 Descend to sea level (no distance credit or fuel used)
 - 10 Reserves: fuel for 30 minutes at sea level at speed for maximum endurance
- Note: Base all performance calculations on standard day conditions with no wind.

Attachment 2

Point Defense Intercept Mission

Configuration: (2)AIM-120 + (2) AIM-9 + M61A1 gun with 500 rounds 20mm ammunition

Phase Description

- 1 Take-off and acceleration allowance (computed at sea level and 59° F).
 - a. Fuel allowance for warm-up
 - b. Fuel to accelerate to climb speed at maximum thrust (no distance credit)
 - 2 Climb from sea level to 35,000 ft and accelerate to maximum speed
 - 3 Dash 200 nm at maximum speed at 35,000 ft
 - 4 Combat allowance: Fuel required to perform the following maneuvers at 35,000 ft with maximum thrust and fuel flow.
 - a. One sustained 360° turn ($P_s = 0$) at Mach = 1.2
 - b. One sustained 360° turn ($P_s = 0$) at Mach = 0.9After maneuvers, fire all missiles and retain gun ammunition.
 - 5 Climb/accelerate to optimum speed and altitude
 - 6 Cruise back 200 nm at optimum speed and altitude
 - 7 Descend to sea level (no distance credit or fuel used)
 - 8 Reserves: fuel for 30 minutes at sea level at speed for maximum endurance
- Note: Base all performance calculations on standard day conditions with no wind.

Attachment 3

Intercept/Escort Mission

Configuration: (2)AIM-120 + (2) AIM-9 + M61A1 gun with 500 rounds 20mm ammunition

Phase Description

- 1 Take-off and acceleration allowance (computed at sea level and 59° F).
 - a. Fuel allowance for warm-up
 - b. Fuel to accelerate to climb speed at maximum thrust (no distance credit)
 - 2 Climb from sea level to 35,000 ft and accelerate to maximum speed
 - 3 Dash out at maximum speed at 35,000 ft
 - 4 Escort for 300 nm at minimum practical airspeed. Retain all weapons.
 - 5 Climb/accelerate to optimum speed and altitude
 - 6 Cruise back at optimum speed and altitude
 - 7 Descend to sea level (no distance credit or fuel used)
 - 8 Reserves: fuel for 30 minutes at sea level at speed for maximum endurance
- Note: Base all performance calculations on standard day conditions with no wind.

Appendix B: Minimum Performance Requirements¹

Minimum Performance Requirements/Constraints

Criteria	Requirement
Intercept Mission Radius.....	200 nm
DCA Mission CAP endurance at 300 nm radius.....	4 hrs
Performance at Maneuver Weight (50% Internal Fuel) for (2)AIM-120 + M61A1 gun with 500 Rounds 20mm Ammunition	
• Maximum Mach Number at 35,000 ft.....	Mach 2.2
• 1-g Specific Excess Power– Military Thrust	
• 0.9M/Sea Level	200 ft/sec
• 0.9M/15,000 ft.....	50 ft/sec
• 1-g Specific Excess Power– Maximum Thrust	
• 0.9M/Sea Level	700 ft/sec
• 0.9M/15,000 ft.....	400 ft/sec
• 5-g Specific Excess Power– Maximum Thrust	
• 0.9M/Sea Level	300 ft/sec
• 0.9M/15,000 ft.....	50 ft/sec
• Sustained Load Factor– Maximum Thrust	
• 0.9M/15,000 ft.....	5.0 g's
• Maximum Instantaneous Turn Rate at 35,000 ft	18.0 deg/s

Appendix C: Government Furnished Equipment¹

Item	Volume, ft ³	Weight, lb	Cost, K\$ (2005)
Avionics			
• Base Suite			
- ICNIA *	3.0	100	200
- 3 x MFDs	1.5	20	60
- Head-Up Display	1.6	35	20
- Data bus	0.5	10	10
• ECM Equipment			
- INEWS [†]	3.0	100	500
Flight and Propulsion Control System			
• Vehicle Management System	1.0	50	200
Fire Control Systems			
• IRSTS [‡]	2.0	50	300
• Active Array Radar	6.0	450	1000
Systems and Equipment			
• Electrical System(2 engines)	4.0	300	50
• Auxiliary Power Unit (APU)	2.0	100	50
• Ejection Seat	8.0	160	100
• OBOGS [§]	1.0	35	10
• OBIGGS ^{**}	1.0	35	10

Air-to-Air Weapons

AIM - 9M Sidewinder Missile

Launch weight:	191 lb
Length:	9.6 ft
Max span:	2.1 ft
Body diameter:	0.4 ft
Launcher rail weight:	50 lb
Launcher rail length:	9.2 ft

AIM - 120 AMRAAM

Launch weight:	327 lb
Length:	12 ft
Max span:	2.1 ft
Body diameter:	0.6 ft

M61A1 20 mm Cannon

Cannon weight:	275 lb
Length:	74 in
Max diameter:	10 in
Ammunition feed system	
(500 rounds) weight:	300 lb
Ammunition drum length: 25 in	
Diameter:	25 in
Ammunition (20 mm)	0.58 each
Returned casings	0.26 each

* Integrated Communication, Navigation, and Identification Avionics

[†] Integrated Electronic Warfare System

[‡] Infrared Search and Track System with laser ranging

[§] Onboard Oxygen Generation System

^{**} Onboard Inert Gas Generation System

Appendix D: Configuration Drawings

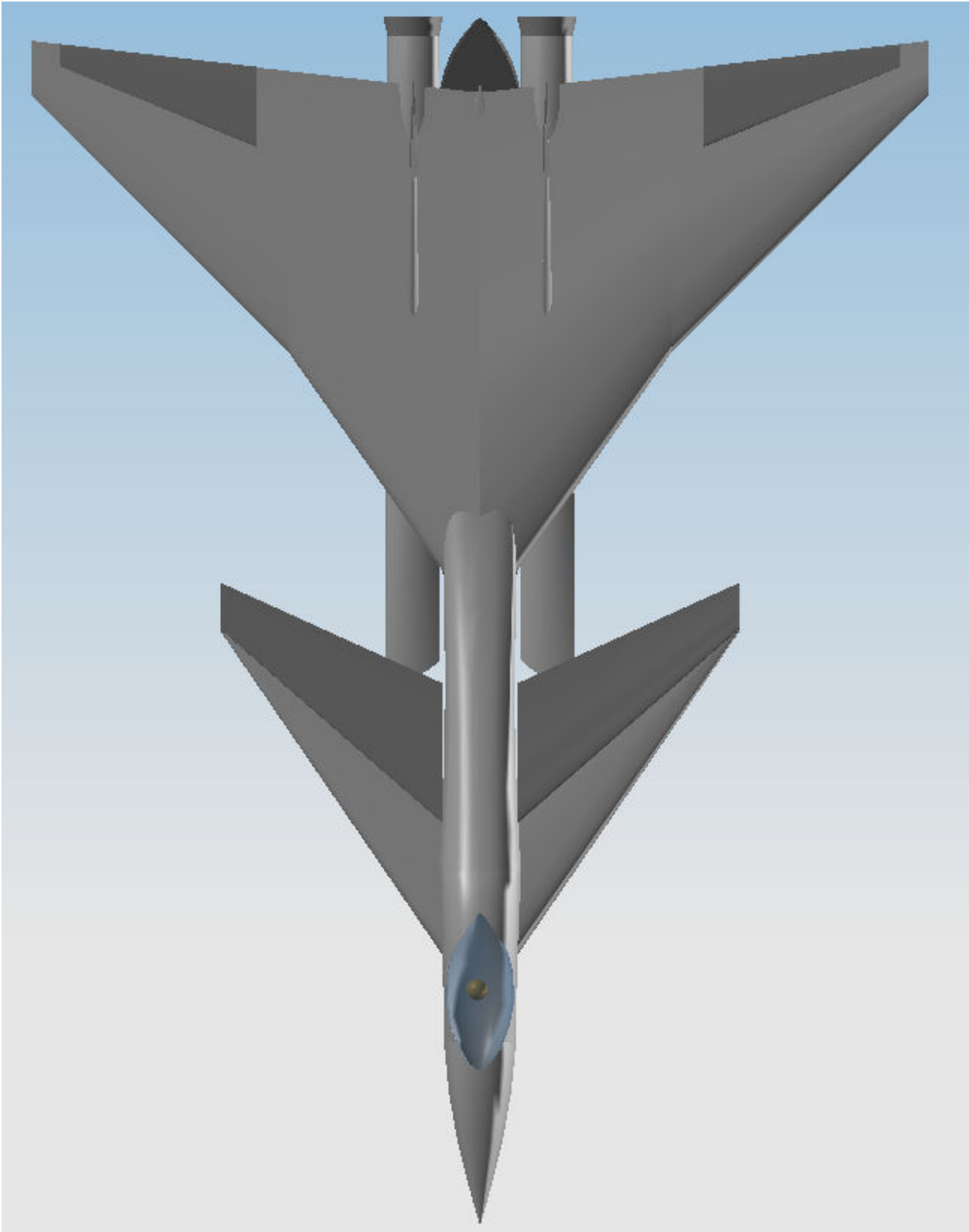


Figure D.1. Top view of *Hedgehog*.

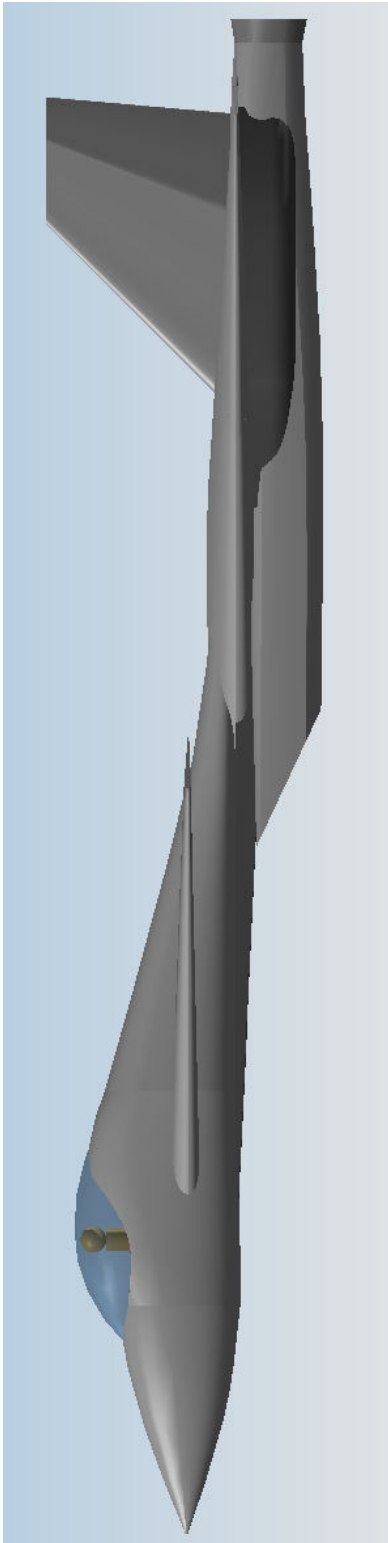


Figure D.2. Side view of *Hedgehog*.

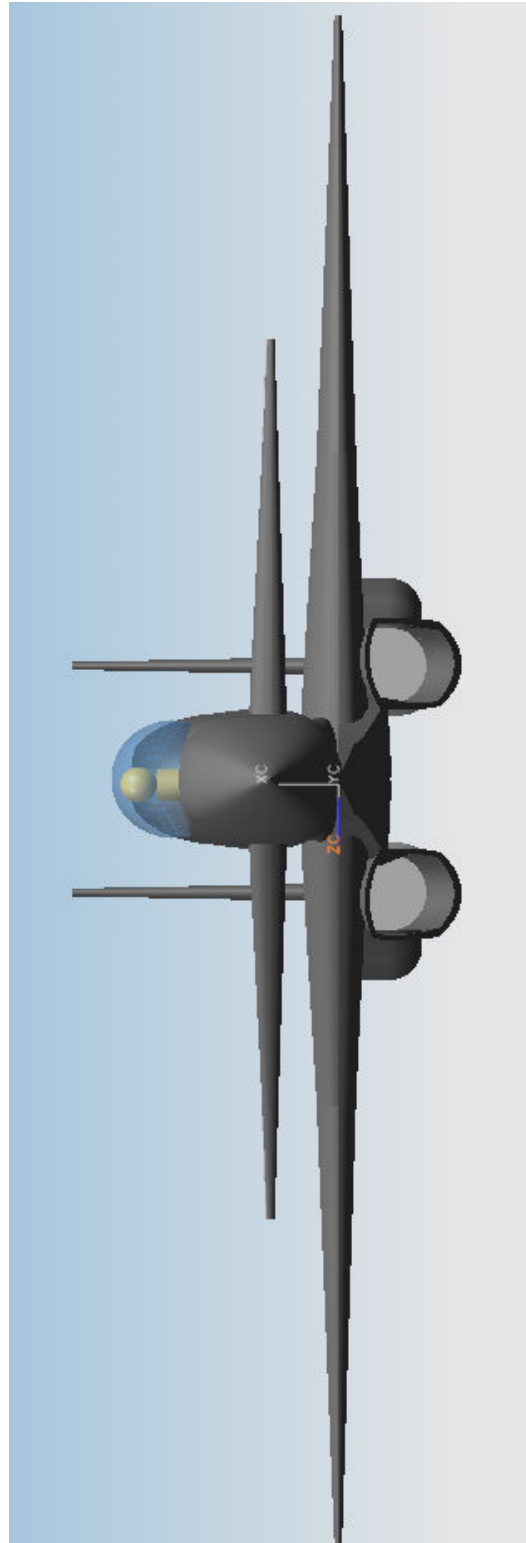


Figure D.3. Front view of *Hedgehog*.

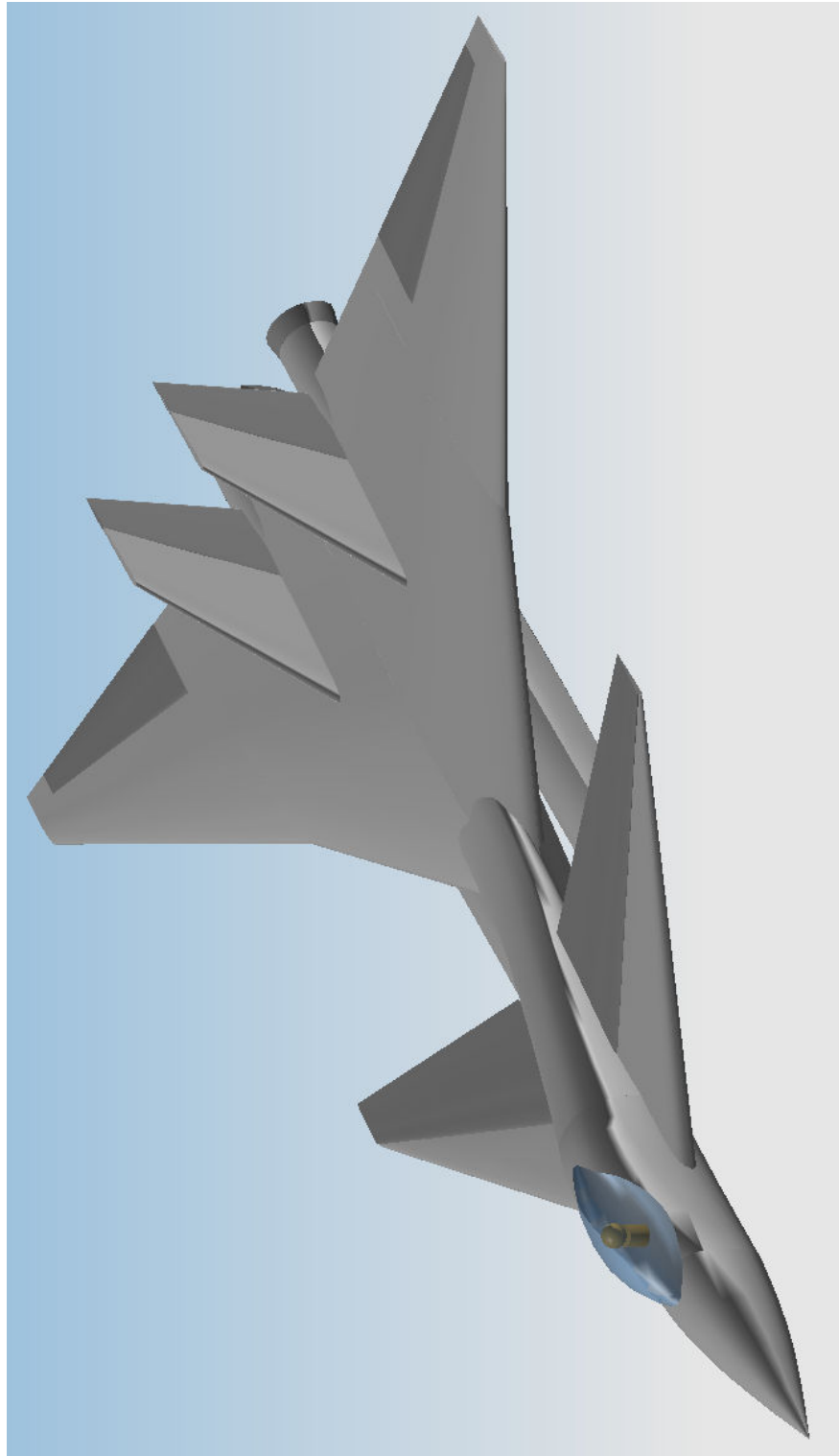


Figure D.4. Isometric view of the *Hedgehog*.

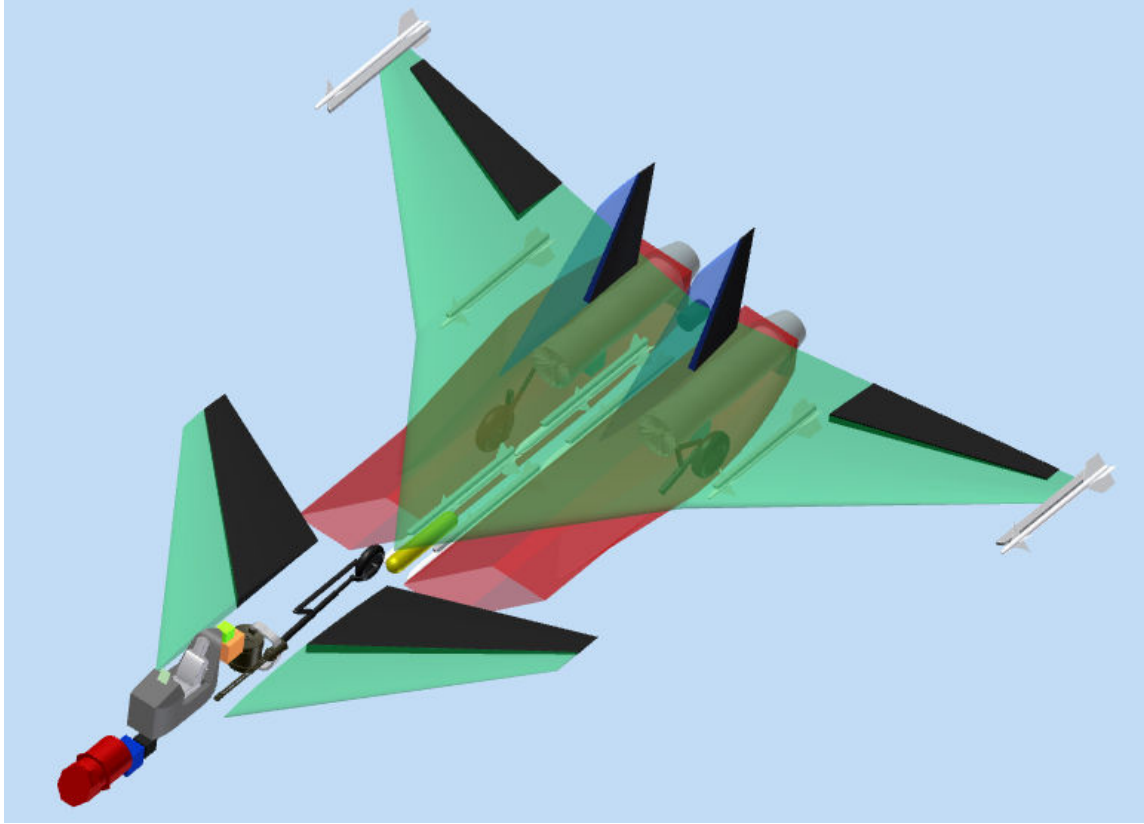


Figure D.5. Isometric systems layout.

References

- ¹ “2005-06 AIAA Foundation Undergrad Team Aircraft Design Competition,” *American Institute of Aeronautics and Astronautics*, URL: http://www.aoe.vt.edu/~mason/Mason_f/AIAAHDIrfp.pdf [cited 6 December 2005].
- ² “Anthrax Attack Could Kill 123,000,” *BBC News*, URL: <http://news.bbc.co.uk/1/hi/health/2857207.stm> [cited 6 December 2005].
- ³ “Coastline of the United States,” *Pearson Education*, URL: <http://www.factmonster.com/ipka/A0001801.html> [cited 6 December 2005].
- ⁴ Raymer, D. P., *Aircraft Design: a Conceptual Approach*, 3rd ed., AIAA Education Series, AIAA, Reston, VA, 1999.
- ⁵ “F-22 Airfoil,” *Aerospaceweb.org*, URL: <http://www.aerospaceweb.org/question/airfoils/q0060a.shtml> [cited 5 May 2006].
- ⁶ “JavaFoil – Analysis of Airfoils,” *JavaFoil*, URL: <http://www.mh-aerotools.de/airfoils/javafoil.htm>
- ⁷ Hom, K.W., Morris, O.A., and Hahne, D.E. “Low-Speed Investigation of the Maneuver Capability of Supersonic Fighter Wings,” AIAA-83-0426. Clean lift reference.
- ⁸ Mason, W. H., “Software for Aerodynamics and Aircraft Design,” *Aerospace Engineering, Virginia Tech*, URL: http://www.aoe.vt.edu/~mason/Mason_f/MRsoft.html [cited 6 December 2005].
- ⁹ Etkin, B., and Reid, L., *Dynamics of Flight: Stability and Control*, 3rd Edition, John Wiley & Sons Inc., NY, 1996.
- ¹⁰ “Military Engines,” *General Electric*, URL: <http://www.geae.com/engines/military/index.html> [cited 5 December 2005].
- ¹¹ “Military Products,” *Pratt and Whitney*, URL: <http://www.pratt-whitney.com/> [cited 5 December 2005].
- ¹² “Defence Aerospace,” *Rolls Royce*, URL: http://www.rolls-royce.com/defence_aerospace/default.jsp [cited 5 December 2005].
- ¹³ Hill, P., and Peterson, C., *Mechanics and Thermodynamics of Propulsion*, 2nd ed., Addison-Wesley Publishing Company, Inc. New York, 1992, Chaps. 3, 6.
- ¹⁴ “Matweb – The Online Materials Information Resource.” URL: www.matweb.com [cited 18 April 2006].
- ¹⁵ “Hexweb Honeycomb Attributes and Properties,” *Hexcel Composites*, URL: <http://www.hexcel.com/NR/rdonlyres/599A3453-316D-46D6-9AEE-C337D8B547CA/0/HexwebAttributesandProperties.pdf> [cited 18 April 2006].
- ¹⁶ Hyer, Michael W., *Stress Analysis of Fiber-Reinforced Composite Materials*. WCB McGraw-Hill, NY, 1998.
- ¹⁷ “Magnamite AS4C, Carbon Fiber,” *Hexcel Composites*, URL: http://www.hexcel.com/NR/rdonlyres/45DE69AE-8330-4BAC-AAF0-76617B888590/0/Magnamite_AS4C.pdf [cited 18 April 2006].
- ¹⁸ Roskam, J., *Airplane Design, Volume V: Component Weight Estimation*. Design Analysis & Research Corporation, 1987.
- ¹⁹ Roskam, J., *Airplane Design, Volume VI: Preliminary Calculation of Aerodynamic, Thrust, and Power Characteristics*. Design Analysis & Research Corporation, 1987.
- ²⁰ “The F/A-22 Common Integrated Processor is the First Fully Integrated Avionics Processing System,” *Raytheon*, URL: http://www.raytheon.com/products/f22_cip/ [cited 6 December 2005].
- ²¹ “F22 Fighter,” *Dewman*, URL: <http://www.f22fighter.com/> [cited 6 December 2005].
- ²² “Advanced Self Protection Integrated Suite,” *Raytheon*, URL: <http://www.raytheon.com/businesses/stellent/groups/sas/documents/asset/aspis.pdf> [cited 6 December 2005].
- ²³ White, R. E., “AN/APG-79 AESA Active Electronically Scanned Array Radar,” *Raytheon*, URL: http://www.raytheon.com/products/stellent/groups/sas/documents/legacy_site/cms01_050831.pdf [cited 6 December 2005].
- ²⁴ Goold, D., “A/N ASQ-228 ATFLIR Advanced Targeting Forward-Looking Infrared Pod,” *Raytheon*, URL: http://www.raytheon.com/products/stellent/groups/public/documents/content/atflir_ds.pdf [cited 6 December 2005].
- ²⁵ “Pilot Support,” *SiteLab Internet Engineering*, URL: http://www.f-22raptor.com/af_pilot.php [cited 6 December 2005].
- ²⁶ “The Ejection Seat Gallery,” *The Ejection Site*, URL: http://www.ejection-site.com/frame_sg.htm [cited 6 December 2005].
- ²⁷ “OC1077 Slimline Oxygen Concentrator,” *Carleton Life Support Systems Inc*, URL: <http://www.carletons.com/productsbu/oc1077.htm> [cited 6 December 2005].
- ²⁸ “NC1029 On-Board Inert Gas Generating System,” *Carleton Life Support Systems Inc*, URL: <http://www.carletons.com/productsbu/nc1029.htm> [cited 6 December 2005].
- ³⁰ Roskam, J., *Airplane Design, Volume IV: Layout Design Of Landing Gear and Systems*. Design Analysis & Research Corporation, 1987.
- ³¹ “Lockheed Martin F-35,” *Moog Inc*. URL: <http://www.moog.com/noq/%5Fprograms%5F%5Fc677/> [cited 18 April 2006].
- ³² E.T. Raymond, C.C. Chenoweth, *Aircraft Flight Control Actuation System Design*. Society of Automotive Engineers, Inc., 1993.
- ³³ “Inflation Calculator,” *Financial Trend Forecaster*. URL: http://inflationdata.com/Inflation/Inflation_Rate/InflationCalculator.asp [cited 18 April 2006].